Journal of Innovative Applied Mathematics and Computational Sciences

JIAMCS

Volume 2, Issue 3

July - December 2022

Publisher

Institute of Sciences and Technology

University Center Abdelhafid Boussouf, Mila.

Publication Center: Algeria

http://jiamcs.centre-univ-mila.dz/

ARK: 49935/jiamcs

ISSN: 2773-4196

Journal of Innovative Applied Mathematics and Computational Sciences (JIAMCS)

Volume 2, No. **3** (2022)

Institute of Sciences and Technology, University Center Abdelhafid Boussouf MILA, ALGERIA.

Contents

Aims and Scope

The Journal of Innovative Applied Mathematics and Computational Sciences (JIAMCS) is an online open access, peer-reviewed semiannual international journal published by the Institute of Sciences and Technology, University Center Abdelhafid Boussouf, Mila, Algeria.

The journal publishes high-quality original research papers from various fields related to applied mathematics, scientific computing, and computer science.

In particular, it publishes original papers in the following areas:

- Differential equations, (ODE's, PDE's, integral equations, difference equations, fractional differential equations)
- Dynamical systems and bifurcation-chaos theory
- Fractional calculus
- Modern control theory and practice
- Operator's theory
- Mathematical physics
- Probability and statistics
- Mathematical optimization
- Mathematical modelling and simulation
- Numerical analysis
- Fuzzy logic and systems
- Lattice theory, number theory and cryptography
- Computer science
- Bioinformatics
- Artificial intelligence

- Pattern recognition
- Computer vision and image processing
- Naturel language processing
- Signal processing
- Communication theory and network security

Editorial Team

Journal of Innovative Applied Mathematics and Computational Sciences

J. Innov. Appl. Math. Comput. Sci. **2**(3) (2022), 01–14. n2t.net/ark:/49935/jiamcs.v2i3.51

http://jiamcs.centre-univ-mila.dz/

Non polynomial fractional spline method for solving Fredholm integral equations

Faraidun K. Hamasalh [1] and Rahel J. Qadir [2]

[1] Department of Mathematics, College of Education, University of Sulaimani, Sulaymaniyah HC7V+H2F, Iraq.

[2] Mathematical Sciences's Department, School of Basic Education, University of Sulaimani, Sulaymaniyah H9G5+HX7, Iraq.

Received 17 July 2022, Accepted 30 October 2022, Published 14 December 2022

Abstract. A new type of non-polynomial fractional spline function for approximating solutions of Fredholm-integral equations has been presented. For this purpose, we used a new idea of fractional continuity conditions by using the Caputo fractional derivative and the Riemann Liouville fractional integration to generate fractional spline derivatives. Moreover, the convergence analysis is studied with proven theorems. The approach is also well-explained and supported by four computational numerical findings, which show that it is both accurate and simple to apply.

Keywords: Non-polynomial fractional spline method, Fredholm integral equations, Fractional derivative.

2020 Mathematics Subject Classification: 45B05, 08A02, 26A99, 65D30, 65K99.

1 Introduction

Consider the second kind of linear integral equation [5-8].

$$y(t) = f(t) + \int_a^b k(t,x)y(x)dx, \tag{1.1}$$

The kernel function of two variables t and x is $k(t,x)$, a and b are constants, $y(t)$ is the unknown function, and $f(t)$ is given. Integral equations can be used to describe some difficulties as well Bellour, A. [5] solving Fredholm integral equations by using two cubic spline methods, in [10] D. Hammad, a new general form of Ten non-polynomial cubic splines for some classes of Fredholm integral equations are presented, Maleknejad, Khosrow, Jalil Rashidinia, and Hamed Jalilian in [22], solved Fredholm integral equation via Quintic Spline functions and in [27] S. Saha Ray, and P. K. Sahu. proposed Numerical methods for solving Fredholm integral equations of the second kind. And for other works see [4] and [25] Non-polynomial spline functions are used to find approximate solutions to a variety of problems, including integral equations [10], [26], [23], and [13], and differential equations [3], [16], [30], [11] and [12],

✉ Corresponding author. Email: faraidun.hamasalh@univsul.edu.iq

ISSN (electronic): 2773-4196

wave equations [8], Burgers equation [1], etc.
We employ a similar technique outlined in [10], [22], and [5], but fractional derivative and fractional models are not used there, it is clear that fractional calculus is one of the most reliable processes for managing complex systems and there are still many models to be suggested, analyzed and used in real-world applications in many fields of science and engineering where locality plays a significant role. Several fractional derivatives and integral definitions have recently been offered. [28]- [20], [7], and [29]. It also contributes significantly to the progress of other fields of science, such as engineering [31], chemistry [14], physics [6], and biology [15]. We hope that much better work on this technique will be done in the future and that this will be the beginning of doing better work.
The following sections of this paper are organized in the given sequence: In Section 2, we give some basic definitions, derivations, and formulations of the non-polynomial fractional spline function for solving second-order integral equations. In section 3, we present the methodology of our technique for Fredholm-integral equations (FIE). In sections 4 and 5, the method's convergence is discussed, and some numerical results are shown for the accurate and simple techniques, respectively. Finally, section 6 consists of the conclusion.

2 Mathematical preliminaries and Non-polynomial fractional spline construction

Here are some key fractional definitions before we get into the details of our approach. Different definitions are available for fractional derivatives. In this paper, both the Riemann-Liouville fractional derivative and the Caputo fractional derivative will be used.

Definition 2.1. [24] The RLD (Riemann- Liouville fractional derivative) of order β can be defined as:

$$ {}_aD_t^{\beta} f(t) = \frac{1}{\Gamma(n-\beta)} \left(\frac{d}{dt}\right)^n \int_a^t (t-u)^{n-\beta-1} f(u)du. $$

for every β, and $n = \lceil \beta \rceil$

Definition 2.2. [24] The CD (Caputo fractional derivative) of order β is defined as:

$$ {}_a^C D_t^{\beta} f(t) = \frac{1}{\Gamma(n-\beta)} \int_a^t (t-u)^{n-\beta-1} \left(\frac{d}{du}\right)^n f(u)du \quad , n = \lceil \beta \rceil \text{ and } \beta > 0. $$

For $\beta = 0$, we introduce the notation:

$$ {}^C D_t^{\beta} f(t) = D^{\beta} f(t). $$

We used the non-polynomial fractional spline function to approximate a solution to the integral equation. For this reason, we consider a finite set of points $\Theta = [a, b]$ with $\Delta : a = t_0 < \cdots < t_m = b$, where $t_i = a + ih$. Let $S_i(t)$ be the interpolating non-polynomial FS (fractional Spline) function with interpolates y at t_i with new fractional continuity conditions, defined on $[t_i, t_{i+1}], i = 0, \ldots, m-1$, as:

$$ S_i(t) = a_i sin(\tau(t-t_i)) + b_i cos(\tau(t-t_i)) + c_i(t-t_i) + d_i(t-t_i)^{\frac{1}{2}} + e_i. \tag{2.1} $$

Where a_i, b_i, c_i, d_i, and e_i are real numbers and τ is the frequency of trigonometric functions. To derive the coefficients a_i, b_i, c_i, d_i and e_i we define boundary conditions:

$$ S_i(t_i) = y_i,\ S_i(t_{i+1}) = y_{i+1},\ S_i'(t_i) = M_i,\ S_i'(t_{i+1}) = M_{i+1}, \text{ and } S_i''(t_i) = y_i''(t_i). \tag{2.2} $$

Then, using algebraic manipulation and a Python program, we get the following expression:

$$a_i = \frac{(\tau M_{i+1} - \tau M_i - \alpha_1 y_i'')}{\tau^2(\alpha_0 - 1)},\ b_i = \frac{-y_i''}{\tau^2},\ c_i = \frac{\tau\alpha_0 M_i - \tau M_{i+1} + \alpha_1 y_i''}{\tau(\alpha_0 - 1)},\ e_i = \frac{(\tau^2 y_i + y_i'')}{\tau^2}, \text{and}$$

$$d_i = \frac{\tau^2(\alpha_0 - 1)y_{i+1} - \tau^2(\alpha_0 - 1)y_i - (\tau^2 h\alpha_0 - \tau\alpha_1)M_i - (\tau\alpha_1 - \tau^2 h)M_{i+1} - (2\alpha_0 + \tau h\alpha_1 - 2)y_i''}{\tau^2\sqrt{h}(\alpha_0 - 1)}. \tag{2.3}$$

Where $\alpha_0 = cos(\tau h)$, and $\alpha_1 = sin(\tau h)$.
We obtained the continuity conditions using fractional derivative from the Caputo fractional derivative:
$D^{(1/2)}S_i(t_i) = D^{(1/2)}S_{i-1}(t_i)$, then we get the following relations:

$$\mu_1 M_{i-1} - \mu_2 M_i + \mu_3 M_{i+1} = \mu_4(y_{i-1} - 2y_i + y_{i+1}) - \mu_5 y_{i-1}'' + \mu_6 y_i''. \tag{2.4}$$

Where
$\mu_1 = \frac{2\sqrt{\pi\tau h}\alpha_2 + (\pi-4)\theta\alpha_0 - \pi\alpha_1}{\sqrt{\tau\pi}}$, $\mu_2 = \frac{2\sqrt{h\pi\theta}(\sqrt{2}\alpha_2 - 1) - \sqrt{h}(2\pi\alpha_1 - \alpha\theta\alpha_0 + (4-\pi)\theta)}{\sqrt{\pi\theta}}$, $\mu_3 = \frac{(\sqrt{\pi\tau}(\theta-\alpha_1) + \sqrt{2h}\tau)}{\tau}$,
$\mu_4 = -\alpha_4\sqrt{\theta}(\alpha_0 - 1)$, $\mu_5 = \frac{2\sqrt{\pi\theta}(\alpha_1\alpha_2 + \alpha_3(\alpha_0 - 1)) + 2\pi(\alpha_0 - 1) + (\pi - 4)\theta\alpha_1}{\sqrt{\pi\tau^3}}$, $\mu_6 = \frac{(\sqrt{\pi}(\alpha_1\theta + 2\alpha_0 - 2) + \sqrt{2\theta}(\alpha_1 + \alpha_0 - 1))}{\sqrt{\tau^3}}$
,
$\theta = h\tau$, $\alpha_0 = cos(h\tau)$, $\alpha_1 = sin(h\tau)$, $\alpha_2 = sin((4h\tau + \pi)/4)$, $\alpha_3 = cos((4h\tau h + \pi)/4)$
and $\alpha_4 = \sqrt{(\pi/h)}$.
The following local truncation error was observed by expanding Eq. (2.4) with Taylor series about t_i:
$T_i = \beta_1 y_i' + \beta_2 y_i'' + \beta_3 y_i''' + \beta_4 y_i^{(4)} + \beta_5 y_i^{(5)} + \beta_6 y_i^{(6)} + O(h^6)$.
Where
$\beta_1 = (-\mu_1 - \mu_2 - \mu_3)$, $\beta_2 = (\mu_1 h - \mu_3 h - \mu_4 h^2 + \mu_5 + \mu_6)$, $\beta_3 = (-\mu_1\frac{h^2}{2!} - \mu_3\frac{h^2}{2!} - \mu_5 h)$,
$\beta_4 = (\mu_1\frac{h^3}{3!} - \mu_3\frac{h^3}{3!} - \mu_4\frac{h^4}{12} + \mu_5\frac{h^2}{2!})$, $\beta_5 = (\mu_1\frac{h^4}{4!} - \mu_3\frac{h^4}{4!} - \mu_4\frac{2h^5}{5!} - \mu_5\frac{h^3}{3!})$,
and $\beta_6 = \mu_5\frac{h^4}{4!}$. Two more equations are required to get the unique solution of the linear system (2.4). Using the Taylor series and the undetermined coefficients technique, which is shown below.

$$\sum_{k=1}^{2}\gamma_k y_k' = \frac{1}{6h}\sum_{k=0}^{4}\eta_k y_k + O(h^5),$$
$$\sum_{k=2}^{3}\gamma_{k-1} y_k' = \frac{1}{12h}\sum_{k=0}^{5}\sigma_k y_k + O(h^5). \tag{2.5}$$

The unknown coefficients in Eq. (2.5) are obtained as follows by using Taylor's expansion:
$(\gamma_1, \gamma_2) = (-\mu_2, \mu_3)$
$(\eta_0, \eta_1, \eta_2, \eta_3, \eta_4) = (-2\mu_2, -3\mu_2 - 2\mu_3, 6\mu_2 - 3\mu_3, 6\mu_3 - \mu_2, -\mu_3)$
$(\sigma_0, \sigma_1, \sigma_2, \sigma_3, \sigma_4, \sigma_5) = (\mu_2, \mu_3 - 8\mu_2, -8\mu_3, 8\mu_2, 8\mu_3 - \mu_2, -\mu_3)$
Rewriting equation (2.4) we get the following in matrix form: $LM = L_1 y + L_2\bar{y}$
And hence

$$M = L^{-1}L_1 y + L^{-1}L_2 L_3 y, \tag{2.6}$$

Where $M = (y_0', y_1', \ldots, y_n')^T, y = (y_0, y_1, \ldots, y_n)^T, \bar{y} = (y_0'', y_1'', \ldots, y_n'')^T$ and $L_3 y = \bar{y}$.
Also L_1 is three-diagonal matrix, L_2 is two-diagonal matrix, L_3 is an integration diagonal

matrix, and

$$L=\begin{bmatrix}
\mu_1 & -\mu_2 & \mu_3 & 0 & 0 & \cdots & 0 & 0 & 0 & 0 & 0\\
0 & \mu_1 & -\mu_2 & \mu_3 & 0 & \cdots & 0 & 0 & 0 & 0 & 0\\
0 & 0 & \mu_1 & -\mu_2 & \mu_3 & \cdots & 0 & 0 & 0 & 0 & 0\\
\vdots & \ddots & \ddots & \ddots & \ddots & \ddots & \vdots & \vdots & \vdots & \vdots & \vdots\\
\vdots & \vdots & \ddots & \ddots & \ddots & \ddots & \ddots & \vdots & \vdots & \vdots & \vdots\\
\vdots & \vdots & \vdots & \ddots & \ddots & \ddots & \ddots & \ddots & \vdots & \vdots & \vdots\\
\vdots & \vdots & \vdots & \vdots & \ddots & \ddots & \ddots & \ddots & \ddots & \vdots & \vdots\\
\vdots & \vdots & \vdots & \vdots & \vdots & \ddots & \ddots & \ddots & \ddots & \ddots & \vdots\\
0 & 0 & 0 & 0 & 0 & 0 & \mu_1 & -\mu_2 & \mu_3 & 0 & 0\\
0 & 0 & 0 & 0 & 0 & 0 & 0 & \mu_1 & -\mu_2 & \mu_3 & 0\\
0 & 0 & 0 & 0 & 0 & 0 & 0 & 0 & \mu_1 & -\mu_2 & \mu_3
\end{bmatrix}, \tag{2.7}$$

3 Method of Non polynomial Analysis

Using the spline polynomial technique, we investigate the second type of integral equation. For Eq. (1.1), a problem has been derived, which discusses the existence and uniqueness of the solution.
From Eq. (1.1) and Eqs. (2.1)-(2.3) we have:

$$y(t_i) \approx f(t_i) + \sum_{j=0}^{m-1} \int_{x_j}^{x_{j+1}} k\,(t_i,x)\,S_j(x)dx,$$

$$= f(t_i) + \sum_{j=0}^{m-1} \int_{x_j}^{x_{j+1}} k\,(t_i,x)\,[a_j sin(\tau(x-x_j)) + b_j cos(\tau(x-x_j)) + c_j(x-x_j) + d_j(x-x_j)^{1/2} + e_j]dx,$$

$$= f(t_i) + \sum_{j=0}^{m-1} \int_{x_j}^{x_{j+1}} k\,(t_i,x)\,[\frac{\sqrt{(x-x_j)}}{h} y_{j+1} + (1 - \frac{\sqrt{(x-x_j)}}{h})y_j + (\frac{\alpha_0}{(\alpha_0-1)}(x-x_j) -$$
$$\frac{sin(\tau(x-x_j))}{\tau(\alpha_0-1)} - \frac{\theta\alpha_0-\alpha_1}{\sqrt{\theta\tau}(\alpha_0-1)})M_j + (\frac{sin(\tau(x-x_j)}{\tau(\alpha_0-1)} - \frac{(x-x_j)}{(\alpha_0-1)} - \frac{(\alpha_1-\theta)}{\sqrt{\tau\theta}(\alpha_0-1)}\sqrt{x-x_j})M_{j+1}$$
$$+(\frac{\alpha}{\theta(\alpha_0-1)}(x-x_j) - \frac{\alpha_1 sin(\tau(x-x_j))}{\tau^2(\alpha_0-1)} - \frac{cos(\tau(x-x_j))}{\tau^2} - \frac{2\alpha_0+\theta\alpha_1-2}{\tau^2\sqrt{h}(\alpha_0-1)}\sqrt{x-x_j} + \frac{1}{\tau^2})y_j'']dx$$

$$= f\left(t_i\right) + \sum_{j=0}^{m-1}\left(\frac{y_{j+1}}{\sqrt{h}} - \frac{\alpha_1-\theta}{\sqrt{\tau\theta}\left(\alpha_0-1\right)}M_{j+1}\right)\int_{x_j}^{x_{j+1}} k\left(t_i,x\right)\ \sqrt{x-x_j}dx + \sum_{j=0}^{m-1}\left(-y_j - \frac{\theta\alpha_0-\alpha_1}{\sqrt{\tau\theta}\left(\alpha_0-1\right)}M_j - \frac{\left(2\alpha_0+\theta\alpha_1-2\right)}{\tau^2\sqrt{h}\left(\alpha_0-1\right)}y_j''\right)\int_{x_j}^{x_{j+1}} k\left(t_i,x\right)\ \sqrt{x-x_j}dx + \sum_{j=0}^{m-1}\left(\frac{\alpha_0}{\alpha_0-1}M_j + \frac{\alpha_1}{\tau\left(\alpha_0-1\right)}y_j''\right)\int_{x_j}^{x_{j+1}} k\left(t_i,x\right)\left(x-x_j\right)dx - \sum_{j=0}^{m-1}\frac{M_{j+1}}{\left(\alpha_0-1\right)}\int_{x_j}^{x_{j+1}} k\left(t_i,x\right)\left(x-x_j\right)dx + \sum_{j=0}^{m-1}\frac{M_{j+1}}{\tau\left(\alpha_0-1\right)}\int_{x_j}^{x_{j+1}} k\left(t_i,x\right)\sin\left(\tau\left(x-x_j\right)\right)dx + \sum_{j=0}^{m-1}\left(\frac{-M_j}{\tau\left(\alpha_0-1\right)} - \frac{\alpha_1}{\tau^2\left(\alpha_0-1\right)}y_j''\right)\int_{x_j}^{x_{j+1}} k\left(t_i,x\right)\sin\left(\tau\left(x-x_j\right)\right)dx + \sum_{j=0}^{m-1}\left(y_j+\frac{y_j''}{\tau^2}\right)\int_{x_j}^{x_{j+1}} k\left(t_i,x\right)dx - \sum_{j=0}^{m-1}\frac{y_j''}{\tau^2}\int_{x_j}^{x_{j+1}} k\left(t_i,x\right)\cos\left(\tau\left(x-x_j\right)\right)dx.$$

Let
$a(i,j) = \int_{x_j}^{x_{j+1}} k\left(t_i,x\right)\ \sqrt{x-x_j}dx = b(i,j+1)$, $c(i,j) = \int_{x_j}^{x_{j+1}} k\left(t_i,x\right)\left(x-x_j\right)dx = d(i,j+1)$,
$q(i,j) = \int_{x_j}^{x_{j+1}} k\left(t_i,x\right) Sin\left(\tau\left(x-x_j\right)\right)dx = r(i,j+1)$, $g(i,j) = \int_{x_j}^{x_{j+1}} k\left(t_i,x\right)dx$
and $p(i,j) = \int_{x_j}^{x_{j+1}} k\left(t_i,x\right)\cos\left(\tau\left(x-x_j\right)\right)dx$
Suppose that $A = a(i,j), B = b(i,j), C = c(i,j), D = d(i,j), Q = q(i,j), R = r(i,j), G = g(i,j)$ and $P = p(i,j)$.
Also $\hat{y}_j, \hat{M}_j, \hat{F}_l$ and $\hat{\hat{y}}_j$ are approximations for y_j, M_j, f_i and $\hat{y}_i$ respectively such satisfy in Eq. (2.4) for i=0, 1, . . . ,m then we get:

$$\hat{y}_j = \hat{F}_i + \frac{B}{\sqrt{h}}\hat{y}_j - \frac{\alpha_1-\theta}{\sqrt{\tau\theta}\left(\alpha_0-1\right)}B\hat{M}_j - A\hat{y}_j - \frac{\theta\alpha_0-\alpha_1}{\sqrt{\tau\theta}\left(\alpha_0-1\right)}A\hat{M}_j - \frac{\left(2\alpha_0+\theta\alpha_1-2\right)}{\tau^2\sqrt{h}\left(\alpha_0-1\right)}A\hat{\hat{y}}_j + \frac{\alpha_0}{\alpha_0-1}C\hat{M}_j + \frac{\alpha_1}{\tau\left(\alpha_0-1\right)}C\hat{\hat{y}}_j - \frac{1}{\alpha_0-1}D\hat{M}_j + \frac{1}{\tau\left(\alpha_0-1\right)}R\hat{M}_j - \frac{1}{\tau\left(\alpha_0-1\right)}Q\hat{M}_j - \frac{\alpha_1}{\tau^2\left(\alpha_0-1\right)}Q\hat{\hat{y}}_j + G\hat{y}_j + \frac{G}{\tau^2}\hat{\hat{y}}_j - \frac{P}{\tau^2}\hat{\hat{y}}_j. \tag{3.1}$$

Then we get:

$$\hat{y}_j = \hat{F}_i + \frac{1}{\sqrt{h}}(B - \sqrt{h}A + G)\hat{y}_j + \frac{1}{\left(\alpha_0-1\right)}\left(\frac{\alpha_1-\theta}{\sqrt{\tau\theta}}B - \frac{\theta\alpha_0-\alpha_1}{\sqrt{\tau\theta}}A + \alpha_0 C - D + \frac{R}{\tau} - \frac{Q}{\tau}\right)\hat{M}_j + \frac{1}{\tau}\left(\frac{2\alpha_0+\theta\alpha_1-2}{\tau\sqrt{h}\left(\alpha_0-1\right)}A + \frac{\alpha_1}{\left(\alpha_0-1\right)}C - \frac{\alpha_1}{\tau\left(\alpha_0-1\right)}Q + \frac{G}{\tau} - \frac{P}{\tau}\right)\hat{\hat{y}}_j.$$

Let

$$A_1 = \frac{1}{\sqrt{h}}(B - \sqrt{h}A + G),\ A_2 = \frac{1}{\left(\alpha_0-1\right)}\left(\frac{\alpha_1-\theta}{\sqrt{\tau\theta}}B - \frac{\theta\alpha_0-\alpha_1}{\sqrt{\tau\theta}}A + \alpha_0 C - D + \frac{R}{\tau} - \frac{Q}{\tau}\right),$$

$$A_3 = \frac{1}{\tau}\left(\frac{2\alpha_0+\theta\alpha_1-2}{\tau\sqrt{h}\left(\alpha_0-1\right)}A + \frac{\alpha_1}{\left(\alpha_0-1\right)}C - \frac{\alpha_1}{\tau\left(\alpha_0-1\right)}Q + \frac{G}{\tau} - \frac{P}{\tau}\right).$$

Then

$$\hat{y}_j = \hat{F}_i + A_1\hat{y}_j + A_2\widehat{M}_j + A_3\hat{\hat{y}}_j \tag{3.2}$$

Substituting Eq. (2.6) in Eq. (3.2) we get:

$$[I - A_1 - L^{-1}L_1A_2 + L^{-1}L_2L_3A_2 + A_3L_3]\hat{y} = \hat{F} + T. \tag{3.3}$$

The vector of local truncation error is $T = [t_0, t_1, \ldots, t_m]$, displayed as the (m+1) dimensional column vector of the exact solution. $\hat{y} = [y_0, y_1, \cdots, y_m]^T$.
According to Eqs. (3.2) and (3.3) we get:

$$[I - A_1 - L^{-1}L_1A_2 + L^{-1}L_2L_3A_2 + A_3L_3]E = T. \tag{3.4}$$

By solving Eq. (3.1), an approximation of Eq. (1.1) will be obtained.
The function y_i can now be approximated by using the non-polynomial fractional spline $\hat{S}_i$, where

$$\hat{S}_i(t) = \frac{\left(\tau^{\frac{5}{2}}\sqrt{\theta}(\alpha_0-1)\hat{y}_i + \tau^{\frac{5}{2}}\sqrt{\theta}(\alpha_0-1)\hat{y}_{i+1} + \tau^2\sqrt{h}(\alpha_0\theta-\alpha_1)\hat{\mathrm{M}}_i + \tau^2\sqrt{h}(\theta-\alpha_1)\hat{\mathrm{M}}_{i+1} + \sqrt{\tau\theta}(2\alpha_0-\theta\alpha_1-2)\hat{y}_i\right)}{\tau^2\theta^{\frac{3}{2}}(\alpha_0-1)}\sqrt{t-t_i} + \frac{(\tau\alpha_0\hat{\mathrm{M}}_i - \tau\hat{\mathrm{M}}_{i+1} + \alpha_1\hat{y}_i)}{\tau\alpha_0-\tau}(t-t_i) + \left(\frac{\hat{\mathrm{M}}_{i+1} - \tau\hat{\mathrm{M}}_i - \alpha_1\hat{y}_i}{\tau^2\alpha_0 - \tau^2}\right)(\sin(\tau(t-t_i))) - \left(\frac{\hat{y}_i}{\tau^2}\right)(\cos(\tau(t-t_i))) + \left(\frac{\tau^2\hat{y}_i + \sqrt{h}\hat{y}_i}{\tau^2\sqrt{h}}\right) + O(h^5). \tag{3.5}$$

In-consequence $\forall i = 1(1)m-1, t \in (t_i, t_{i+1})$, then we get:

$$\left|\mathrm{S_i(t)} - \hat{\mathrm{S}}_\mathrm{i}(\mathrm{t})\right| \equiv \varphi \mathrm{h}^5. \tag{3.6}$$

4 Convergence of the method

This section includes some important theorems and lemmas, as well as the study of non-polynomial fractional spline convergence.

Lemma 4.1. *[10] Let L be a square Matrix with $\|L\|_\infty < 1$, then the matrix $(I - L)$ is invertible. Furthermore, $\left\|(I-L)^{-1}\right\|_\infty \le \frac{1}{1-\|L\|_\infty}$,*
Where I is the identity matrix and $\|L\|_\infty$ is the infinity norm of the matrix, $L = (l_{ij})$ that is described as following:

$$\|\mathrm{L}\|_\infty = \max_{1\le i\le n}\left(\sum_{j=0}^{n}\left|\mathrm{l_{ij}}\right|\right).$$

Lemma 4.2. *Let $S(t)$ satisfy in (2.1)-(2.4) and be the unique non-polynomial fractional spline, for a given function $y \in C^5[a,b]$. Then:$\|S^\alpha - y^\alpha\| \le O(h^3)$, where $\alpha \in R$.*
proof. *We investigate the continuity of sufficiently high-order derivatives of y by applying (2.1)-(2.4), and we obtain*

$$\begin{aligned}
S_i^{\left(\frac{1}{2}\right)}(t_i) &= -\gamma_0 y_i + \gamma_1 y_i^{\left(\frac{1}{2}\right)} + \gamma_2 y_i' + \gamma_3 y_i^{\left(\frac{3}{2}\right)} + \gamma_4 y_i'' + \gamma_5 y_i^{\left(\frac{5}{2}\right)} + \gamma_6 y_i^{(3)} + \gamma_7 y_i^{\left(\frac{7}{2}\right)} + \gamma_8 y_i^{(4)}(\alpha_1),\\
S_i^{\left(\frac{3}{2}\right)}(t_i) &= \gamma_9 \mathrm{y_i}^{\left(\frac{3}{2}\right)} + \gamma_{10}\mathrm{y_i''} + \gamma_{11}\mathrm{y_i}^{\left(\frac{5}{2}\right)} + \gamma_{12}\mathrm{y_i}^{(3)} + \gamma_{13}\mathrm{y_i}^{\left(\frac{7}{2}\right)} + \gamma_{14}\mathrm{y_i}^{(4)}(\alpha_1),\\
S_i^{\left(\frac{5}{2}\right)}(t_i) &= -\gamma_{15}\mathrm{y_i}^{\left(\frac{3}{2}\right)} + \gamma_{16}\mathrm{y_i''} + \gamma_{17}\mathrm{y_i}^{\left(\frac{5}{2}\right)} + \gamma_{18}\mathrm{y_i}^{(3)} + \gamma_{19}\mathrm{y_i}^{\left(\frac{7}{2}\right)} + \gamma_{20}\mathrm{y_i}^{(4)}(\alpha_1).
\end{aligned} \tag{4.1}$$

Where, $\gamma_0 = \frac{\sqrt{\pi}(\sin(\tau \mathrm{h})-\tau \mathrm{h})}{2\tau\sqrt{\mathrm{h}}(\cos(\tau \mathrm{h})-1)}$, $\gamma_1 = \frac{(\sqrt{\varepsilon \mathrm{h}}-1)(\tau\sqrt{\mathrm{h}(\cos(\tau \mathrm{h})-1)}) - \sqrt{\varepsilon \mathrm{h}}(\sin(\tau \mathrm{h})-\tau \mathrm{h})}{\tau\sqrt{\mathrm{h}}(\cos(\tau \mathrm{h})-1)}$,
$\gamma_2 = \frac{\sqrt{\pi}\varepsilon h^{\frac{3}{2}}\tau(\cos(\tau h)-1) + \sqrt{\pi}\sin(\tau h) - \sqrt{h}\varepsilon(\sin(\tau h)-\tau h) - \sqrt{\pi}\tau\,\mathrm{h}\cos(\tau h)}{2\tau\sqrt{h}(\cos(\tau h)-1)}$,

$\gamma_3 = \frac{3\cdot\sqrt{2}\sqrt{\varepsilon}\sqrt{\tau}+2\sqrt{\pi}\tau\varepsilon^{\frac{3}{2}}h^2(\cos(\tau h)-1)-2\sqrt{\pi}\tau\varepsilon^2h^2(\sin(\tau h)-\tau h)}{3\tau\sqrt{\pi h}(\cos(\tau h)-1)}$,
$\gamma_4 = \frac{\varepsilon(2h)^{\frac{3}{2}}+4\sqrt{\pi}\varepsilon^2h^{\frac{3}{2}}\tau(\cos(\tau h)-1)-\sqrt{\pi}(\varepsilon h)^2(\sin(\tau h)-\tau h)+4\sqrt{\pi}(\cos(\tau h)-1)}{4\tau\sqrt{h}(\cos(\tau h)-1)}$,
$\gamma_5 = \frac{5\sqrt{\tau}(2\varepsilon)^{\frac{3}{2}}h^2+4\sqrt{\pi}\varepsilon^{\frac{5}{2}}h^3\tau-2\sqrt{\pi}(\varepsilon h)^{\frac{3}{2}}(\sin(\tau h)-\tau h)}{15\tau\sqrt{\pi h}(\cos(\tau h)-1)}$, $\gamma_6 = \frac{6\sqrt{\tau}(h)^{\frac{3}{2}}\varepsilon^2+\tau(2)^{\frac{3}{2}}\varepsilon^3h^{\frac{5}{2}}(\cos(\tau h)-1)-\sqrt{2\pi}(\sin(\tau h)-\tau h)}{12\tau\sqrt{2}\,h(\cos(\tau h)-1)}$,
$\gamma_7 = \frac{(2\,h\varepsilon)^{\frac{5}{2}}}{15\sqrt{\pi\tau}(\cos(\tau h)-1)}$, $\gamma_8 = \frac{(\varepsilon h)^3}{6\tau\sqrt{2\tau}(\cos(\tau h)-1)}$, $\gamma_9 = \frac{\sqrt{2\tau\varepsilon h}}{\sqrt{\pi}(\cos(\tau h)-1)}$, $\gamma_{10} = \frac{\tau\varepsilon h-\sin(\tau h)+\sqrt{\tau}(\cos(\tau h)-1)}{\sqrt{\tau}(\cos(\tau h)-1)}$,
$\gamma_{11} = \frac{4\sqrt{\tau}(\varepsilon h)^{\frac{3}{2}}}{3\sqrt{\pi}(\cos(\tau h)-1)}$, $\gamma_{12} = \frac{\sqrt{\tau}(\varepsilon h)^2}{2(\cos(\tau h)-1)}$, $\gamma_{13} = \frac{8\sqrt{\tau}(\varepsilon h)^{\frac{5}{2}}}{15\sqrt{\pi}(\cos(\tau h)-1)}$, $\gamma_{14} = \frac{\sqrt{\tau}(\varepsilon h)^3}{6(\cos(\tau h)-1)}$,
$\gamma_{15} = \frac{\tau\sqrt{2\varepsilon\tau h}}{\sqrt{\pi}}$, $\gamma_{16} = \frac{\varepsilon h\tau^2\sqrt{2}+\sqrt{2\tau}\sin(\tau h)-1}{\sqrt{2\tau}}$, $\gamma_{17} = \frac{4(\varepsilon\tau h)^{\frac{3}{2}}}{3\sqrt{\pi}}$, $\gamma_{18} = \frac{4(\varepsilon h)^2(\tau)^{\frac{3}{2}}}{2}$, $\gamma_{19} = \frac{8(\varepsilon h)^{\frac{5}{2}}(\tau)^{\frac{3}{2}}}{15\sqrt{\pi}}$
and $\gamma_{20} = \frac{(\varepsilon h)^3(\tau)^{\frac{3}{2}}}{6}$.
Now, let $e(t) = S(t) - y(t)$*, then for* $0 \le t \le 1$,

$$e\,(t_i + \varepsilon h) = e\,(t_i) + \frac{2}{\sqrt{\pi}}\varepsilon^{\frac{1}{2}}h^{\frac{1}{2}}y_i^{\left(\frac{1}{2}\right)} + \varepsilon h y_i^{(1)} + \frac{4}{3\sqrt{\pi}}\varepsilon^{\frac{3}{2}}h^{\frac{3}{2}}y_i^{\left(\frac{3}{2}\right)} + \frac{1}{2!}\varepsilon^2h^2y_i^{(2)} + \frac{8}{15\sqrt{\pi}}\varepsilon^{\frac{5}{2}}h^{\frac{5}{2}}y_i^{\left(\frac{5}{2}\right)} + \frac{1}{3!}\varepsilon^3h^3y_i^{(3)} + \frac{16}{105\sqrt{\pi}}\varepsilon^{\frac{7}{2}}h^{\frac{7}{2}}y_i^{\left(\frac{7}{2}\right)}\left(\alpha_j\right). \tag{4.2}$$

For $0 \le \varepsilon \le 1$ *Putting Eq. (4.1) in Eq. (4.2), we get:*
$\|e\,(x_i + \varepsilon h)\| \le \frac{\sqrt{\tau}(\varepsilon h)^3}{6}y_i^{(4)}\,(\alpha_1)$.

Lemma 4.3. *The matrix* $[I - A_1 - L^{-1}L_1A_2 + L^{-1}L_2L_3A_2 + A_3L_3]$ *is invertible, if* $\varphi\|k\|_\infty(b-a)\left(\frac{2}{3} - \frac{2\sqrt{h}}{3} + \sigma_1\sigma_2\sigma_3\tau^{\frac{3}{2}}\frac{h}{2} - \tau\sigma_3\sigma_4\right) < 1$.
Proof:
Clearly, for $j = 0, 1, \ldots, n$*, then:*

$$\begin{aligned}
&\|A\|_\infty = \|B\|_\infty \le \|k\|_\infty(b-a)\frac{2h^{\frac{1}{2}}}{3},\\
&\|C\|_\infty = \|D\|_\infty \le \|k\|_\infty(b-a)\frac{h}{2},\\
&\|Q\|_\infty = \|R\|_\infty \le \|k\|_\infty(b-a)|\sin(\tau h)|,\\
&\|G\|_\infty \le \|k\|_\infty(b-a),\\
&\|P\|_\infty \le \|k\|_\infty(b-a)\frac{1}{\tau}|\cos(\tau h)|,\\
&\|L_1\|_\infty \le \sigma_1\frac{|\cos(\tau h)|}{\sqrt{\tau\pi}},\\
&\|L_2\|_\infty \le \sigma_2\tau^{\frac{3}{2}},\\
&\|A_1\|_\infty \le \|k\|_\infty(b-a)\frac{2(1-\sqrt{h})}{3},\\
&\|A_2\|_\infty \le \|k\|_\infty(b-a)\frac{h}{2},\\
&\|A_3\|_\infty \le \|k\|_\infty(b-a)\tau\sigma_4.
\end{aligned} \tag{4.3}$$

Where

$$\sigma_4 = \frac{2(2\cos(\tau h) - 2 + \tau\sin(\tau h))}{3\tau^2(\cos(\tau h) - 1)} + \frac{h\sin(\tau h)}{2(\cos(\tau h) - 1)} + \frac{\sin(\tau h)^2}{\tau(\cos(\tau h) - 1)} + \frac{cos(\tau h - 1)}{\tau^3}.$$

From Eq. (3.4) of matrix representation we get:

$$\left(\|A_1\| + \left\|L^{-1}\right\| \|L_2\| \|L_3\| \|A_2\| - \|A_3\| \|L_3\|\right) < 1,$$

Then we use lemma (4.1), the matrix $\left[\mathrm{I} - \mathrm{A}_1 - \mathrm{L}^{-1}\ \mathrm{L}_1\ \mathrm{A}_2 + \mathrm{L}^{-1}\ \mathrm{L}_2\ \mathrm{L}_3\ \mathrm{A}_2 + \mathrm{A}_3\ \mathrm{L}_3\right]$ *, is invertible, if* $\left\|A_1 + L^{-1}L_1A_2 - L^{-1}L_2L_3A_2 - A_3L_3\right\|_\infty < 1$, *we get:*

$$\varphi\|k\|_\infty(b-a)\left(\frac{2}{3} - \frac{2\sqrt{h}}{3} + \sigma_1\sigma_2\sigma_3\tau^{\frac{3}{2}}\frac{h}{2} - \tau\sigma_3\sigma_4\right) < 1.$$

Theorem 4.4. *[10]. Let* $y(t) \in C^5(I), k(t,x) \in C^5(I \times I)$ *such that*

$$\varphi\|k\|_\infty(b-a)\left(\frac{2}{3} - \frac{2\sqrt{h}}{3} + \sigma_1\sigma_2\sigma_3\tau^{\frac{3}{2}}\frac{h}{2} - \tau\sigma_3\sigma_4\right) < 1.$$

As a result, consider single numerical solutions and the error obtained. $E = y - \hat{S}$ *satisfies* $\|E\| \equiv O(h^3), \quad \forall\Omega \subset I$ *Where* $\tau, \theta, h, \sigma_1, \cdots, \sigma_4$, *and* σ_5 *are constants, and* $I := [a, b]$.

Proof:

We use Eq. (3.4) and lemma (4.1) we get

$$\|E\| \leq \frac{\|T\|}{1 - (\|A_1\| + \|L^{-1}\| \|L_2\| \|L_3\| \|A_2\| - \|A_3\| \|L_3\|)}, \tag{4.4}$$

By substituting $\|T\| \leq \omega h^3$ *and Eq. (4.3) in Eq. (4.4) we get:* $\|E\| \equiv O\left(h^3\right)$,

Therefore, we have

$$\|y - \hat{S}\|_\infty \leq \varphi_1 h^3, \tag{4.5}$$

And applying Eq. (3.6) and Eq. (4.5), $\|y - \hat{S}\|_\infty \leq \|y - S\|_\infty + \|S - \hat{S}\|_\infty \leq \varphi_1 h^3 + \varphi \mathrm{h}^5 \equiv \mathrm{O}(\mathrm{h}^3)$

Thus, it is as follows: $\|E\| \to 0$ *as* $h \to 0$, *then we explained the convergence of the third order proposed method.*

See [10].

5 Results and Discussion

The proposed technique is applied to some FIE (Fredholm-integral equations) test problems in this section, with a comparison of the presented method and the exact solution to illustrate the suggested technique's correctness and effectiveness, as well as to compare it with some other existing methods for solving three integral equations test problems. We calculate the results for x = 0, 0.2, 0.4, 0.6, 0.8, 1, and n = 10, 40. Python software handles all of the calculations. The absolute error $||E||$ in theorem 4.4 is applied to compute the efficiency of the proposed technique.

Example 5.1. [5] Consider the FIE:

$$g(x) = f(x) + \int_0^1 k(x,t)g(t)dt, x \in [0,1].$$

Where $k(x,t) = \frac{1}{12}\frac{tx-1}{1+x^2}$, and $f(x)$ is chosen so that the exact solution of this equation $g(x) = sin(x) + 1$. Presented the exact and approximation solutions in Table 5.1. and Figure 5.1. and the absolute errors of the proposed method and NSI method in [5] in Table 5.2.

x	Exact solutions	Proposed method
0	1.0	0.9998809889969068
0.2	1.0998334166468282	1.0997366950959002
0.4	1.1986693307950613	1.198566011640177
0.6	1.2955202066613396	1.295421184579774
0.8	1.3894183423086506	1.3893240990734304
1	1.479425538604203	1.4793383323910736

Table 5.1: Difference between exact and approximation solutions with h=0.1, and $\tau = 10^6$.

x	Best in [5] of NSI with n=20	Presented method with n=10
0	0.46×10^{-3}	1.19×10^{-4}
0.2	0.61×10^{-3}	9.67×10^{-5}
0.4	0.68×10^{-3}	1.03×10^{-4}
0.6	0.66×10^{-3}	9.90×10^{-5}
0.8	0.60×10^{-3}	9.42×10^{-5}
1	0.51×10^{-3}	8.72×10^{-5}

Table 5.2: Absolute errors E(n) for different points.

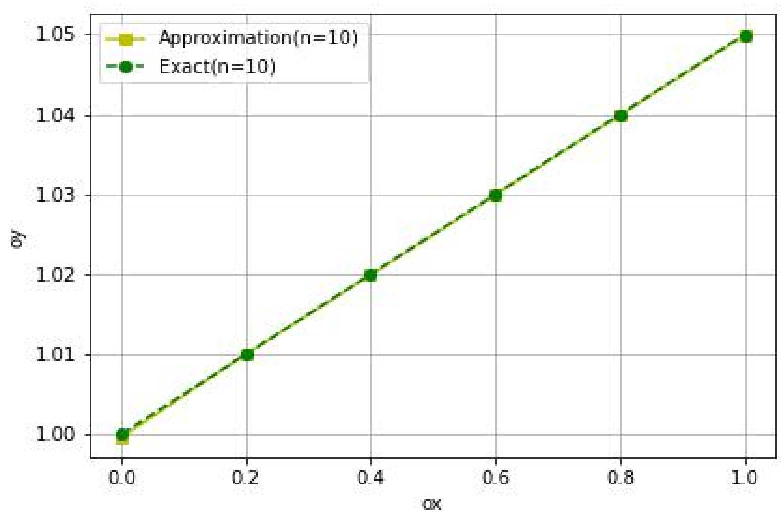

Figure 5.1: Comparison between the exact solution and approximate solution using the proposed method.

Example 5.2. [21] Consider the FIE:

$$g(x) = f(x) + \int_0^1 k(x,t)g(t)dt, x \in [0,1].$$

Where $k(x,t) = \frac{t^4}{24}x, f(x) = e^x - \frac{x^4}{24}$ and $g(x) = e^x$, is the exact solution. Presented the absolute errors of solutions in Table 5.3. and Figure 5.2.

$n=10$ and $\tau=10^5$			$n=40$ and $\tau=10^6$			$n=10^6$ and $\tau=10^{10}$		
$g(x_i)$	$S(x_i)$	$\lvert E(x_i)\rvert$	$g(x_i)$	$S(x_i)$	$\lvert E(x_i)\rvert$	$g(x_i)$	$S(x_i)$	$\lvert E(x_i)\rvert$
1.0	1.0	0.0	1.0	1.0	0.0	1.0	1.0	0.0
1.10517	1.10525	8.5×10^{-5}	1.025315	1.025312	2.1×10^{-6}	1.000001	1.000001	0.0
1.22140	1.22050	8.9×10^{-4}	1.051271	1.051262	8.2×10^{-6}	1.000002	1.000002	0.0
1.34985	1.34929	5.6×10^{-4}	1.077884	1.077849	3.4×10^{-5}	1.000003	1.000003	0.0
1.49182	1.48824	3.5×10^{-3}	1.105170	1.105097	7.3×10^{-5}	1.000004	1.000004	0.0
1.64872	1.64836	3.5×10^{-4}	1.133148	1.133007	1.4×10^{-4}	1.000005	1.000005	0.0

Table 5.3: Absolute error E(n) for different points.

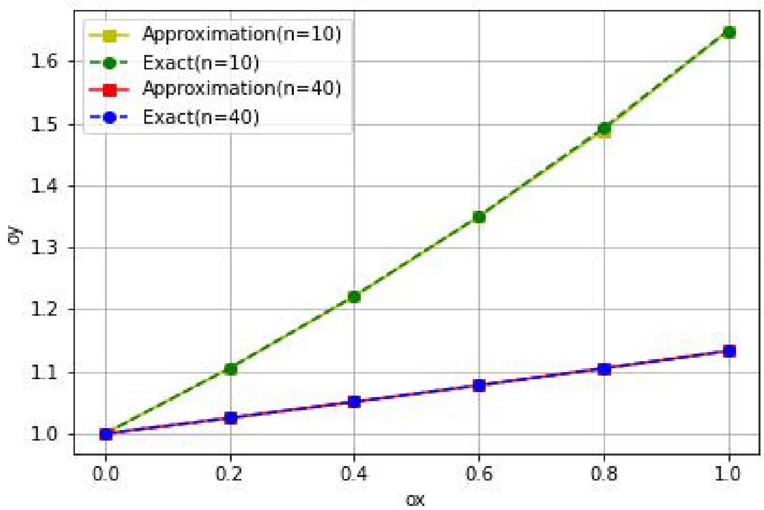

Figure 5.2: Comparison between the exact solution and approximate solution using the proposed method.

Example 5.3. [21] consider the FIE:

$$g(x) = f(x) + \int_{-1}^{1} k(x,t)g(t)dt, x \in [0,1],$$

where, $k(x,t) = \frac{x^4}{24}$, $f(x) = e^{-x} - \frac{x^2}{2} + \frac{x^3 e^{-1}}{6}$ and $g(x) = e^{-x} - \frac{x^2}{2}$ is the exact solution.
Presented the absolute errors of solutions in Table 5.4 and Figure 5.3.

Example 5.4. [21] consider the IDE:

$$g(x) = f(x) + \int_{0}^{1} k(x,t)g(t)dt, x \in [0,1].$$

where, $k(x,t) = (\frac{x^4}{24} - \frac{tx^3}{6}), f(x) = xe^x + 1 - \frac{x^4}{24} + \frac{x^3(e-2)}{6}$ and $g(x) = xe^x + 1$ is the exact solution.
Presented the absolute errors of solutions in Table 5.5 and Figure 5.4.

$n=10$ and $\tau=0.1$			$n=40$ and $\tau=0.1$			$n=10^6$ and $\tau=0.1$		
$g(x_i)$	$S(x_i)$	$\|E(x_i)\|$	$g(x_i)$	$S(x_i)$	$\|E(x_i)\|$	$g(x_i)$	$S(x_i)$	$\|E(x_i)\|$
1.0	1.0	0.0	1.0	1.0	0.0	1.0	1.0	0.0
0.89983	0.89989	6.04×10^{-5}	0.974997	0.974998	9.57×10^{-7}	0.99	0.99	0.0
0.79873	0.79919	4.6×10^{-4}	0.949979	0.949987	7.64×10^{-6}	0.99	0.99	0.0
0.69581	0.69730	1.48×10^{-3}	0.924930	0.924956	2.56×10^{-5}	0.99	0.99	0.0
0.59032	0.59351	3.19×10^{-3}	0.899837	0.899897	6.04×10^{-5}	0.99	0.99	4.5×10^{-25}
0.48153	0.48714	5.61×10^{-3}	0.874684	0.874801	1.17×10^{-4}	0.99	0.99	7.2×10^{-25}

Table 5.4: Absolute error E(n) for different points.

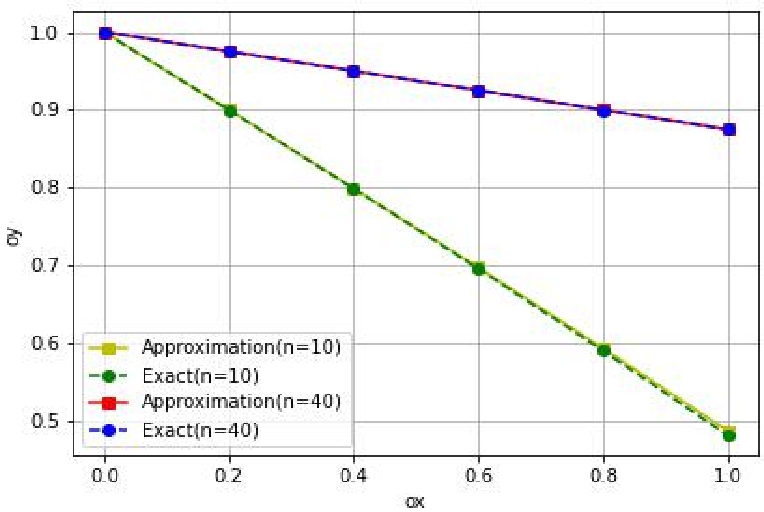

Figure 5.3: Comparison between the exact solution and approximate solution using the proposed method.

6 Conclusion

This paper presents a new general form of non-polynomial fractional spline function to approximate the Fredholm-integral equation of the second kind, and the proposed approach is innovative. The current scheme was developed by running four different examples through the Python program. The results were compared to the exact solution and show that the proposed technique is better than the method in [5]. The physical behavior of approximation and exact solutions can be evaluated in 2D for various points, and it is clear that adding step sizes ensures no error.

Acknowledgements

The author thanks the reviewers and the editor for their helpful comments and careful corrections.

$n = 10$ and $\tau = 10^4$			$n = 40$ and $\tau = 10^4$			$n = 10^6$ and $\tau = 10^9$		
$g(x_i)$	$S(x_i)$	$\lvert E(x_i)\rvert$	$g(x_i)$	$S(x_i)$	$\lvert E(x_i)\rvert$	$g(x_i)$	$S(x_i)$	$\lvert E(x_i)\rvert$
1.0	1.0	0.0	1.0	1.0	0.0	1.0	1.0	0.0
1.11051	1.11074	2.2×10^{-4}	1.025632	1.025637	4.9×10^{-6}	1.000001	1.000001	0.0
1.24428	1.24422	5.9×10^{-5}	1.052563	1.052553	9.9×10^{-6}	1.000002	1.000002	0.0
1.40495	1.40532	3.6×10^{-4}	1.080841	1.080870	2.8×10^{-5}	1.000003	1.000003	0.0
1.59672	1.59583	8.9×10^{-4}	1.110517	1.110525	8.8×10^{-6}	1.000004	1.000004	0.0
1.82436	1.82086	3.4×10^{-3}	1.141643	1.141698	5.4×10^{-5}	1.000005	1.000005	0.0

Table 5.5: Absolute error E(n) for different points.

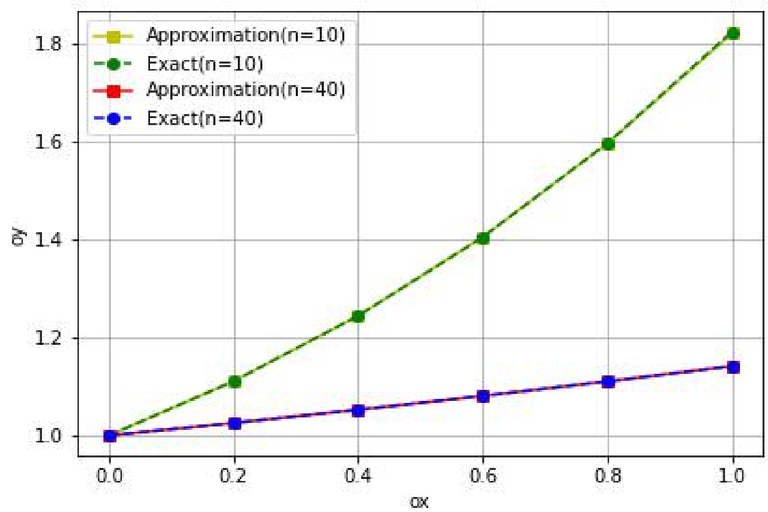

Figure 5.4: Comparison between the exact solution and approximate solution using the proposed method.

Conflict of interest

The authors have no conflicts of interest to declare.

References

[1] K. K. Ali, K. R. Raslan and T. S. El-Danaf, *Non-polynomial spline method for solving coupled Burgers equations*, Comput. methods differ. equ., **3**(3) (2015), 218-230.

[2] M. Al-Refai and T. Abdeljawad, *Fundamental results of conformable Sturm-Liouville eigenvalue problems*, J. Complex. **2017** (2017), 3720471. DOI

[3] M. Amin, M. Abbas, M. K. Iqbal and D. Baleanu, *Non-polynomial quintic spline for numerical solution of fourth-order time fractional partial differential equations*, Adv. Difference Equ., **2019** (2019), 1-22. DOI

[4] S. Amiri, M. Hajipour and D. Baleanu, *A spectral collocation method with piecewise trigonometric basis functions for nonlinear Volterra-Fredholm integral equations*, Appl. Math. Comput., **370** (2020), 124915. DOI

[5] A. Bellour, D. Sbibih and A. Zidna, *Two cubic spline methods for solving Fredholm integral equations*, Appl. Math. Comput., **276** (2016), 1-11. DOI

[6] D. Baleanu and D. Kumer, *Fractional calculus and its applications in physics*, Frontiers in Physics, Lausanne: Frontiers Media, 2019. DOI

[7] M. Benbachir and A. Boutiara, *Measure of noncompactness for nonlinear Hilfer fractional differential equation with mixed fractional integral boundary conditions in Banach space*, J. innov. appl. math. comput. sci., **2**(1) (2022), 27-42. URL

[8] N. G. Chegini, A. Salaripanah, R. Mokhtari and D. Isvand, *Numerical solution of the regularized long wave equation using nonpolynomial splines*, Nonlinear. Dyn, **69** (2012), 459-471. DOI

[9] M. Dalir and M. Bashour, *Applications of fractional calculus1*, Appl. Math. Sci., **4**(21) (2010), 1021-1032. URL

[10] D. A. Hammad, M. S. Semary and A. G. Khattab, *Ten non-polynomial cubic splines for some classes of Fredholm integral equations*, Ain Shams Eng. J., **13**(4) (2022), 101666. DOI

[11] F. K. Hamasalh and M. A. Headayat, *The applications of non-polynomial spline to the numerical solution for fractional differential equations*, AIP Conference Proceedings., 2334(1) AIP Publishing, 2021. DOI

[12] F. K. Hamasalh and P. O. Muhammed, *Computational Method for Fractional Differential Equations Using Nonpolynomial Fractional Spline*, Math. Sci. Lett., **5**(2) (2016), 131-136. DOI

[13] N. N. Hasan and M. R. Nasif, *Cubic trigonometric spline for solving nonlinear volterra integral equations*, Iraqi J. Sci., **60**(12) (2019), 2697-2705. DOI

[14] R.T. Hernandez, V. R. Ramirez, G. A. I. Silve and U. M. Diwekar, *A fractional calculus approach to the dynamic optimization of biological reactive systems. Part I: Fractional models for biological reactions*, Chem. Eng. Sci., **117** (2014), 217-228. DOI

[15] C. Ionescua, A. Lopesb, D. Copota, J. A. T. Machadoc and J. H. T. Batesa, *The role of fractional calculus in modeling biological phenomena: A review*, Commun. Nonlinear Sci. Numer. Simul., **51** (2017), 141-159. DOI

[16] A. Khalid, A. Ghaffar, M. N. Naeem, K. S. Nisar and D. Baleanu, *Solutions of BVPs arising in hydrodynamic and magnetohydro-dynamic stability theory using polynomial and non-polynomial splines*, Alex. Eng. J., **60**(1) (2021), 941-953. DOI

[17] R. Khalila, M. Al Horania, A. Yousefa and M. Sababheh, *A new definition of fractional derivative*, J. Comput. Appl. Math., 264 (2014), 65-70. DOI

[18] A. Kurt, Y. Çenesiz and O. Tasbozan, *On the solution of Burgers equation with the new fractional derivative*, Open Physics, **13**(1) (2015), 355-360. DOI

[19] Z. Laadjal, T. Abdeljawad and F. Jarad, *Sharp estimates of the unique solution for two-point fractional boundary value problems with conformable derivative*, Numer. Methods Partial Differ. Equ. (2021). DOI

[20] A. Pal Singh, D. Deb, H. Agrawal, K. Bingi and S. Ozana, *Modeling and control of robotic manipulators: A fractional calculus point of view*, Arab J Sci Eng., **46**(10) (2021), 9541-9552. DOI

[21] R. J. Qadir and F. Hamasalh, *Fractional Spline Model for Computing Fredholm Integral Equations*, 2022 International Conference on Computer Science and Software Engineering (CSASE). IEEE, 2022. URL

[22] K. Maleknejad, J. Rashidinia and H. Jalilian, *Quintic Spline functions and Fredholm integral equation*, Numer. Methods Partial Differ. Equ., **9**(1) (2021), 211-224.

[23] K. Maleknejad, J. Rashidinia and H. Jalilian, *Non-polynomial spline functions and Quasi-linearization to approximate nonlinear Volterra integral equation*, Filomat **32**(11) (2018), 3947-3956. DOI

[24] C. Milici, G. Draganescu and J. T. Machado, *Introduction to fractional differential equations*, Springer International Publishing, 2018. URL

[25] M. Mutaz and A. Trounev, *Fractional nonlinear Volterra-Fredholm integral equations involving Atangana-Baleanu fractional derivative: framelet applications*, Adv. Difference Equ., **2020** (2020), 1-15. DOI

[26] J. Rashidinia, K. Maleknejad and H. Jalilian, *Convergence analysis of non-polynomial spline functions for the Fredholm integral equation*, Int. J. Comput. Math., **97**(6) (2020), 1197-1211. DOI

[27] S. S. Ray and P. K. Sahu, *Numerical methods for solving Fredholm integral equations of second kind*, Abstr. Appl. Anal., 2013 (2013),1-17. DOI

[28] J. Sabatier, O. P. Agrawal and J. A. T. Machado, *Advances in fractional calculus*, Springer Dordrecht, 2007. DOI

[29] B. Safa, M. S. Abdelouahab and R. Lozi, *On periodic solutions of fractional-order differential systems with a fixed length of sliding memory*, J. innov. appl. math. comput. sci., **1**(1) (2021), 64-78. URL

[30] P. K. Srivastava, *Study of differential equations with their polynomial and nonpolynomial spline based approximation*, Acta Technica Corviniensis-Bulletin of Engineering, **7**(3) (2014),1-12. URL

[31] H. G. Sun, Y. Zhang, D. Baleanu, W. Chen and Y.Q. Chen, *A new collection of real world applications of fractional calculus in science and engineering*, Commun. Nonlinear Sci. Numer. Simul., *64* (2018), 213-231. DOI

[32] T. Tahernezhad and R. Jalilian, *Exponential spline for the numerical solutions of linear Fredholm integro-differential equations*, Adv. Difference Equ., **2020** (2020), 1-15. DOI

[33] A. M. Wazwaz, *Linear and nonlinear integral equations*, Springer Berlin, Heidelberg, 2011. DOI

Journal of Innovative Applied Mathematics and Computational Sciences

J. Innov. Appl. Math. Comput. Sci. **2**(3) (2022), 15–28. n2t.net/ark:/49935/jiamcs.v2i3.46

http://jiamcs.centre-univ-mila.dz/

An approximate solution for the time-fractional diffusion equation

Sayed Ali Ahmad Mosavi

Baghlan University, Pol-e-khomri city, Afghanistan.

Received 18 June 2022, Accepted 22 November 2022, Published 15 December 2022

Abstract. In this paper, a numerical method based on a finite difference scheme is proposed for solving the time-fractional diffusion equation (TFDE). The TFDE is obtained from the standard diffusion equation by replacing the first-order time derivative with Caputo fractional derivative. At first, we introduce a time discrete scheme. Then, we prove the proposed method is unconditionally stable and the approximate solution converges to the exact solution with order $O(\Delta t^{2-\alpha})$, where Δt is the time step size and α is the order of Caputo derivative. Finally, some examples are presented to verify the order of convergence and show the application of the present method.

Keywords: Time-fractional diffusion equation, Caputo derivative, Convergence rates, Stability.

2020 Mathematics Subject Classification: 65Mxx, 65Nxx, 65Axx. MSC2020

1 Introduction

In recent years, the use of fractional ordinary differential equations (FODEs) and fractional partial differential equations (FPDEs) in finance problems [10, 21, 22], hydrology problems [1,3–5,26], physics problems [2,6–8,12,18–20,23,24,29], and mathematical models have become increasingly popular. The numerical and the analytical solutions of the time-fractional partial differential equations are studied using Fourier-Laplace transforms or Green's functions (see e.g. [9, 16, 25, 27, 28]). However, published papers on the numerical solution of the time-fractional diffusion equation (TFDE) are limited. The authors of [11] have proposed finite element methods for time-fractional partial differential equations; the authors of [17] have used a meshless method for the(TFDE); Liu et al. [15] used an explicit finite-difference scheme for TFDE (this method is a lowe-order method); Lin and Xu et al. [14] have proposed finite difference/spectral methods for TFDE, they used Legendre spectral methods in space and a finite difference scheme in time and show that the methods for α order TFDE have convergence rate $O(\Delta t^{2-\alpha} + N^{-m}/(\Delta t)^{\alpha})$, where Δt, N and m are the time step size, polynomial degree and the regularity of the exact solution respectively. The convergence rate in their paper is not optimal.

Email: aliahmadmosavi1370@gmail.com

ISSN (electronic): 2773-4196

In this paper, we propose a numerical scheme based on the finite difference method for solving time-fractional diffusion equation and prove an optimal convergence rate. We consider the time-fractional diffusion equation of the form:

$$\frac{\partial^\alpha u(x,t)}{\partial t^\alpha} - \frac{\partial^2 u(x,t)}{\partial x^2} = f(x,t), \qquad (x,t) \in [0,1] \times [0,T], \tag{1.1}$$

subject to the boundary and initial conditions:

$$u(0,t) = u(1,t) = 0, \qquad t \in (0,T], \tag{1.2}$$

$$u(x,0) = u_0(x), \qquad x \in [0,1], \tag{1.3}$$

where $0 < \alpha < 1$, u_0 and f are given smooth functions, the time-fractional derivative $\frac{\partial^\alpha u(x,t)}{\partial t^\alpha}$ is the Caputo derivative defined by

$$\frac{\partial^\alpha u(x,t)}{\partial t^\alpha} = \frac{1}{\Gamma(1-\alpha)} \int_0^t \frac{\partial u(x,s)}{\partial s} \frac{ds}{(t-s)^\alpha}. \tag{1.4}$$

2 The numerical method for the TFDE

In this section, we will estimate the time-fractional derivative $\frac{\partial^\alpha u}{\partial t^\alpha}$ at t_{m+1} by forward finite difference approximation to discretize the time-fractional derivative. Let $t_m := m\Delta t$, $m = 0, 1, ..., M$, where $\Delta t := T/M$ is the time step and M is a positive integer.

$$\begin{aligned}\frac{\partial^\alpha (x, t_{m+1})}{\partial t^\alpha} &= \frac{1}{\Gamma(1-\alpha)} \int_{t_0}^{t_{m+1}} \frac{\partial u(x,s)}{\partial s} \frac{ds}{(t_{m+1}-s)^\alpha} \\ &= \frac{1}{\Gamma(1-\alpha)} = \sum_{k=0}^{m} \int_{t_k}^{t_{k+1}} \frac{\partial u(x,s)}{\partial s} \frac{ds}{(t_{m+1}-s)^\alpha}.\end{aligned} \tag{2.1}$$

For the forward finite difference, we have

$$\frac{\partial u(x,s)}{\partial t} \mid_{(x,t_k)} = \frac{u(x,t_{k+1}) - u(x,t_k)}{\Delta t} + O(\Delta t), \tag{2.2}$$

Substituting (2.2) into (2.1), we obtain

$$\begin{aligned}\frac{\partial^\alpha (x, t_{m+1})}{\partial t^\alpha} &= \frac{1}{\Gamma(1-\alpha)} \sum_{k=0}^{m} \int_{t_k}^{t_{k+1}} \frac{\partial u(x,t_{k+1}) - u(x,t_k)}{\Delta t} \frac{ds}{(t_{m+1}-s)^\alpha} + R_{\Delta t}^{k+1} \\ &= \frac{1}{\Gamma(1-\alpha)} \sum_{k=0}^{m} \frac{\partial u(x,t_{k+1}) - u(x,t_k)}{\Delta t} \int_{t_k}^{t_{k+1}} \frac{ds}{(t_{m+1}-s)^\alpha} + R_{\Delta t}^{k+1},\end{aligned} \tag{2.3}$$

where $R_{\Delta t}^{k+1}$ is the truncation error, which we will get it later in proposition 2.1, for the integral at the RHS of (2.3), we have

$$\begin{aligned}\int_{t_k}^{t_{k+1}} \frac{ds}{(t_{m+1}-s)^\alpha} &= -\int_{t_{m+1}-t_k}^{t_{m+1}-t_k} p^{-\alpha} dp \\ &= \frac{(t_{m+1}-t_k)^\alpha - (t_{m+1}-t_{k+1})^{1-\alpha}}{1-\alpha}.\end{aligned} \tag{2.4}$$

By using $t_m = m\Delta t$, we have

$$t_{m+1} - t_{k+1} = (m-k)\Delta t, \qquad t_{m+1} - t_k = (m+1-k)\Delta t, \tag{2.5}$$

Substituting (2.5) into (2.4), we obtain

$$\int_{t_k}^{t_{k+1}} \frac{ds}{(t_{m+1}-s)^{\alpha}} = \frac{((m+1-k)\Delta t^{1-\alpha}) - ((m-k)\Delta t^{1-\alpha})}{1-\alpha}$$
$$= \frac{\Delta t^{1-\alpha}}{1-\alpha}((m+1-k)^{1-\alpha} - (m-k)^{1-\alpha}, \tag{2.6}$$

substituting (2.6) into (2.3), we obtain

$$\frac{\partial^{\alpha} u(x,t_{m+1})}{\partial t^{\alpha}} = \frac{\Delta^{-\alpha}(t)}{(1-\alpha)(\Gamma(1-\alpha)} \sum_{k=0}^{m} a_{m-k}(u(x,t_{k+1}) - u(x,t_k)) + R_{\Delta t}^{k+1}$$
$$= \frac{\Delta^{-\alpha}(t)}{\Gamma(2-\alpha)} \sum_{k=0}^{m} a_{m-k}(u(x,t_{k+1}) - u(x,t_k)) + R_{\Delta t}^{k+1}. \tag{2.7}$$

Here $a_k := (k+1)^{1-\alpha} - k^{1-\alpha}, k = 0,1,...,M$. Let $\gamma = \Gamma(2-\alpha)\Delta t^{\alpha}$. Substituting (2.7) into (1.1), the following form is obtained

$$u(x,t_{m+1}) - \gamma\left(\frac{\partial^2 u(x,t_{m+1})}{\partial x^2}\right)$$
$$= u(x,t_m) - \sum_{k=1}^{m} a_k(u(x,t_{m-k+1} - u(x,t_{m-k})) + \gamma f(x,t_{m+1}) + R_{\Delta t}^{(1)}, \tag{2.8}$$

where

$$R_{\Delta t}^{(1)} \le C_0 \Delta t^2,$$

and C_0 is a constant.

Let u^m be the numerical solution to $u(x,t_m)$ and $f^{m+1} = f(x,t_{m+1})$, by removing the small term $R_{\Delta t}^{(1)}$ from (2.8), we can create the following discrete scheme for solving 1.1.

$$u^{m+1} - \gamma\left(\frac{\partial^2 u^{m+1}}{\partial x^2}\right) = u^m - \sum_{k=1}^{m} a_k(u^{m-k+1} - u^{m-k}) + \gamma f^{m+1}, m = 0,1,...,M. \tag{2.9}$$

Proposition 2.1. *The truncation error $R_{\Delta t}^{k+1}$ has the following form*

$$R_{\Delta t}^{k+1} \le C_1 \left| \frac{1}{\Gamma(1-\alpha)} \sum_{k=0}^{m} \int_{t_k}^{t_{k+1}} \frac{2s - t_{k+1} - t_k}{(t_{m+1}-s)^{\alpha}} ds + O(\Delta t^2) \right| \le C_2 \Delta t^{2-\alpha}, \tag{2.10}$$

Where C_1 and C_2 are constant.

proof: First we show that

$$R_{\Delta t}^{k+1} \le C_1 \left| \frac{1}{\Gamma(1-\alpha)} \sum_{k=0}^{m} \int_{t_k}^{t_{k+1}} \frac{2s - t_{k+1} - t_k}{(t_{m+1}-s)^{\alpha}} ds + O(\Delta t^2) \right|.$$

By using the Taylor series, we have

$$\frac{u(x,t_{k+1}) - u(x,t_k)}{\Delta t} = \frac{\partial u(x,t_k)}{\partial t} + \frac{\Delta t}{2} \frac{\partial^2 u(x,t_k)}{\partial t^2} + O(\Delta t^2),$$

In addition, from (2.3), the truncation error has the following form

$$R_{\Delta t}^{k+1} = \frac{1}{\Gamma(1-\alpha)} \int_{t_k}^{t_{k+1}} \left(\frac{\partial u(x,s)}{s} - \frac{\partial u(x,t_k)}{\partial t} - \frac{\Delta t}{2}\frac{\partial^2 u(x,t_k)}{\partial t^2} + O(\Delta t)\right)\left(\frac{ds}{(t_{m+1}-s)^{\alpha}}\right), \tag{2.11}$$

Now we write the Taylor expansion of $\frac{\partial u(x,s)}{\partial s}$ at t_k

$$\frac{\partial u(x,s)}{\partial s} = \frac{\partial u(x,t_k)}{\partial t} + (s-t_k)\frac{\partial^2 u(x,t_k)}{\partial t^2} + O((s-t_k)^2), \tag{2.12}$$

Substituting (2.12) into (2.11), we obtain

$$\begin{aligned} R_{\Delta t}^{k+1} &= \frac{1}{\Gamma(1-\alpha)}\sum_{k=0}^{m}\int_{t_k}^{t_{k+1}}\left((s-t_k-\frac{\Delta t}{2})\frac{\partial^2 u(x,t_k)}{\partial t^2} + O(\Delta t^2)\right)\left(\frac{ds}{(t_{m+1}-s)^\alpha}\right) \\ &= \frac{1}{\Gamma(1-\alpha)}\sum_{k=0}^{m}\int_{t_k}^{t_{k+1}}\left(\frac{2s-t_{k+1}-t_k}{2}\frac{\partial^2 u(x,t_k)}{\partial t^2} + O(\Delta t^2)\right)\left(\frac{ds}{(t_{m+1}-s)^\alpha}\right), \end{aligned}$$

the absolute value of the truncation error is as follows

$$R_{\Delta t}^{k+1} \le C_1\left|\frac{1}{\Gamma(1-\alpha)}\sum_{k=0}^{m}\int_{t_k}^{t_{k+1}}\frac{2s-t_{k+1}-t_k}{2}\frac{\partial^2 u(x,t_k)}{\partial t^2}ds + O(\Delta t^2)\right|,$$

where $C_1 \le \frac{1}{2}\left|\frac{\partial^2 u(x,t_k)}{\partial t^2}\right|$.

Now, we show that

$$\left|\frac{1}{\Gamma(1-\alpha)}\sum_{k=0}^{m}\int_{t_k}^{t_{k+1}}\frac{2s-t_{k+1}-t_k}{2}\frac{\partial^2 u(x,t_k)}{\partial t^2}ds + O(\Delta t^2)\right| \le C_2(\Delta t^{2-\alpha}).$$

We have

$$\begin{aligned} &\frac{1}{\Gamma(1-\alpha)}\sum_{k=0}^{m}\int_{t_k}^{t_{k+1}}\frac{2s-t_{k+1}-t_k}{2}\frac{\partial^2 u(x,t_k)}{\partial t^2}ds + O(\Delta t^2) \\ &\quad = -\frac{1}{\Gamma(1-\alpha)}\sum_{k=0}^{m}\frac{1}{\Gamma(1-\alpha)}(2k+1)(\Delta t)^{2-\alpha}\left[(m-k)^{1-\alpha}-(m+1-k)^{1-\alpha}\right] \\ &\qquad + \frac{1}{\Gamma(1-\alpha)}\sum_{k=0}^{m}\frac{2}{(1-\alpha)}(\Delta t)^{2-\alpha}\left[(k+1)(m-k)^{1-\alpha}-k(m+1-k)^{1-\alpha}\right] \\ &\qquad + \frac{1}{\Gamma(1-\alpha)}\sum_{k=0}^{m}\frac{2}{(1-\alpha)(2-\alpha)}(\Delta t)^{2-\alpha}\left[(m-k)^{2-\alpha}-(m+1-k)^{2-\alpha}\right] \\ &\quad = \frac{(\Delta t)^{2-\alpha}}{\Gamma(2-\alpha)}\left[(m+1)^{1-\alpha}+2(m^{1-\alpha}+(m-1)^{1-\alpha}+(m-2)^{1-\alpha}+...+1^{1-\alpha})\right] \\ &\qquad\qquad - \frac{2(\Delta t)^{2-\alpha}}{\Gamma(3-\alpha)}(m+1)^{2-\alpha} \\ &\quad = \frac{(\Delta t)^{2-\alpha}}{\Gamma(2-\alpha)}\left[(m+1)^{1-\alpha}+2(m^{1-\alpha}+(m-1)^{1-\alpha}+(m-2)^{1-\alpha}+...+1^{1-\alpha})-\frac{2}{2-\alpha}(m+1)^{2-\alpha}\right]. \end{aligned}$$

Let

$$p(m) = (m+1)^{1-\alpha}+2(m^{1-\alpha}+(m-1)^{1-\alpha}+(m-2)^{1-\alpha}+...+1^{1-\alpha})-\frac{2}{2-\alpha}(m+1)^{2-\alpha}.$$

We will show that the $|p(m)|$ is bounded for all $\alpha \in [0,1]$ and all $m \ge 1$, as proven in the following lemma.

Lemma 2.2. *for all $\alpha \in [0,1]$ and all $m \ge 1$, we have*

$$|p(m)| \le C_3,$$

where C_3 is a constant independent of α, m.

Proof. First, for $\alpha = 0$ and $m \geq 1$, we will show that $p(m) = 0$.

We have

$$\begin{aligned} p(m) &= (m+1) + 2(m + (m-1) + (m-2) + ... + 1) - (m+1)^2 \\ &= m + 1 + 2\left[\frac{m}{2}(m+1)\right] - (m+1)^2 \\ &= (m+1)^2 - (m+1)^2 = 0. \end{aligned}$$

Now we prove for $\alpha \in (0, 1]$, we can write $p(m)$ as follows

$$p(m) = (m+1)^{1-\alpha} + 2(m^{1-\alpha} + (m-1)^{1-\alpha} + (m-2)^{1-\alpha} + \cdots + 1^{1-\alpha}) - \frac{2}{2-\alpha}(m+1)^{2-\alpha} = \sum_{i=0}^{m} b_i,$$

where

$$b_i = (i+1)^{1-\alpha} + i^{1-\alpha} - \frac{2}{2-\alpha}((i+1)^{2-\alpha} - i^{2-\alpha}).$$

It suffices to prove that the $\sum_{i=0}^{\infty} b_i$ convergent. It is well known that the series $\sum_{i=0}^{\infty} \frac{1}{i^{\beta}}$ is a geometric series and converges for all $\beta > 1$. Now we will show that the $|b_i| \leq \frac{1}{i^{1+\alpha}}$ for big enough i. For $i \geq 2$, we have

$$\begin{aligned} |b_i| =& i^{1-\alpha}\left|\left(1+\frac{1}{i}\right)^{1-\alpha} + 1 - \frac{2i}{2-\alpha}\left(\left(1+\frac{1}{i}\right) - 1\right)\right| \\ =& i^{1-\alpha} \mid 1 + 1 + (1-\alpha)\frac{1}{i} + \frac{(1-\alpha)(-\alpha)}{2!}\frac{1}{i^2} + \frac{(1-\alpha)(\alpha)(-\alpha-1)}{3!}\frac{1}{i^3} + \ldots \\ & - \frac{2i}{2-\alpha}\left(-1 + 1 + (2-\alpha)\frac{1}{i} + \frac{(2-\alpha)(1-\alpha)}{2!}\frac{1}{i^2} + \frac{(2-\alpha)(1-\alpha)(-\alpha)}{3!}\frac{1}{i^3} + \ldots\right) \mid \\ =& i^{1-\alpha}\left|\left(\frac{1}{2!} - \frac{2}{3!}\right)(1-\alpha)(-\alpha)\frac{1}{i^2} + \left(\frac{1}{3!} - \frac{2}{4!}\right)(1-\alpha)(-\alpha)(-\alpha-1)\frac{1}{i^3} + \ldots\right| \\ \leq& i^{1-\alpha}\frac{1}{3!}(1-\alpha)\alpha\frac{1}{i^2}\left(1 + \frac{2(\alpha+1)}{4}\frac{1}{i} + \frac{3(\alpha+1)(\alpha+2)}{20}\frac{1}{i^2} + \ldots\right) \\ \leq& \frac{1}{3!}(1-\alpha)\alpha\frac{1}{i^{1+\alpha}}\left(1 + \frac{1}{i} + \frac{1}{i^2} + \frac{1}{i^3} + \ldots\right) \leq \frac{2}{3!}(1-\alpha)\alpha\frac{1}{i^{1+\alpha}} \leq \frac{1}{i^{1+\alpha}}. \end{aligned}$$

The proof is completed. □

3 Stability of the method

In this section, by using the following lemma, we will prove the proposed method is unconditionally stable, in other words, we will prove the stability of Eq. (2.9).

Lemma 3.1. *[13] Let Ω be a bounded domain in R^n with piecewise smooth boundary $\partial\Omega$, if V and U are two functions defined on the closed region containing Ω and have continuous partial derivatives, then*

$$\int_{\Omega} V\frac{\partial U}{\partial x_i}d\Omega = \int_{\partial\Omega} VUcos(\overrightarrow{n}, x_i)dS - \int_{\Omega} U\frac{\partial V}{\partial x_i}d\Omega, \tag{3.1}$$

Where $\overrightarrow{n}$ is the outward vector, dS stands for the surface area element on $\partial\Omega$.

Lemma 3.2. *The coefficient, a_i, satisfy*

1. $a_i > 0, \quad i = 1, 2, ...$
2. $a_i > a_{i+1}, \quad i = 0, 1, 2, ...$

Proof. Let

$$s(i) := a_i = (i+1)^{1-\alpha} - i^{1-\alpha}, \quad i = 0, 1, 2, ...$$

We have

$$s'(i) = (1-\alpha)[(i+1)^{-\alpha} - i^{-\alpha}] < 0 \Rightarrow a_i > a_{i+1}, \quad i = 0, 1, ...$$

□

Lemma 3.3. *[30] If $u^m \in H_0^1, m = 0, 1, .., M$ is the solution of (2.9), then*

$$||u^m||_2 \le ||u^0||_2 + \gamma a_{m-1}^{-1} \max_{0 \le l \le M} ||f^l||_2.$$

Proof. We will prove this Lemma by mathematical induction. When $m = 0$, by using (2.9), we will have

$$u^1 - \gamma \frac{\partial u^1}{\partial x^2} = u^0 + \gamma f^1.$$

Multiplying the above relation by u^1 and integrating on Ω, we will obtain the following relation

$$(u^1, u^1) - \gamma (\frac{\partial^2 u^1}{\partial x^2}, u^1) = (u^0, u^1) + \gamma (f^1, u^1),$$

i.e.

$$||u^1||_2^2 - \gamma \left(\frac{\partial^2 u^1}{\partial x_1^2}, u^1 \right) = (u^0, u^1) + \gamma (f^1, u^1). \tag{3.2}$$

By using Lemma 3.1, we get

$$(\frac{\partial^2 u^1}{\partial {x_1}^2}, u^1) = \int_\Omega \frac{\partial}{\partial x_1} \left(\frac{\partial u^1}{\partial x_1} \right) u^1 d\Omega = \underbrace{\int_{\partial\Omega} \frac{\partial u^1}{\partial x_1} u^1 ds}_{0} - \int_\Omega \frac{\partial u^1}{\partial x_1} \frac{\partial u^1}{\partial x_1} d\Omega$$

$$= - \int_\Omega \frac{\partial u^1}{\partial x_1} \frac{\partial u^1}{\partial x_1} d\Omega = -(\frac{\partial u^1}{\partial x_1}, \frac{\partial u^1}{\partial x_1}), \tag{3.3}$$

Substituting (3.3) into (3.2), we obtain

$$||u^1||_2^2 + \gamma \left(\frac{\partial^2 u^1}{\partial x_1^2}, \frac{\partial^2 u^1}{\partial x_1^2} \right) = (u^0, u^1) + \gamma (f^1, u^1), \tag{3.4}$$

Since $\gamma > 0$ and $\left(\frac{\partial^2 u^1}{\partial x_1^2}, \frac{\partial^2 u^1}{\partial x_1^2} \right) \ge 0$, we will rewrite the (3.4), as follows

$$||u^1||_2^2 \le (u^0, u^1) + \lambda (f^1, u^1),$$

using Schwarz inequality, we get

$$||u^1||_2 \le ||u^0||_2 + \gamma ||f^1||_2 \le ||u^0||_2 + \gamma a_0^{-1} \max_{0 \le l \le M} ||f^l||_2.$$

Suppose now we have

$$||u^k||_2 \le ||u^0||_2 + \gamma a_{k-1}^{-1} \max_{0 \le l \le M} ||f^l||_2, \quad k = 1, 2, \ldots, m. \tag{3.5}$$

Multiplying (2.9) by u^{m+1} and integrating on Ω, we will obtain

$$||u^{m+1}||_2^2 - \gamma(\frac{\partial^2 u^{m+1}}{\partial x_{m+1}^2}, u^{m+1}) = (1-a_1)(u^m, u^{m+1}) + \left(\sum_{k=1}^{m-1}(a_k - a_{k+1})u^{m-k}, u^{m+1}\right)$$
$$+ (a_m u^0, u^m + 1) + \gamma(f^{m+1}, u^{m+1}),$$

By using Schwarz inequality and the inequality in Lemma 3.2

$$a_k \geq a_{k+1}, \qquad k = 1, 2, ..., m.$$

We obtain

$$||u^{m+1}||_2 \leq (1 - a_1)||u^m||_2 + \sum_{k=1}^{m-1}(a_k - a_{k+1})||u^{m-k}||_2 + a_m||u^0||_2 + \gamma||f^{m+1}||_2.$$

By using (3.5), we get

$$\begin{aligned} ||u^{m+1}||_2 &\leq ||u^0||_2 + \left(\sum_{k=1}^{m-1}(a_k - a_{k+1})a_{m-k-1}^{-1} + 1\right) \max_{0\leq l\leq M} ||\gamma f^l||_2 \\ &\leq ||u^0||_2 + \left(\sum_{k=1}^{m-1}(a_k - a_{k+1})a_m^{-1} + 1\right) \max_{0\leq l\leq M} ||\gamma f^1||_2 \\ &\leq ||u^0|| + \gamma a_m^{-1} \max_{0\leq l\leq M} ||f^l||_2. \end{aligned}$$

Hence, the proof is completed. □

Now, we will prove the stability theorem, to simplify the notations without loss of generality, let U^m be an exact solution of (2.9), we consider the case $f \equiv 0$ in stability analysis.

Theorem 3.4 (Stability theorem)**.** *The numerical implicit method defined by* (2.9)*, is unconditionally stable.*

Proof. Denote the error:

$$\xi^m = U^m - u^m, \tag{3.6}$$

It satisfies

$$\xi^{m+1} - \gamma\frac{\partial^2 \xi^{m+1}}{\partial^2 x^{m+1}} = (1 - a_1)\xi^m + \sum_{k=1}^{m-1}(a_k - a_{k+1})\xi^{m-k} + a_m\xi^0, \tag{3.7}$$

and

$$\xi^{m+1}|_{\partial\Omega} = 0, \qquad t \in [0, T].$$

By using Lemma 3.1, similar to the proof of Lemma 3.3, we will obtain

$$||\xi^m||_2 \leq ||\xi^0||_2, \qquad m = 1, 2, ..., M. \tag{3.8}$$

This proves the theorem. □

4 Convergence of the method

In this section, we will show that the approximate solution converges to the exact solution with order $O(\Delta t^{2-\alpha})$ and we will obtain an error bound for the time discrete scheme.

Theorem 4.1. *Let $u^m, m = 0, 1, 2, ..., M$ be the approximate solution of Eq. (2.9) and the $u(x, t^m), m = 0, 1, ..., M$ be the exact solution of Eq. (1.1) with the above initial and boundary condition, then we have the following error estimates*

$$||u(x,t^m) - u^m||_2 \leq C^\star(\Delta t^{2-\alpha}), \quad m = 1, 2, ..., M. \tag{4.1}$$

Where $C^\star$ is, constant.

Proof. Denote

$$\epsilon^m = u(x,t^m) - u^m. \tag{4.2}$$

From (2.8) and (2.9), we get

$$\epsilon^{m+1} - \gamma\frac{\partial^2 \epsilon^{m+1}}{\partial^2 x^{m+1}} = \epsilon^m - \sum_{k=1}^{m} a_k(\epsilon^{m-k+1} - \epsilon^{m-k}) + R^1(\Delta t), \tag{4.3}$$

$$\epsilon^0 = 0, \quad \epsilon^m|\partial_\Omega = 0,$$

by using Lemma 3.3, we obtain

$$||\epsilon^m||_2 \leq a_{m-1}^{-1} \max_{0\leq l\leq M} ||R^l||_2 \leq C_3(\Delta t)^2. \tag{4.4}$$

Because

$$\lim_{m\to\infty} a_{m-1}^{-1} m^{-\alpha} = \lim_{m\to\infty} \frac{m^{-\alpha}}{m^{1-\alpha} - (m-1)^{1-\alpha}} = \lim_{m\to\infty} \frac{1}{m - (m-1)(m/m-1)^\alpha} = \frac{1}{1-\alpha}, \tag{4.5}$$

thus, $a_{m-1}^{-1}(\Delta t)^2$ is bounded, from (4.4), we will obtain

$$||u(x,t^m) - u^m||_2 \leq C^\star(\Delta t^{2-\alpha}), \quad m = 1, 2, \ldots, M. \tag{4.6}$$

This proves the theorem. □

5 Numerical results

In this section, we present an example to verify our theoretical finding. In this example, we will check the convergence of the numerical solution with respect to Δt.

Example 5.1. We consider the same equation as that in [11]:

$$\frac{\partial^{[\alpha} u(x,t)}{\partial t^\alpha} - \frac{\partial^2 u(x,t)}{\partial x^2} = f(x,t), \qquad (x,t) \in [0,1] \times [0,1], \tag{5.1}$$

with

$$f(x,t) = \frac{2}{\Gamma(3-\alpha)} t^{2-\alpha} sin(2\pi x) + 4\pi^2 t^2 sin(2\pi x),$$

subject to the initial condition $u_0(x) = 0$ and the homogeneous boundary conditions: $u(0,t) = u(1,t) = 0$.

Table 5.1: The error and the convergence rate for $\alpha = 0.1$

M	N	The error	Convergence rate
30	30	0.00355	–
60	60	$8.90771 * 10^{-4}$	1.99469
100	100	$3.20611 * 10^{-4}$	2.00041
150	150	$1.42463 * 10^{-4}$	2.00053
200	200	$8.01563 * 10^{-5}$	1.99910

Table 5.2: The error and the convergence rate for $\alpha = 0.5$

M	N	The error	Convergence rate
30	30	0.00358	–
60	60	$9.05205 * 10^{-4}$	1.98357
100	100	$3.28401 * 10^{-4}$	1.98497
150	150	$1.47078 * 10^{-4}$	1.98111
200	200	$8.33012 * 10^{-5}$	1.97614

The exact solution to the problem is given by $u = t^2 sin(2\pi x)$. Taking $\Delta(t) = \frac{1}{M}$ and $h = \frac{1}{N}$, where N and M are the numbers of meshes in space and time, in this example, we use $N = M$. The $\frac{\partial^2 u(x,t_{m+1})}{\partial x^2}$ is approximated as follows:

$$\frac{\partial^2 u(x,t_{m+1})}{\partial x^2} \approx \frac{u(x_{n+1},t_{m+1}) - 2u(x_n,t_{m+1}) + u(x_{n-1},t_{m+1})}{h^2}. \tag{5.2}$$

The rates of convergence are computed by

$$\text{rate} = \frac{Ln(e_{\text{new}}/e_{\text{old}})}{Ln\left((\Delta t)_{\text{new}}/(\Delta t)_{\text{old}}\right)}.$$

The errors in our examples are denoted by $max\{|u^m - U^m| : m = 1,2,...,M\}$. The convergence rate and the errors for different α and M are presented in Tables (5.1-5.4). We can see that the convergence rate for time is close to Δt^2. The numerical results are consistent with our theoretical results in theorem 3.4. The comparison of the exact and approximate solutions with $\alpha = 0.1$ at different M and the comparison of the exact and approximate solutions with $\alpha = 0.9$ at different M are shown (see Figs5.1 and 5.2). All the calculations in this example are performed using MATLAB 2016.

Table 5.3: The error and the convergence rate for $\alpha = 0.7$

M	N	The error	Convergence rate
30	30	0.00369	–
60	60	$9.55878 * 10^{-4}$	1.94872
100	100	$3.56404 * 10^{-4}$	1.93132
150	150	$1.64371 * 10^{-4}$	1.97877
200	200	$9.55343 * 10^{-5}$	1.88625

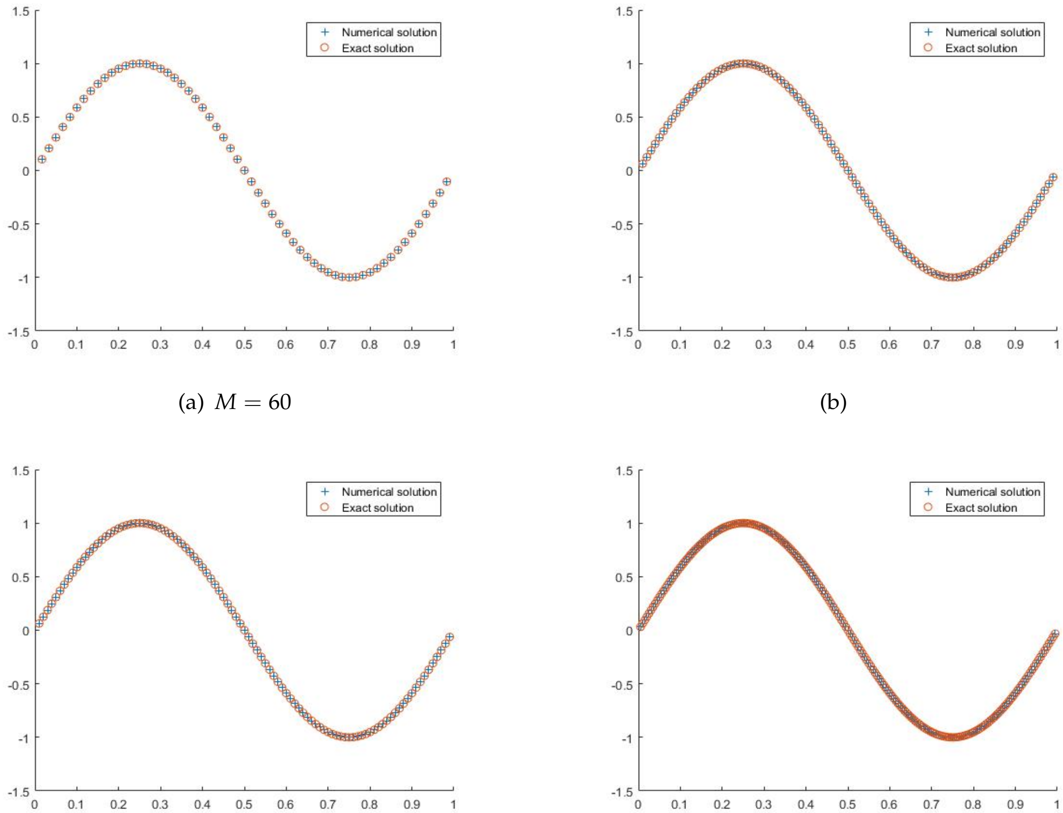

(a) $M = 60$ (b)

(c) $M = 150$ (d) $M = 200$

Figure 5.1: The comparison of the exact and approximate solutions with $\alpha = 0.1$ at different M for test problem 5.1.

Table 5.4: The error and the convergence rate for $\alpha = 0.9$

M	N	The error	Convergence rate
30	30	0.00400	–
60	60	0.00112	1.83650
100	100	$4.53413 * 10^{-4}$	1.77023
150	150	$2.28800 * 10^{-4}$	1.68684
200	200	$1.43598 * 10^{-4}$	1.61925

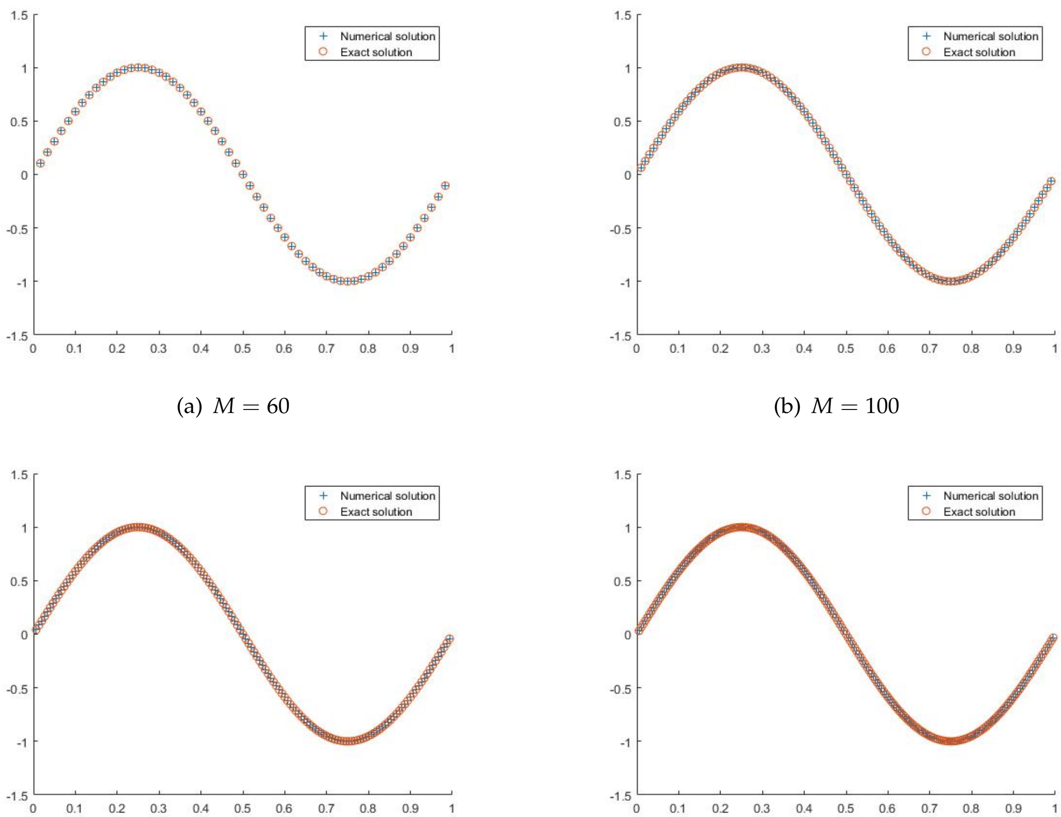

(a) $M = 60$

(b) $M = 100$

(c) $M = 150$

(d) $M = 200$

Figure 5.2: The comparison of the exact and approximate solutions with $\alpha = 0.9$ at different M for test problem 5.1.

6 Concluding remarks

In this paper, we studied an implicit discrete scheme to solve the time-fractional diffusion equation. The error estimates and the stability of the proposed method are discussed. The convergence rate of the proposed method was proved to be optimal. An example was provided to illustrate the capability and accuracy of the method. Constructing more efficient algorithms is also our goal in future works.

Acknowledgments

The author thanks very much editors and referees for their valuable and kind comments, suggestions, correcting errors and improving written language, which helped me to improve this paper.

Conflict of Interest

The authors have no conflicts of interest to declare.

References

[1] B. Baeumer, M. M. Meerschaert, D. A. Benson and S. W. Wheatcraft , *Subordinated advection–dispersion equation for contaminant transport*, Water Resour. Res. **37** (2001) 1543-1550.

[2] E. Barkai, R. Metzler and J. Klafter, *From continuous time random walks to the fractional Fokker-Planck equation*, Phys. Rev. E **61** (2000) 132-138.

[3] D. Benson, R. Schumer, M. Meerschaert and S. Wheatcraft, *Fractional dispersion, Levy motions, and the MADE tracer tests*, Transport Porous Media **42** (2001) 211-240.

[4] D. Benson, S. Wheatcraft and M. Meerschaert, *Application of a fractional advection-dispersion equation*, Water Resour. Res. **36** (2000) 1403-1412.

[5] D. Benson, S. Wheatcraft and M. Meerschaert, *The fractional-order governing equation of Levy motion*, Water Resour. Res. **36** (2000) 1413-1424.

[6] A. Blumen, G. Zumofen and J. Klafter , *Transport aspects in anomalous diffusion: Levy walks*, Phys. Rev. A**40** (1989) 3964-3973.

[7] J. P. Bouchaud and A. Georges, *Anomalous diffusion in disordered media—statistical mechanisms*, models and physical applications, Phys. Rep. **195**(1990) 127-293.

[8] A.Chaves, *Fractional diffusion equation to describe Levy flights*, Phys. Lett. A **239** (1998) 13-16.

[9] R. Gorenflo, Y. Luchko and F. Mainradi, *Wright function as scale-invariant solution of the diffusion-wave equation*, J. Comp. Appl. Math. **118** (2000) 175-191.

[10] R. Gorenflo, F. Mainardi, E. Scalas and M. Raberto, *Fractional calculus and continuous-time finance*, III, The diffusion limit. Mathematical finance (Konstanz, 2000), Trends in Math., Birkhuser, Basel, 2001, pp.171-180.

[11] Y. J. Jiang and J. T. Ma, *High order finite element methods for time-fractional partial differential equations*, J. Comput. Appl. Math. **235** (2011) 3285-3290.

[12] J. Klafter, A. Blumen and M. F. Shlesinger, *Stochastic pathways to anomalous diffusion*, Phys. Rev. A **35** (1987)3081-3085.

[13] L. Li and X. G. Hu, *The Green's formula and its proof*, J. Chongqing Uni. Arts. Sci. (Nat. Sci. Ed.) **26** (2007) 40-41.

[14] Y. M. Lin and C. J. Xu, *Finite difference/spectral approximations for the time fractional diffusion equation*, J. Compute. phys. **225**(2007) 1533-1552.

[15] F. Liu, S. Shen, V. Anh and I. Turner, *Analysis of a discrete non-Markovian random walk approximation for time fractional diffusion equation*, ANZIAM J. **46** (E) (2005) 488-504.

[16] F. Liu, V. Anh, I. Turner and P. Zhuang, *Time fractional advection-dispersion equation*, J. Appl. Math. Compute. **13**(2003) 233-245.

[17] Q. Liu, Y. T. Gu, P. Zhuang, F. Liu and Y. F. Nie, *An implicit RBF meshless approach for time fractional diffusion equations*, Comput. Mech. **48**(2011) 1-12.

[18] M. Meerschaert, D. Benson and B. Baeumer, *Operator Levy motion and multiscaling anomalous diffusion*, Phys. Rev. E **63** (2001) 1112-1117.

[19] M. Meerschaert, D. Benson, H. P. ScheXer and B. Baeumer, *Stochastic solution of space-time fractional diffusion equations*, Phys. Rev. E **65** (2002) 1103-1106.

[20] M. M. Meerschaert and H. P. ScheXer, *Semistable Levy Motion*, Frac. Calc. Appl. Anal. **5** (2002) 27-54.

[21] M. Raberto, E. Scalas and F. Mainardi, *Waiting-times and returns in high-frequency 5nancial data: an empirical study*, Physica A **314** (2002) 749-755.

[22] L. Sabatelli and S. Keating, J. Dudley, P. Richmond, *Waiting time distributions in 5nancial markets*, Eur. Phys. J. B **27**(2002) 273-275.

[23] A. I. Saichev and G. M. Zaslavsky, *Fractional kinetic equations: solutions and applications*, Chaos **7** (1997) 753-764.

[24] E. Scalas, R. Gorenflo and F. Mainardi, *Fractional calculus and continuous-time finance*, Phys. A **284**(2000) 376-384.

[25] W. R. Schneider and W. Wyss, *fractional diffusion and wave equations*, J.Math. Phys. **30**(1989)34-144.

[26] R. Schumer, D. A. Benson, M. M. Meerschaert and B. Baeumer, *Multiscaling fractional advection–dispersion equations and their solutions*, Water Resour. Res. **39** (2003) 1022-1032.

[27] T. Tang, *A finite difference scheme for partial integro-differential equations with a weakly singular kernel*, Appl. Numer. Math. **11**(4) (1993) 309-319.

[28] W. Wyss, *The fractional diffusion equation*, J. Math. Phys.**27** (1986) 2782-2785.

[29] G. Zaslavsky, *Fractional kinetic equation for Hamiltonian chaos. Chaotic advection, tracer dynamics and turbulent dispersion*, Phys. D **76**(1994) 110-122.

[30] J. Zhang, X. Zhang and B. Yang, *An approximation scheme for the time fractional convection–diffusion equation*, J. App. Math. Comp. **335** (2018) 305-312.

Journal of Innovative Applied Mathematics and Computational Sciences

J. Innov. Appl. Math. Comput. Sci. **2**(3) (2022), 29–40. n2t.net/ark:/49935/jiamcs.v2i3.48

http://jiamcs.centre-univ-mila.dz/

Generalized contraction theorems in $\mathfrak{M}$-fuzzy cone metric spaces

Mookiah Suganthi [1*], Mathuraiveeran Jeyaraman ✉[2] and Avulichikkanan Ramachandran [3]

[1]PG and Research Department of Mathematics, Raja Doraisingam Government Arts College, Sivagangai 630561, Affiliated to Alagappa University, Karaikudi, India, *Department of Mathematics, Government Arts College, Melur 625106.

[2]PG and Research Department of Mathematics, Raja Doraisingam Government Arts College, Sivagangai 630561, Affiliated to Alagappa University, Karaikudi, India.

[3]Research Scholar, Suvarna Karnataka Institute of Studies and Research Center, Tumkur 572102, Karnataka.

Received 23 June 2022, Accepted 14 November 2022, Published 15 December 2022

Abstract. This work defines $\mathfrak{M}$-Fuzzy Cone Metric Space, as a new metric space. It also analyzes possible forms of contractive conditions and groups them accordingly to set up generalized contractive conditions for self-mappings defined over $\mathfrak{M}$-fuzzy cone metric spaces. We prove the existence of fixed points of these mappings and exhibit the same through a suitable example.

Keywords: Fixed point, Cone, Triangular, Fuzzy contractive, Symmetric.

2020 Mathematics Subject Classification: 54H25; 47H10 MSC2020

1 Introduction

A self-mapping f, defined on a metric space (M, d), is said to be a contraction if for some $k \in [0, 1)$, it fulfills the condition $d(f(x), f(y)) \leq kd(x, y)$, for all $x, y \in M$. Stefan Banach, a Polish mathematician, used these contractions to bring out his fixed point theorem, a remarkable finding, known as Banach Contraction Principle.

Theorem 1.1. *(Banach [1])*
(X, d) is a complete metric space and $f : X \to X$ is a contraction mapping. Thus, there exists a constant $r < 1$ such that $d(f(x), f(y)) \leq rd(x, y)$ for each $x, y \in X$. From this, one draws three conclusions:
(i) f has a unique fixed point, say x_0;
(ii) For each $x \in X$ the Picard sequence $\{f^n(x)\}$ converges to x_0;
(iii) The convergence is uniform if X is bounded.

✉Corresponding author. Email: jeya.math@gmail.com

ISSN (electronic): 2773-4196

This principle has made a great impact in the domain of research. Since then, it has been the origin of numerous findings as all these findings are its modifications. These modifications are made to the contractive conditions and the settings of the domain. One of the remarkable extensions is due to Hardy and Rogers in the year 1973. His work is an extension of Reich's fixed point theorem.

Theorem 1.2. *(Hardy and Rogers) [10]*
Let (M, d) be a metric space and T a self-mapping of M satisfying the condition for $x, y \in M$

$$(1)\ d(Tx, Ty) \leq ad(x, Tx) + bd(y, Ty) + cd(x, Ty) + d(y, Tx) + fd(x, y),$$

where a, b, c, d, e, f are nonnegative and we set $\alpha = a + b + c + d + e + f$. Then
(a) If M is complete and $\alpha < 1$, T has a unique fixed point.
(b) If (1) is modified to the condition

$$(1')\ d(Tx, Ty) \leq ad(x, Tx) + bd(y, Ty) + cd(x, Ty) + d(y, Tx) + fd(x, y),$$

and in this case, we assume M is compact, T is continuous and $\alpha = 1$, then T has a unique fixed point.

Likewise, the Banach Contraction Principle has seen numerous extensions and generalizations. Besides, in the year 1965, Zadeh [19] made a great contribution to the field of mathematics by introducing the definition of fuzzy set, an idea to handle uncertainties well. Since then, new metrics are being discovered over fuzzy sets. A few fuzzy metrics, that were found at the initial stage, can be found in [2, 4, 12, 13]. Making a slight change in the definition of Kramosil and Michalek [13], George and Veeramani [5] present a fuzzy metric space which is more adaptable due to its topological structure. In the year 2000, Gregori and Sapena [7] defined fuzzy contractive mappings and proved fixed point theorems on both of these fuzzy metric spaces

Sedghi and Shobe [16] presented $\mathfrak{M}$-fuzzy metric spaces in the year 2006. Huang and Zhang [11] defined cone metric spaces as a generalization of metric spaces in the year 2007. Combining the concept of cone metric spaces and fuzzy metric spaces [5], Oner et. al. [14] came up with the concept of fuzzy cone metric spaces.

Here, we aim to present $\mathfrak{M}$-fuzzy cone metric spaces in the sense of [16] and [14]. We also define generalized fuzzy cone contractive conditions and prove some fixed point theorems for self-mappings in the settings of $\mathfrak{M}$-fuzzy cone metric spaces.

2 Preliminaries

Definition 2.1. [14] Let E be a real Banach space and $\mathscr{C}$ be a subset of E. $\mathscr{C}$ is called a cone if and only if:
[C1] $\mathscr{C}$ is closed, nonempty, and $\mathscr{C}$ is not equal to $\{0\}$,
[C2] $a, b \in \mathbb{R}$, $a, b \geq 0$, $\mathbf{c}_1, \mathbf{c}_2 \in \mathscr{C}$ imply $a\mathbf{c}_1 + b\mathbf{c}_2 \in \mathscr{C}$,
[C3] $\mathbf{c} \in \mathscr{C}$ and $-\mathbf{c} \in \mathscr{C}$ imply $\mathbf{c} = 0$.
The cones considered here are subsets of a real Banach space E and are with nonempty interiors.

Definition 2.2. An $\mathfrak{M}$-Fuzzy Cone Metric Space (briefly, $\mathfrak{M}$-FCM Space) is a 3-tuple $(\mathcal{Z}, \mathfrak{M}, *)$ where $\mathcal{Z}$ is an arbitrary set, $*$ is a continuous t-norm, $\mathscr{C}$ is a cone and $\mathfrak{M}$ a fuzzy set in $\mathcal{Z}^3 \times int(\mathscr{C})$ satisfying the following conditions: For all $\zeta, \eta, \omega, \mathsf{u} \in \mathcal{Z}$ and $\mathbf{c}, \mathbf{c}' \in int(\mathscr{C})$,
[MFC1] $\mathfrak{M}(\zeta, \eta, \omega, \mathbf{c}) > 0$,
[MFC2] $\mathfrak{M}(\zeta, \eta, \omega, \mathbf{c}) = 1$ if and only if $\zeta = \eta = \omega$,
[MFC3] $\mathfrak{M}(\zeta, \eta, \omega, \mathbf{c}) = \mathfrak{M}(p\{\zeta, \eta, \omega\}, \mathbf{c})$, where p is a permutation,
[MFC4] $\mathfrak{M}(\zeta, \eta, \omega, \mathbf{c} + \mathbf{c}') \geq \mathfrak{M}(\zeta, \eta, \mathsf{u}, \mathbf{c}) * \mathfrak{M}(\mathsf{u}, \omega, \omega, \mathbf{c}')$,
[MFC5] $\mathfrak{M}(\zeta, \eta, \omega, \cdot) : int(\mathscr{C}) \to [0, 1]$ is continuous.
Here, $\mathfrak{M}$ is called $\mathfrak{M}$-Fuzzy Cone Metric on $\mathcal{Z}$. The function $\mathfrak{M}(\zeta, \eta, \omega, \mathbf{c})$ denote the degree of nearness between ζ, η and ω with respect to $\mathbf{c}$.

Example 2.3. Let $E = \mathbb{R}^2$ and consider the cone $\mathscr{C} = \{(\mathbf{c}_1, \mathbf{c}_2) \in \mathbb{R}^2 : \mathbf{c}_1 \geq 0, \mathbf{c}_2 \geq 0\}$ in E. Let the t-norm $*$ be defined by $\mathfrak{a} * \mathfrak{b} = \mathfrak{a}\mathfrak{b}$. Define the function $\mathfrak{M} : \mathbb{R}^3 \times int(\mathscr{C}) \to [0, 1]$ by $\mathfrak{M}(\zeta, \eta, \omega, \mathbf{c}) = \frac{1}{e^{\frac{|\zeta - \eta| + |\eta - \omega| + |\omega - \zeta|}{\|c\|}}}$, for all $\zeta, \eta, \omega \in \mathbb{R}$ and $\mathbf{c} \in int(\mathscr{C})$. Then $(\mathbb{R}, \mathfrak{M}, *)$ is an $\mathfrak{M}$-Fuzzy Cone Metric Space.

Definition 2.4. A symmetric $\mathfrak{M}$-FCM Space is an $\mathfrak{M}$-FCM Space $(\mathcal{Z}, \mathfrak{M}, *)$ satisfying

$$\mathfrak{M}(\eta, \omega, \omega, \mathbf{c}) = \mathfrak{M}(\omega, \eta, \eta, \mathbf{c}), \text{ for all } \eta, \omega \in \mathcal{Z} \text{ and } \mathbf{c} \in int(\mathscr{C}).$$

Definition 2.5. Let $(\mathcal{Z}, \mathfrak{M}, *)$ be an $\mathfrak{M}$-FCM Space. A self-mapping $\mathcal{K} : \mathcal{Z} \to \mathcal{Z}$ is said to be $\mathfrak{M}$-fuzzy cone contractive if there exists $k \in (0, 1)$ such that

$$\left(\frac{1}{\mathfrak{M}(\mathcal{K}(\zeta), \mathcal{K}(\eta), \mathcal{K}(\omega), \mathbf{c})} - 1\right) \leq k \left(\frac{1}{\mathfrak{M}(\zeta, \eta, \omega, \mathbf{c})} - 1\right),$$

for all $\zeta, \eta, \omega \in \mathcal{Z}$ and $\mathbf{c} \in int(\mathscr{C})$.

Remark 2.6. In the above definition, k excludes the value zero, for if $k = 0$, then it is possible to have

$$\left(\frac{1}{\mathfrak{M}(\mathcal{K}(\zeta), \mathcal{K}(\eta), \mathcal{K}(\omega), \mathbf{c})} - 1\right) > \left(\frac{1}{\mathfrak{M}(\zeta, \eta, \omega, \mathbf{c})} - 1\right),$$

for all distinct $\zeta, \eta, \omega \in \mathcal{Z}$ and $\mathbf{c} \in \text{int}(\mathscr{C})$, and $\mathcal{K}$ cannot have any fixed point.

Definition 2.7. In an $\mathfrak{M}$-FCM Space $(\mathcal{Z}, \mathfrak{M}, *)$, $\mathfrak{M}$ is said to be triangular if, for all $\zeta, \eta, \omega, \mathsf{u} \in \mathcal{Z}$ and $\mathbf{c} \in \text{int}(\mathscr{C})$,

$$\left(\frac{1}{\mathfrak{M}(\zeta, \eta, \omega, \mathbf{c})} - 1\right) \leq \left(\frac{1}{\mathfrak{M}(\zeta, \eta, \mathsf{u}, \mathbf{c})} - 1\right) + \left(\frac{1}{\mathfrak{M}(\mathsf{u}, \omega, \omega, \mathbf{c})} - 1\right).$$

Definition 2.8. Let $(\mathcal{Z}, \mathfrak{M}, *)$ be an $\mathfrak{M}$-FCM Space. For $\mathsf{u} \in \mathcal{Z}, r > 0$ and $\mathbf{c} \in int(\mathscr{C})$, the open ball $B_{\mathscr{C}}(\mathsf{u}, r, \mathbf{c})$, with center at u and radius r, is defined by

$$B_{\mathscr{C}}(\mathsf{u}, r, \mathbf{c}) = \{\mathsf{w} \in \mathcal{Z} : \mathfrak{M}(\mathsf{u}, \mathsf{w}, \mathsf{w}, \mathbf{c}) > 1 - r\}.$$

Lemma 2.9. *[18] For each $\mathbf{c}_1 \in int(\mathscr{C})$ and $\mathbf{c}_2 \in int(\mathscr{C})$, there exists $\mathbf{c} \in int(\mathscr{C})$ such that $\mathbf{c}_1 - \mathbf{c} \in int(\mathscr{C})$ and $\mathbf{c}_2 - \mathbf{c} \in int(\mathscr{C})$.*

Theorem 2.10. *Let $(\mathcal{Z}, \mathfrak{M}, *)$ is an $\mathfrak{M}$-FCM Space. Then $\tau_{\mathscr{C}}$, defined hereunder, is a topology:*

$$\tau_{\mathscr{C}} = \left\{ \begin{array}{c} \mathscr{D} \subseteq \mathcal{Z} : a \in \mathscr{D} \quad \text{if and only if there exists} \quad r \in (0,1) \\ \text{and} \quad \mathbf{c} \in int(\mathscr{C}) \quad \text{such that} \quad \mathscr{B}_{\mathscr{C}}(a, r, \mathbf{c}) \subset \mathscr{D} \end{array} \right\}.$$

Proof. **(i)** It is obvious that $\emptyset \in \tau_{\mathscr{C}}$ and $\mathcal{Z} \in \tau_{\mathscr{C}}$.
(ii) Suppose $\mathscr{D}_1 \in \tau_{\mathscr{C}}$ and $\mathscr{D}_2 \in \tau_{\mathscr{C}}$ and $a \in \mathscr{D}_1 \cap \mathscr{D}_2$. Then $a \in \mathscr{D}_1$ and $a \in \mathscr{D}_2$.
Then, there exists $r_1, r_2 \in (0,1)$ and $\mathbf{c}_1, \mathbf{c}_2 \in int(\mathscr{C})$ such that

$$\mathscr{B}_{\mathscr{C}}(a, r_1, \mathbf{c}_1) \subset \mathscr{D}_1 \quad \text{and} \quad \mathscr{B}_{\mathscr{C}}(a, r_2, \mathbf{c}_2) \subset \mathscr{D}_2.$$

By Lemma 2.9, there exists $\mathbf{c} \in int(\mathscr{C})$ such that $\mathbf{c}_1 - \mathbf{c} \in int(\mathscr{C}), \mathbf{c}_2 - \mathbf{c} \in int(\mathscr{C})$.
Let $r = \min\{r_1, r_2\}$. Then $\mathscr{B}_{\mathscr{C}}(a, r, \mathbf{c}) \subset \mathscr{B}_{\mathscr{C}}(a, r_1, \mathbf{c}_1) \cap \mathscr{B}_{\mathscr{C}}(a, r_2, \mathbf{c}_2) \subset \mathscr{D}_1 \cap \mathscr{D}_2$.
Hence, $\mathscr{D}_1 \cap \mathscr{D}_2 \in \tau_{\mathscr{C}}$.
(iii) Let $\mathscr{D}_j \in \tau_{\mathscr{C}}$ for each $j \in J$, an index set, and let $a \in U_{j\in J}\mathscr{D}_j$. Then $a \in \mathscr{D}_{j_0}$ for some $j_0 \in J$.
Hence, there exists $r \in (0,1)$ and $\mathbf{c} \in int(\mathscr{C})$ such that $\mathscr{B}_{\mathscr{C}}(a, r, \mathbf{c}) \subset D_{j_0}$.
As $D_{j_0} \subset U_{j\in J}\mathscr{D}_j$, we have that $\mathscr{B}_{\mathscr{C}}(a, r, \mathbf{c}) \subset U_{j\in J}\mathscr{D}_j$.
Thus, $U_{j\in J}\mathscr{D}_j \in \tau_{\mathscr{C}}$.
From (i), (ii) and (iii), $\tau_{\mathscr{C}}$ is a topology. □

Remark 2.11. [5] For any $r_1 > r_2$, there exists r_3 such that $r_1 * r_3 \geq r_2$ and for any r_4 there exists $r_5 \in (0,1)$ such that $r_5 * r_5 \geq r_4$, where $r_1, r_2, r_3, r_4, r_5 \in (0,1)$.

Theorem 2.12. *Let $(\mathcal{Z}, \mathfrak{M}, *)$ be an $\mathfrak{M}$-FCM Space. Then $(\mathcal{Z}, \tau_{\mathscr{C}})$ is Hausdorff.*

Proof. Let $\zeta, \omega \in \mathcal{Z}$ be distinct. Then $0 < \mathfrak{M}(\zeta, \omega, \omega, \mathbf{c}) < 1$ for all $\mathbf{c} \in int(\mathscr{C})$.
Let $\mathfrak{M}(\zeta, \omega, \omega, \mathbf{c}) = r$.
Now, for each $r_0 \in (r, 1)$, there exists $r_1 \in (0,1)$ such that $r_1 * r_1 \geq r_0$.
Suppose $\mathscr{B}_{\mathscr{C}}\left(\zeta, 1 - r_1, \frac{\mathbf{c}}{2}\right) \cap \mathscr{B}_{\mathscr{C}}\left(\omega, 1 - r_1, \frac{\mathbf{c}}{2}\right)$ is nonempty.
Then there exists $z \in \mathscr{B}_{\mathscr{C}}\left(\zeta, 1 - r_1, \frac{\mathbf{c}}{2}\right) \cap \mathscr{B}_{\mathscr{C}}\left(\omega, 1 - r_1, \frac{\mathbf{c}}{2}\right)$ and we have that

$$r = \mathfrak{M}(\zeta, \omega, \omega, \mathbf{c}) \geq \mathfrak{M}\left(\zeta, \omega, \zeta, \frac{\mathbf{c}}{2}\right) * \mathfrak{M}\left(\zeta, \omega, \omega, \frac{\mathbf{c}}{2}\right) \geq r_1 * r_1 \geq r_0 > r.$$

This is a contradiction. Hence, $\mathscr{B}_{\mathscr{C}}\left(\zeta, 1 - r_1, \frac{\mathbf{c}}{2}\right) \cap \mathscr{B}_{\mathscr{C}}\left(\omega, 1 - r_2, \frac{\mathbf{c}}{2}\right)$ is empty.
Therefore, $(\zeta, \tau_{\mathscr{C}})$ is Hausdorff. □

Definition 2.13. Let $(\mathcal{Z}, \mathfrak{M}, *)$ be an $\mathfrak{M}$-FCM Space, $\zeta' \in \mathcal{Z}$ and $\{\zeta_n\}$ be a sequence in $\mathcal{Z}$.

(i) $\{\zeta_n\}$ is said to converge to ζ' if for all $\mathbf{c} \in int(\mathscr{C})$, $\lim_{n\to\infty}\left(\frac{1}{M(\zeta_n, \zeta', \zeta', \mathbf{c})} - 1\right) = 0$. It is denoted by $\lim_{n\to\infty} \zeta_n = \zeta'$ or by $\zeta_n \to \zeta'$ as $n \to \infty$.

(ii) $\{\zeta_n\}$ is said to be a Cauchy sequence if for all $\mathbf{c} \in int(\mathscr{C})$ and $m \in \mathbb{N}$, we have that $\lim_{n\to\infty}\left(\frac{1}{\mathfrak{M}(\zeta_{n+m}, \zeta_n, \zeta_n, \mathbf{c})} - 1\right) = 0$.

(iii) $(\mathcal{Z}, \mathfrak{M}, *)$ is called a complete $\mathfrak{M}$-FCM space if every Cauchy sequence in $\mathcal{Z}$ converges.

Definition 2.14. Let $(\mathcal{Z}, M, *)$ be an $\mathfrak{M}$-FCM Space. A sequence $\{\zeta_n\}$ in $\mathcal{Z}$ is $\mathfrak{M}$-fuzzy cone contractive if there exists $k \in (0,1)$ such that

$$\left(\frac{1}{\mathfrak{M}(\zeta_n, \zeta_{n+1}, \zeta_{n+1}, \mathbf{c})} - 1\right) \leq k\left(\frac{1}{\mathfrak{M}(\zeta_{n-1}, \zeta_n, \zeta_n, \mathbf{c})} - 1\right), \text{ for all } \mathbf{c} \in int(\mathscr{C}).$$

Lemma 2.15. *An $\mathfrak{M}$-FCM Space $(\mathcal{Z}, \mathfrak{M}, *)$ is symmetric.*

Proof. Let $\eta, w \in \mathcal{Z}$ and $\mathbf{c} \in int(\mathscr{C})$. Then,

$$\lim_{r\to 0} \mathfrak{M}(\eta,\eta,\omega,\mathbf{c}+r) \geq \lim_{r\to 0} \big(\mathfrak{M}(\eta,\eta,\eta,r) * \mathfrak{M}(\eta,\omega,\omega,\mathbf{c})\big),$$
$$\lim_{r\to 0} \mathfrak{M}(\omega,\omega,\eta,\mathbf{c}+r) \geq \lim_{r\to 0} \big(\mathfrak{M}(\omega,\omega,\omega,r) * \mathfrak{M}(\omega,\eta,\eta,\mathbf{c})\big).$$

These inequalities imply that

$$\mathfrak{M}(\eta,\eta,\omega,\mathbf{c}) \geq \mathfrak{M}(\eta,\omega,\omega,\mathbf{c}) \quad \text{and} \quad \mathfrak{M}(\omega,\omega,\eta,\mathbf{c}) \geq \mathfrak{M}(\omega,\eta,\eta,\mathbf{c}).$$

Hence, $\mathfrak{M}(\eta,\omega,\omega,\mathbf{c}) = \mathfrak{M}(\omega,\eta,\eta,\mathbf{c})$. □

Lemma 2.16. *Let $(\mathcal{Z},\mathfrak{M},*)$ be an $\mathfrak{M}$-FCM Space, where M is triangular. Then any $\mathfrak{M}$-fuzzy cone contractive sequence in $\mathcal{Z}$ is a Cauchy sequence.*

Proof. Let the sequence $\{\zeta_n\}$ be $\mathfrak{M}$-fuzzy cone contractive in $\mathcal{Z}$. Then, there exists $k \in (0,1)$, such that

$$\left(\frac{1}{\mathfrak{M}(\zeta_n,\zeta_{n+1},\zeta_{n+1},\mathbf{c})} - 1\right) \leq k\left(\frac{1}{\mathfrak{M}(\zeta_{n-1},\zeta_n,\zeta_n,\mathbf{c})} - 1\right). \tag{2.1}$$

Since $\mathfrak{M}$ is triangular, by Lemma(2.15), for $m > n$,

$$\begin{aligned}\left(\frac{1}{\mathfrak{M}(\zeta_n,\zeta_n,\zeta_m,\mathbf{c})} - 1\right) &\leq \left(\left(\frac{1}{\mathfrak{M}(\zeta_n,\zeta_n,\zeta_{n+1},\mathbf{c})} - 1\right) + \left(\frac{1}{\mathfrak{M}(\zeta_{n+1},\zeta_{n+1},\zeta_m,\mathbf{c})} - 1\right)\right)\\ &\leq \left(\left(\frac{1}{\mathfrak{M}(\zeta_n,\zeta_n,\zeta_{n+1},\mathbf{c})} - 1\right) + \left(\frac{1}{\mathfrak{M}(\zeta_{n+1},\zeta_{n+1},\zeta_{n+2},\mathbf{c})} - 1\right)\right.\\ &\quad \left. + \left(\frac{1}{\mathfrak{M}(\zeta_{n+2},\zeta_{n+2},\zeta_m,\mathbf{c})} - 1\right)\right).\end{aligned}$$

Continuing the process, and using (2.1), we finally arrive at

$$\begin{aligned}\left(\frac{1}{\mathfrak{M}(\zeta_n,\zeta_n,\zeta_m,\mathbf{c})} - 1\right) &\leq \begin{pmatrix} \left(\frac{1}{\mathfrak{M}(\zeta_n,\zeta_n,\zeta_{n+1},\mathbf{c})} - 1\right) + \left(\frac{1}{\mathfrak{M}(\zeta_{n+1},\zeta_{n+1},\zeta_{n+2},\mathbf{c})} - 1\right) \\ + \cdots + \left(\frac{1}{\mathfrak{M}(\zeta_{m-1},\zeta_{m-1},\zeta_m,\mathbf{c})} - 1\right) \end{pmatrix}\\ &\leq k^n\left(\frac{1}{\mathfrak{M}(\zeta_0,\zeta_0,\zeta_1,\mathbf{c})} - 1\right) + \cdots + k^{m-1}\left(\frac{1}{\mathfrak{M}(\zeta_0,\zeta_0,\zeta_1,\mathbf{c})} - 1\right)\\ &= (k^n + \cdots + k^{m-1})\left(\frac{1}{\mathfrak{M}(\zeta_0,\zeta_0,\zeta_1,\mathbf{c})} - 1\right)\\ &\leq \frac{k^n}{1-k}\left(\frac{1}{\mathfrak{M}(\zeta_0,\zeta_0,\zeta_1,\mathbf{c})} - 1\right).\end{aligned} \tag{2.2}$$

From (2.2), we have that $\left(\frac{1}{\mathfrak{M}(\zeta_n,\zeta_n,\zeta_m,\mathbf{c})} - 1\right) \to 0$ as $n \to \infty$.
Hence, $\{\zeta_n\}$ is a Cauchy sequence. □

3 Main Results

This section aims to prove the existence of fixed points of self-mappings under generalized $\mathfrak{M}$-fuzzy cone contractive conditions in a complete $\mathfrak{M}$-FCM Space.

Theorem 3.1. *Let $(\mathcal{Z}, \mathfrak{M}, *)$ be a complete $\mathfrak{M}$-FCM Space where $\mathfrak{M}$ is triangular. If $\mathcal{K} : \mathcal{Z} \to \mathcal{Z}$ is such that, for all $\zeta, \eta, \omega \in \mathcal{Z}$ and $\mathbf{c} \in int(\mathscr{C})$,*

$$\left(\frac{1}{\mathfrak{M}(\mathcal{K}\zeta, \mathcal{K}\eta, \mathcal{K}\omega, \mathbf{c})} - 1\right) \leq \left\{ \begin{array}{l} k_1\left(\frac{1}{\mathfrak{M}(\zeta,\eta,\omega,\mathbf{c})} - 1\right) + k_2\left(\frac{1}{\mathfrak{M}(\zeta,\mathcal{K}\zeta,\mathcal{K}\zeta,\mathbf{c})} - 1\right) + \\ k_3\left(\frac{1}{\mathfrak{M}(\eta,\mathcal{K}\omega,\mathcal{K}\omega,\mathbf{c})} - 1\right) + k_4\left(\frac{1}{\mathfrak{M}(\eta,\mathcal{K}\eta,\mathcal{K}\eta,\mathbf{c})} - 1\right) + \\ k_5\left(\frac{1}{\mathfrak{M}(\omega,\mathcal{K}\omega,\mathcal{K}\omega,\mathbf{c})} - 1\right) + k_6\left(\frac{1}{\mathfrak{M}(\omega,\mathcal{K}\eta,\mathcal{K}\eta,\mathbf{c})} - 1\right) + \\ k_7\left(\frac{1}{\mathfrak{M}(\eta,\mathcal{K}\zeta,\omega,\mathbf{c})} - 1\right) \end{array} \right\}, \tag{3.1}$$

where $k_i \in [0, \infty], i = 1, \ldots, 7$ and $\sum_{i=1}^{6} k_i < 1$. Then $\mathcal{K}$ has a fixed point and such a point is unique if $k_1 + k_7 < 1$.

Proof. Let $\zeta_0 \in \mathcal{Z}$ be arbitrary. Generate a sequence $\{\zeta_n\}$ with $\zeta_n = \mathcal{K}\zeta_{n-1}$ for $n \in \mathbb{N}$. If there exists a non-negative integer m such that $\zeta_{m+1} = \zeta_m$, then $\mathcal{K}\zeta_m = \zeta_m$ and ζ_m becomes a fixed point of $\mathcal{K}$.
Suppose $\zeta_n \neq \zeta_{n-1}$ for any $n \in \mathbb{N}$.
From (3.1),

$$\begin{aligned} \left(\frac{1}{\mathfrak{M}(\zeta_n, \zeta_{n+1}, \zeta_{n+1}, \mathbf{c})} - 1\right) &\leq \left(\frac{1}{\mathfrak{M}(\mathcal{K}\zeta_{n-1}, \mathcal{K}\zeta_n, \mathcal{K}\zeta_n, \mathbf{c})} - 1\right) \\ &\leq \left\{ \begin{array}{l} k_1\left(\frac{1}{\mathfrak{M}(\zeta_{n-1},\zeta_n,\zeta_n,\mathbf{c})} - 1\right) + k_2\left(\frac{1}{\mathfrak{M}(\zeta_{n-1},\mathcal{K}\zeta_{n-1},\mathcal{K}\zeta_{n-1},\mathbf{c})} - 1\right) \\ +k_3\left(\frac{1}{\mathfrak{M}(\zeta_n,\mathcal{K}\zeta_n,\mathcal{K}\zeta_n,\mathbf{c})} - 1\right) + k_4\left(\frac{1}{\mathfrak{M}(\zeta_n,\mathcal{K}\zeta_n,\mathcal{K}\zeta_n,\mathbf{c})} - 1\right) \\ +k_5\left(\frac{1}{\mathfrak{M}(\zeta_n,\mathcal{K}\zeta_n,\mathcal{K}\zeta_n,\mathbf{c})} - 1\right) + k_6\left(\frac{1}{\mathfrak{M}(\zeta_n,\mathcal{K}\zeta_n,\mathcal{K}\zeta_n,\mathbf{c})} - 1\right) \\ +k_7\left(\frac{1}{\mathfrak{M}(\zeta_n,\mathcal{K}\zeta_{n-1},\mathcal{K}\zeta_n,\mathbf{c})} - 1\right) \end{array} \right\} \\ &= \left\{ \begin{array}{l} k_1\left(\frac{1}{\mathfrak{M}(\zeta_{n-1},\zeta_n,\zeta_n,\mathbf{c})} - 1\right) + k_2\left(\frac{1}{\mathfrak{M}(\zeta_{n-1},\zeta_n,\zeta_n,\mathbf{c})} - 1\right) \\ +k_3\left(\frac{1}{\mathfrak{M}(\zeta_n,\zeta_{n+1},\zeta_{n+1},\mathbf{c})} - 1\right) + k_4\left(\frac{1}{\mathfrak{M}(\zeta_n,\zeta_{n+1},\zeta_{n+1},\mathbf{c})} - 1\right) \\ +k_5\left(\frac{1}{\mathfrak{M}(\zeta_n,\zeta_{n+1},\zeta_{n+1},\mathbf{c})} - 1\right) + k_6\left(\frac{1}{\mathfrak{M}(\zeta_n,\zeta_{n+1},\zeta_{n+1},\mathbf{c})} - 1\right) \\ +k_7\left(\frac{1}{\mathfrak{M}(\zeta_n,\zeta_n,\zeta_n,\mathbf{c})} - 1\right) \end{array} \right\} \\ &= \left\{ \begin{array}{l} (k_1 + k_2)\left(\frac{1}{\mathfrak{M}(\zeta_{n-1},\zeta_n,\zeta_n,\mathbf{c})} - 1\right) \\ +(k_3 + k_4 + k_5 + k_6)\left(\frac{1}{\mathfrak{M}(\zeta_n,\zeta_{n+1},\zeta_{n+1},\mathbf{c})} - 1\right). \end{array} \right\}. \end{aligned}$$

Hence, we have that

$$\left(\frac{1}{\mathfrak{M}(\zeta_n, \zeta_{n+1}, \zeta_{n+1}, \mathbf{c})} - 1\right) \leq \frac{k_1 + k_2}{1 - (k_3 + k_4 + k_5 + k_6)}\left(\frac{1}{\mathfrak{M}(\zeta_{n-1}, \zeta_n, \zeta_n, \mathbf{c})} - 1\right). \tag{3.2}$$

Put $k = \frac{k_1+k_2}{1-(k_3+k_4+k_5+k_6)}$. Then, $k < 1$ and (3.2) becomes

$$\left(\frac{1}{\mathfrak{M}(\zeta_n, \zeta_{n+1}, \zeta_{n+1}, \mathbf{c})} - 1\right) \leq k\left(\frac{1}{\mathfrak{M}(\zeta_{n-1}, \zeta_n, \zeta_n, \mathbf{c})} - 1\right). \tag{3.3}$$

(3.3) makes the sequence $\{\zeta_n\}$ $\mathfrak{M}$-fuzzy cone contractive. Hence, by Lemma(2.16), $\{\zeta_n\}$ is Cauchy in $\mathcal{Z}$. As $\mathcal{Z}$ is complete, there exists $\zeta' \in \mathcal{Z}$ such that

$$\lim_{n\to\infty}\left(\frac{1}{\mathfrak{M}(\zeta_n, \zeta', \zeta', \mathbf{c})} - 1\right) = 0. \tag{3.4}$$

By repeated application of (3.3), we obtain that

$$\left(\frac{1}{\mathfrak{M}(\zeta_n,\zeta_{n+1},\zeta_{n+1},\mathbf{c})}-1\right)\leq k^n\left(\frac{1}{\mathfrak{M}(\zeta_0,\zeta_1,\zeta_1,\mathbf{c})}-1\right).$$

Therefore, we have that

$$\lim_{n\to\infty}\left(\frac{1}{\mathfrak{M}(\zeta_n,\zeta_{n+1},\zeta_{n+1},\mathbf{c})}-1\right)=0. \tag{3.5}$$

Now,

$$\begin{aligned}
\left(\frac{1}{\mathfrak{M}(\zeta_{n+1},\mathcal{K}\zeta',\mathcal{K}\zeta',\mathbf{c})}-1\right) &= \left(\frac{1}{\mathfrak{M}(\mathcal{K}\zeta_n,\mathcal{K}\zeta',\mathcal{K}\zeta',\mathbf{c})}-1\right)\\
&\leq \left\{\begin{array}{l} k_1\left(\frac{1}{\mathfrak{M}(\zeta_n,\zeta',\zeta',\mathbf{c})}-1\right)+k_2\left(\frac{1}{\mathfrak{M}(\zeta_n,\mathcal{K}\zeta_n,\mathcal{K}\zeta_n,\mathbf{c})}-1\right)\\ +k_3\left(\frac{1}{\mathfrak{M}(\zeta',\mathcal{K}\zeta',\mathcal{K}\zeta',\mathbf{c})}-1\right)+k_4\left(\frac{1}{\mathfrak{M}(\zeta',\mathcal{K}\zeta',\mathcal{K}\zeta',\mathbf{c})}-1\right)\\ +k_5\left(\frac{1}{\mathfrak{M}(\zeta',\mathcal{K}\zeta',\mathcal{K}\zeta',\mathbf{c})}-1\right)+k_6\left(\frac{1}{\mathfrak{M}(\zeta',\mathcal{K}\zeta',\mathcal{K}\zeta',\mathbf{c})}-1\right)\\ +k_7\left(\frac{1}{\mathfrak{M}(\zeta',\mathcal{K}\zeta_n,\zeta',\mathbf{c})}-1\right)\end{array}\right\}\\
&= \left\{\begin{array}{l} k_1\left(\frac{1}{\mathfrak{M}(\zeta_n,\zeta',\zeta',\mathbf{c})}-1\right)+k_2\left(\frac{1}{\mathfrak{M}(\zeta_n,\zeta_{n+1},\zeta_{n+1},\mathbf{c})}-1\right)\\ +k_3\left(\frac{1}{\mathfrak{M}(\zeta',\mathcal{K}\zeta',\mathcal{K}\zeta',\mathbf{c})}-1\right)+k_4\left(\frac{1}{\mathfrak{M}(\zeta',\mathcal{K}\zeta',\mathcal{K}\zeta',\mathbf{c})}-1\right)\\ +k_5\left(\frac{1}{\mathfrak{M}(\zeta',\mathcal{K}\zeta',\mathcal{K}\zeta',\mathbf{c})}-1\right)+k_6\left(\frac{1}{\mathfrak{M}(\zeta',\mathcal{K}\zeta',\mathcal{K}\zeta',\mathbf{c})}-1\right)\\ +k_7\left(\frac{1}{\mathfrak{M}(\zeta',\zeta_{n+1},\zeta',\mathbf{c})}-1\right)\end{array}\right\}\\
&\to k'\left(\frac{1}{\mathfrak{M}(\zeta',\mathcal{K}\zeta',\mathcal{K}\zeta',\mathbf{c})}-1\right) \text{ as } n\to\infty,\\
&\text{where } k'=k_3+k_4+k_5+k_6, \text{since by (3.4) and (3.5).}
\end{aligned}$$

Hence,

$$\limsup_{n\to\infty}\left(\frac{1}{\mathfrak{M}(\zeta_{n+1},\mathcal{K}\zeta',\mathcal{K}\zeta',\mathbf{c})}-1\right)\leq k'\left(\frac{1}{\mathfrak{M}(\zeta',\mathcal{K}\zeta',\mathcal{K}\zeta',\mathbf{c})}-1\right). \tag{3.6}$$

As $\mathfrak{M}$ is triangular,

$$\left(\frac{1}{\mathfrak{M}(\mathcal{K}\zeta',\mathcal{K}\zeta',\zeta',\mathbf{c})}-1\right)\leq\left(\frac{1}{\mathfrak{M}(\mathcal{K}\zeta',\mathcal{K}\zeta',\zeta_{n+1},\mathbf{c})}-1\right)+\left(\frac{1}{\mathfrak{M}(\zeta_{n+1},\zeta',\zeta',\mathbf{c})}-1\right). \tag{3.7}$$

From (3.5) to (3.7), we can bring that

$$\left(\frac{1}{\mathfrak{M}(\mathcal{K}\zeta',\mathcal{K}\zeta',\zeta',\mathbf{c})}-1\right)\leq k'\left(\frac{1}{\mathfrak{M}(\zeta',\mathcal{K}\zeta',\mathcal{K}\zeta',\mathbf{c})}-1\right).$$

This gives, $\left(\frac{1}{\mathfrak{M}(\mathcal{K}\zeta',\mathcal{K}\zeta',\zeta',t)}-1\right)=0$ since $k'<1$, and, hence we have

$$\mathcal{K}\zeta'=\zeta'.$$

Thus, we can conclude that ζ' is a fixed point of $\mathcal{K}$. Suppose $\mathcal{K}\zeta''=\zeta''$. From (3.1),

$$\left(\frac{1}{\mathfrak{M}(\mathcal{K}\zeta',\mathcal{K}\zeta'',\mathcal{K}\zeta'',\mathbf{c})}-1\right)\leq\left\{\begin{array}{l} k_1\left(\frac{1}{\mathfrak{M}(\zeta',\zeta'',\zeta'',\mathbf{c})}-1\right)+k_2\left(\frac{1}{\mathfrak{M}(\zeta',\mathcal{K}\zeta',\mathcal{K}\zeta',\mathbf{c})}-1\right)\\ +k_3\left(\frac{1}{\mathfrak{M}(\zeta'',\mathcal{K}\zeta'',\mathcal{K}\zeta'',\mathbf{c})}-1\right)+k_4\left(\frac{1}{\mathfrak{M}(\zeta'',\mathcal{K}\zeta'',\mathcal{K}\zeta'',\mathbf{c})}-1\right)\\ +k_5\left(\frac{1}{\mathfrak{M}(\zeta'',\mathcal{K}\zeta'',\mathcal{K}\zeta'',\mathbf{c})}-1\right)+k_6\left(\frac{1}{\mathfrak{M}(\zeta'',\mathcal{K}\zeta'',\mathcal{K}\zeta'',\mathbf{c})}-1\right)\\ +k_7\left(\frac{1}{\mathfrak{M}(\zeta'',\mathcal{K}\zeta',\zeta'',\mathbf{c})}-1\right)\end{array}\right\}.$$

This gives that

$$\left(\frac{1}{\mathfrak{M}(\zeta',\zeta'',\zeta'',\mathbf{c})}-1\right)\leq(k_1+k_7)\left(\frac{1}{\mathfrak{M}(\zeta',\zeta'',\zeta'',\mathbf{c})}-1\right).$$

Therefore, $\left(\frac{1}{\mathfrak{M}(\zeta',\zeta'',\zeta'',\mathbf{c})}-1\right)=0,\ \text{ if } k_1+k_7<1.$
Hence, we can conclude that $\mathcal{K}$ has a unique fixed point if $k_1+k_7<1$. □

Example 3.2. Let $\mathcal{Z}=[0,\infty)$ with metric d defined by $d(\zeta,\eta)=|\zeta-\eta|$ for all $\zeta,\eta\in\mathcal{Z}$ and let $\mathscr{C}=\mathbb{R}^+$. Define the t-norm $*$ by $i*j=\min\{i,j\}$. Define $\mathfrak{M}$ by

$$\mathfrak{M}(\zeta,\eta,\omega,\mathbf{c})=\frac{c}{c+(|\zeta-\eta|+|\eta-\omega|+|\omega-\zeta|)},$$

for all $\zeta,\eta,\omega\in\mathcal{Z}$ and $t\in int(\mathscr{C})$.
Then, it is clear that $(\mathcal{Z},\mathfrak{M},*)$ is a complete $\mathfrak{M}$-FCM Space, and, that $\mathfrak{M}$ is triangular.
Consider the self-mapping, $\mathcal{K}:\mathcal{Z}\to\mathcal{Z}$, given by $\mathcal{K}u=\begin{cases}\frac{5}{4}u+3, & u\in[0,1],\\ \frac{3}{4}u+\frac{7}{2}, & u\in[1,\infty).\end{cases}$
Then,

$$\left(\frac{1}{\mathfrak{M}(\mathcal{K}\zeta,\mathcal{K}\eta,\mathcal{K}\omega,\mathbf{c})}-1\right)=\frac{5}{4}\left(\frac{1}{\mathfrak{M}(\zeta,\eta,\omega,\mathbf{c})}-1\right),$$

where $\zeta,\eta,\omega\in[0,1]$. Hence $\mathcal{K}$ is not $\mathfrak{M}$-fuzzy cone contractive. Therefore, we cannot assure the existence of fixed points using the contraction theorem. But, here $\mathcal{K}$ satisfies the condition (3.1) with

$$k_1=\frac{3}{80},k_2=\frac{17}{80},k_3=k_4=k_5=\frac{1}{20},k_6=0,k_7=\frac{1}{20}.$$

Therefore, $\mathcal{K}$ has a unique fixed point and this point is $u=14$.

Corollary 3.3. *Let $(\mathcal{Z},\mathfrak{M},*)$ be a complete $\mathfrak{M}$-FCM Space where $\mathfrak{M}$ is triangular. If $\mathcal{K}:\mathcal{Z}\to\mathcal{Z}$ is such that for all $\zeta,\eta,\omega\in\mathcal{Z},\mathtt{c}\in int(\mathscr{C})$,*

$$\left(\frac{1}{\mathfrak{M}(\mathcal{K}\zeta,\mathcal{K}\eta,\mathcal{K}\omega,\mathbf{c})}-1\right)\leq\left\{\begin{array}{l}k_1\left(\frac{1}{\mathfrak{M}(\zeta,\eta,\omega,\mathbf{c})}-1\right)+k_2\left(\frac{1}{\mathfrak{M}(\zeta,\mathcal{K}\zeta,\mathcal{K}\zeta,\mathbf{c})}-1\right)\\ +k_3\left(\frac{1}{\mathfrak{M}(\eta,\mathcal{K}\omega,\mathcal{K}\omega,\mathbf{c})}-1\right)+k_4\left(\frac{1}{\mathfrak{M}(\eta,\mathcal{K}\zeta,\omega,\mathbf{c})}-1\right)\end{array}\right\},$$

where $k_i\in[0,\infty],i=1,\ldots,4$ and $k_1+k_2+k_3<1$. Then $\mathcal{K}$ has a fixed point and such a point is unique if $k_1+k_4<1$.

Corollary 3.4. *Let $(\mathcal{Z},\mathfrak{M},*)$ be a complete $\mathfrak{M}$-FCM Space, where $\mathfrak{M}$ is triangular. If $\mathcal{K}:\mathcal{Z}\to\mathcal{Z}$ is such that for all $\zeta,\eta,\omega\in\mathcal{Z},\mathtt{c}\in int(\mathscr{C})$,*

$$\left(\frac{1}{\mathfrak{M}(\mathcal{K}\zeta,\mathcal{K}\eta,\mathcal{K}\omega,\mathbf{c})}-1\right)\leq\left\{\begin{array}{l}k_1\left(\frac{1}{\mathfrak{M}(\zeta,\eta,\omega,\mathbf{c})}-1\right)+k_2\left(\frac{1}{\mathfrak{M}(\zeta,\mathcal{K}\zeta,\mathcal{K}\zeta,\mathbf{c})}-1\right)\\ +k_3\left(\frac{1}{\mathfrak{M}(\eta,\mathcal{K}\omega,\mathcal{K}\omega,\mathbf{c})}-1\right)+k_4\left(\frac{1}{\mathfrak{M}(\eta,\mathcal{K}\eta,\mathcal{K}\eta,\mathbf{c})}-1\right)\\ +k_5\left(\frac{1}{\mathfrak{M}(\omega,\mathcal{K}\omega,\mathcal{K}\omega,\mathbf{c})}-1\right)+k_6\left(\frac{1}{\mathfrak{M}(\omega,\mathcal{K}\eta,\mathcal{K}\eta,\mathbf{c})}-1\right)\end{array}\right\},$$

where $k_i\in[0,\infty],i=1,\ldots,6$ and $\sum_{i=1}^{6}k_i<1$. Then $\mathcal{K}$ has a unique fixed point.

Corollary 3.5. *Let $(\mathcal{Z},\mathfrak{M},*)$ be a complete $\mathfrak{M}$-FCM Space, where $\mathfrak{M}$ is triangular. If $\mathcal{K}:\mathcal{Z}\to\mathcal{Z}$ satisfies (3.1) with $\sum_{i=1}^{7}k_i<1$, then $\mathcal{K}$ has a unique fixed point.*

The following theorem gives a more generalized contractive condition which considers almost all forms of possible restrictions.

Theorem 3.6. *Let $(\mathcal{Z}, \mathfrak{M}, *)$ be a complete $\mathfrak{M}$-FCM Space, where $\mathfrak{M}$ is triangular. If $\mathcal{K} : \mathcal{Z} \to \mathcal{Z}$ is such that for all $\zeta, \eta, \omega \in \mathcal{Z}, \mathsf{c} \in int(\mathscr{C})$,*

$$\left(\frac{1}{\mathfrak{M}(\mathcal{K}\zeta, \mathcal{K}\eta, \mathcal{K}\omega, \mathbf{c})} - 1\right) \leq \left\{ \begin{array}{l} k_1\left(\frac{1}{\mathfrak{M}(\zeta,\eta,\omega,\mathbf{c})} - 1\right) + k_2\left(\frac{1}{\mathfrak{M}(\zeta,\mathcal{K}\zeta,\omega,\mathbf{c})} - 1\right) \\ +k_3\left(\frac{1}{\mathfrak{M}(\zeta,\zeta,\mathcal{K}\zeta,\mathbf{c})} - 1\right) + k_4\left(\frac{1}{\mathfrak{M}(\zeta,\mathcal{K}\zeta,\mathcal{K}\zeta,\mathbf{c})} - 1\right) \\ +k_5\left(\frac{1}{\mathfrak{M}(\eta,\mathcal{K}\eta,\omega,\mathbf{c})} - 1\right) + k_6\left(\frac{1}{\mathfrak{M}(\eta,\mathcal{K}\omega,\omega,\mathbf{c})} - 1\right) \\ +k_7\left(\frac{1}{\mathfrak{M}(\mathcal{K}\zeta,\mathcal{K}\eta,\omega,\mathbf{c})} - 1\right) + k_8\left(\frac{1}{\mathfrak{M}(\mathcal{K}\zeta,\mathcal{K}\omega,\eta,\mathbf{c})} - 1\right) \\ +k_9\left(\frac{1}{\mathfrak{M}(\eta,\eta,\mathcal{K}\eta,\mathbf{c})} - 1\right) + k_{10}\left(\frac{1}{\mathfrak{M}(\omega,\omega,\mathcal{K}\omega,\mathbf{c})} - 1\right) \\ +k_{11}\left(\frac{1}{\mathfrak{M}(\eta,\mathcal{K}\eta,\mathcal{K}\eta,\mathbf{c})} - 1\right) + k_{12}\left(\frac{1}{\mathfrak{M}(\omega,\mathcal{K}\omega,\mathcal{K}\omega,\mathbf{c})} - 1\right) \\ +k_{13}\left(\frac{1}{\mathfrak{M}(\omega,\mathcal{K}\eta,\mathcal{K}\eta,\mathbf{c})} - 1\right) + k_{14}\left(\frac{1}{\mathfrak{M}(\eta,\mathcal{K}\omega,\mathcal{K}\omega,\mathbf{c})} - 1\right) \\ +k_{15}\left(\frac{1}{\mathfrak{M}(\mathcal{K}\eta,\mathcal{K}\omega,\zeta,\mathbf{c})} - 1\right) + k_{16}\left(\frac{1}{\mathfrak{M}(\zeta,\mathcal{K}\eta,\omega,\mathbf{c})} - 1\right) \end{array} \right\}, \tag{3.8}$$

where $k_i \in [0, \infty], i = 1, \ldots, 16$ and $k_1 + \cdots + k_{14} + 2(k_{15} + k_{16}) < 1$. Then $\mathcal{K}$ has a unique fixed point.

Proof. Let $\zeta_0 \in \mathcal{Z}$ be arbitrary. Generate a sequence $\{\zeta_n\}$ with $\zeta_n = \mathcal{K}\zeta_{n-1}$ for $n \in \mathbb{N}$. If there exists a non-negative integer m such that $\zeta_{m+1} = \zeta_m$, then $\mathcal{K}\zeta_m = \zeta_m$ and ζ_m becomes a fixed point of $\mathcal{K}$.
Suppose $\zeta_n \neq \zeta_{n-1}$ for any $n \in \mathbb{N}$.
As $\mathfrak{M}$ is triangular,

$$\left(\frac{1}{\mathfrak{M}(\zeta_{n+1}, \zeta_{n+1}, \zeta_{n-1}, \mathbf{c})} - 1\right) \leq \left(\frac{1}{\mathfrak{M}(\zeta_{n-1}, \zeta_{n-1}, \zeta_n, \mathbf{c})} - 1\right) + \left(\frac{1}{\mathfrak{M}(\zeta_n, \zeta_{n+1}, \zeta_{n+1}, \mathbf{c})} - 1\right), \tag{3.9}$$

$$\left(\frac{1}{\mathfrak{M}(\zeta_{n-1}, \zeta_n, \zeta_{n+1}, \mathbf{c})} - 1\right) \leq \left(\frac{1}{\mathfrak{M}(\zeta_{n-1}, \zeta_n, \zeta_n, \mathbf{c})} - 1\right) + \left(\frac{1}{\mathfrak{M}(\zeta_n, \zeta_{n+1}, \zeta_{n+1}, \mathbf{c})} - 1\right). \tag{3.10}$$

Using (3.8) as in Theorem(3.1), together with (3.9) to (3.10), we arrive at

$$\left(\frac{1}{\mathfrak{M}(\zeta_n, \zeta_{n+1}, \zeta_{n+1}, \mathbf{c})} - 1\right) \leq \frac{k_1 + \cdots + k_4 + k_{15} + k_{16}}{1 - (k_5 + \cdots + k_{16})}\left(\frac{1}{\mathfrak{M}(\zeta_{n-1}, \zeta_n, \zeta_n, \mathbf{c})} - 1\right).$$

Putting $k = \frac{k_1+\cdots+k_4+k_{15}+k_{16}}{1-(k_5+\cdots+k_{16})}$, the above inequality becomes

$$\left(\frac{1}{\mathfrak{M}(\zeta_n, \zeta_{n+1}, \zeta_{n+1}, \mathbf{c})} - 1\right) \leq k\left(\frac{1}{\mathfrak{M}(\zeta_{n-1}, \zeta_n, \zeta_n, \mathbf{c})} - 1\right). \tag{3.11}$$

And, this makes the sequence $\{\zeta_n\}$ $\mathfrak{M}$-fuzzy cone contractive. Hence, by Lemma 2.16, $\{\zeta_n\}$ is Cauchy in $\mathcal{Z}$. As $\mathcal{Z}$ is complete, there exists $\zeta' \in \mathcal{Z}$ such that

$$\lim_{n\to\infty}\left(\frac{1}{\mathfrak{M}(\zeta_n, \zeta', \zeta', \mathbf{c})} - 1\right) = 0. \tag{3.12}$$

By repeated application of (3.11), we obtain that

$$\left(\frac{1}{\mathfrak{M}(\zeta_n,\zeta_{n+1},\zeta_{n+1},\mathbf{c})}-1\right)\leq k^n\left(\frac{1}{\mathfrak{M}(\zeta_0,\zeta_1,\zeta_1,\mathbf{c})}-1\right),$$
$$\lim_{n\to\infty}\left(\frac{1}{\mathfrak{M}(\zeta_n,\zeta_{n+1},\zeta_{n+1},\mathbf{c})}-1\right)=0. \tag{3.13}$$

From (3.8),

$$\left(\frac{1}{\mathfrak{M}(\zeta_{n+1},\mathcal{K}\zeta',\mathcal{K}\zeta',\mathbf{c})}-1\right)=\left(\frac{1}{\mathfrak{M}(\mathcal{K}\zeta_n,\mathcal{K}\zeta',\zeta',\mathbf{c})}-1\right)\leq k'\left(\frac{1}{\mathfrak{M}(\mathcal{K}\zeta',\mathcal{K}\zeta',\zeta',\mathbf{c})}-1\right),$$

where $k'=k_5+\cdots+k_{16}$.
Hence,

$$\limsup_{n\to\infty}\left(\frac{1}{\mathfrak{M}(\zeta_{n+1},\mathcal{K}\zeta',\mathcal{K}\zeta',\mathbf{c})}-1\right)\leq k'\left(\frac{1}{\mathfrak{M}(\mathcal{K}\zeta',\mathcal{K}\zeta',\zeta',\mathbf{c})}-1\right).$$

As $\mathfrak{M}$ is triangular,

$$\left(\frac{1}{\mathfrak{M}(\zeta',\mathcal{K}\zeta',\mathcal{K}\zeta',\mathbf{c})}-1\right)\leq\left(\frac{1}{\mathfrak{M}(\mathcal{K}\zeta',\mathcal{K}\zeta',\zeta_{n+1},\mathbf{c})}-1\right)+\left(\frac{1}{\mathfrak{M}(\zeta_{n+1},\zeta',\zeta',\mathbf{c})}-1\right). \tag{3.14}$$

From (3.13) and (3.14), we can bring that

$$\left(\frac{1}{\mathfrak{M}(\zeta',\mathcal{K}\zeta',\mathcal{K}\zeta',\mathbf{c})}-1\right)\leq k'\left(\frac{1}{\mathfrak{M}(\zeta',\mathcal{K}\zeta',\mathcal{K}\zeta',\mathbf{c})}-1\right).$$

This gives that $\left(\frac{1}{\mathfrak{M}(\zeta',\mathcal{K}\zeta',\mathcal{K}\zeta',\mathbf{c})}-1\right)=0$, as $k'<1$, and, hence we have $\mathcal{K}\zeta'=\zeta'$. Thus, we can conclude that ζ' is a fixed point of $\mathcal{K}$.
Suppose $\mathcal{K}\zeta''=\zeta''$. Then from (3.8) and by Lemma 2.15,

$$\left(\frac{1}{\mathfrak{M}(\zeta',\zeta'',\zeta'',\mathbf{c})}-1\right)\leq k''\left(\frac{1}{\mathfrak{M}(\zeta',\zeta'',\zeta'',\mathbf{c})}-1\right),$$

where $k''=k_1+k_2+k_7+k_8+k_{15}+k_{16}$.
This implies $\left(\frac{1}{\mathfrak{M}(\zeta',\zeta'',\zeta'',\mathbf{c})}-1\right)=0$, as $k''<1$, and hence we have $\zeta'=\zeta''$.
Thus, we can conclude that $\mathcal{K}$ has a unique fixed point. □

Corollary 3.7. *Let $(\mathcal{Z},\mathfrak{M},*)$ be a complete $\mathfrak{M}$-FCM Space, where $\mathfrak{M}$ is triangular. If $\mathcal{K}:\mathcal{Z}\to\mathcal{Z}$ is such that for all $\zeta,\eta,\omega\in\mathcal{Z}$, $\mathbf{c}\in int(c)$,*

$$\left(\frac{1}{\mathfrak{M}(\mathcal{K}\zeta,\mathcal{K}\eta,\mathcal{K}\omega,\mathbf{c})}-1\right)\leq\left\{\begin{array}{l}k_1\left(\frac{1}{\mathfrak{M}(\zeta,\eta,\omega,\mathbf{c})}-1\right)+k_2\left(\frac{1}{\mathfrak{M}(\zeta,\mathcal{K}\zeta,\omega,\mathbf{c})}-1\right)+\\ k_3\left(\frac{1}{\mathfrak{M}(\mathcal{K}\zeta,\mathcal{K}\eta,\omega,\mathbf{c})}-1\right)+k_4\left(\frac{1}{\mathfrak{M}(\eta,\mathcal{K}\omega,\mathcal{K}\omega,\mathbf{c})}-1\right)+\\ k_5\left(\frac{1}{\mathfrak{M}(\mathcal{K}\eta,\mathcal{K}\omega,\zeta,\mathbf{c})}-1\right)+k_6\left(\frac{1}{\mathfrak{M}(\zeta,\mathcal{K}\eta,\omega,\mathbf{c})}-1\right)\end{array}\right\},$$

where $k_i\in[0,\infty]$, $i=1,\ldots,6$ and $k_1+k_2+k_3+k_4+2(k_5+k_6)<1$. Then $\mathcal{K}$ has a unique fixed point.

Conclusion:

We constructed some fixed point theorems as an extension of Banach contraction theorem by giving a general form of contractive conditions for self-mappings and proved the existence of fixed points for these self-mappings.

Conflict of Interest

The authors have no conflicts of interest to declare.

References

[1] S. Banach, *Sur les opérations dans les ensembles abstraits et leur application aux équations intégrales*, Fund. Math., **3** (1922), 133-181. DOI

[2] Z. Deng, *Fuzzy pseudo-metric spaces*, J. Math. Anal. Appl., **86**(1) (1982), 74-95. DOI

[3] P. Diamond and P. Kloeden, *Metric spaces of fuzzy sets*, Fuzzy Sets and Systems, 35(2)(1990), 241-249. DOI

[4] M. A. Erceg, *Metric spaces in fuzzy set theory*, J. Math. Anal. Appl., **69**(1) (1979), 205-230. DOI

[5] A. George and P. Veeramani, *On some results in fuzzy metric spaces*, Fuzzy Sets and Systems, **64** (1994), 395-399. DOI

[6] A. George and P. Veeramani, *On some results of analysis for fuzzy metric spaces*, Fuzzy Sets and Systems, **90**(3)(1997), 365-368. DOI

[7] V. Gregori and A. Sapena, *On fixed point theorems in fuzzy metric spaces*, Fuzzy sets and Systems, **125** (2002), 245-252. DOI

[8] V. Gupta, S. S. Chauhan and I. K. Sandhu, *Banach Contraction Theorem on Extended Fuzzy Cone b-metric Space*, Thai J. Math., 20(1)(2022), 177-194. URL

[9] V. Gupta, A. Kaushik and M. Verma, *Some new fixed point results on $V-\psi$-fuzzy contraction endowed with graph*, Journal of Intelligent & Fuzzy Systems, **36**(6) (2019), 6549-6554. DOI

[10] G. E. Hardy and T. D. Rogers, *A generalization of a fixed point theorem of Reich*, Canad. Math. Bull., **16**(2) (1973), 201-206. DOI

[11] L.-G. Huang and X. Zhang, *Cone metric spaces and fixed point theorems of contractive mappings*, J. Math. Anal. Appl., **332**(2) (2007), 1468-1476. DOI

[12] O. Kaleva and S. Seikkala, *On fuzzy metric spaces*, Fuzzy Sets and Systems, **12**(3) (1984), 215-229. DOI

[13] I. Kramosil and J. Michálek, *Fuzzy metric and statistical metric spaces*, Kybernetica, **11**(5) (1975), 326-334. URL

[14] T. Öner, M. B. Kandemir and B. Tanay, *Fuzzy cone metric spaces*, J. Nonlinear Sci. Appl., **5** (2015), 610-616. URL

[15] U. R. Saif and L. Hong-Xu, *Fixed point theorems in fuzzy cone metric spaces,* J. Nonlinear Sci. Appl., **10** (2017), 5763-5769. DOI

[16] S. Sedghi and N. Shobe, *Fixed point theorem in $\mathfrak{M}$-fuzzy metric spaces with property (E)*, Advances in Fuzzy Mathematics, **1**(1) (2006), 55-65. URL

[17] T. Turkoglu and M. Abuloha, *Cone metric spaces and fixed point theorems in diametrically contractive mappings,* Acta Math. Sin. (Engl. Ser.), **26** (2010), 489-496. DOI

[18] C. S. Wong, *Generalized contractions and fixed point theorems*, Proc. Amer. Math. Soc., **42**(2) (1974), 409-417. DOI

[19] L. A. Zadeh, *Fuzzy sets*, Information and Control, 8 (1965), 338-353. DOI

Journal of Innovative Applied Mathematics and Computational Sciences

J. Innov. Appl. Math. Comput. Sci. **2**(3) (2022), 41–68. n2t.net/ark:/49935/jiamcs.v2i3.47

http://jiamcs.centre-univ-mila.dz/

Effect of dispersal in two-patch environment with Richards growth on population dynamics

Elbetch Bilel ✉ [1]

[1]Department of Mathematics, University Dr. Moulay Tahar of Saida, Algeria.

Received 23 June 2022, Accepted 18 November 2022, Published 18 December 2022

Abstract. In this paper, we consider a two-patch model coupled by migration terms, where each patch follows a Richards law. First, we prove the global stability of the model. Second, in the case when the migration rate tends to infinity, the total carrying capacity is given, which in general is different from the sum of the two carrying capacities and depends on the parameters of the growth rate and also on the migration terms. Using the theory of singular perturbations, we give an approximation of the solutions of the system in this case. Finally, we determine the conditions under which fragmentation and migration can lead to a total equilibrium population which might be greater or smaller than the sum of two carrying capacities and we give a complete classification for all possible cases. The total equilibrium population formula for a large migration rate plays an important role in this classification. We show that this choice of local dynamics has an influence on the effect of dispersal. Comparing the dynamics of the total equilibrium population as a function of the migration rate with that of the logistic model, we obtain the same behavior. In particular, we have only three situations that the total equilibrium population can occur: it is always greater than the sum of two carrying capacities, always smaller, and a third case, where the effect of dispersal is beneficial for lower values of the migration rate and detrimental for the higher values. We end by examining the two-patch model where one growth rate is much larger than the second one, we compare the total equilibrium population with the sum of the two carrying capacities.

Keywords: Population dynamics, Richards Model, Asymmetric dispersal, Singular Perturbation.

2020 Mathematics Subject Classification: 92B05, 92D25, 34D15, 34D05.

1 Introduction

Population dynamics is a wide field of mathematics, which contains many problems, among them the effect of migration on the general dynamics of the population. Bibliographies can be found in the work of Levin [18, 19] and Holt [15]. There are ecological situations that motivate the representation of space as a finite set of patches connected by migrations, for

✉Corresponding author. Email: elbetchbilal@gmail.com

ISSN (electronic): 2773-4196

instance, an archipelago with bird populations and predators. It is an example of insular biogeography. A reference work on mathematical models is the book of Levin, Powell and Steele [20], whereas Hanski and Gilpin [13] give a more ecological account of the subject. The standard question in this type of biomathematical problem is to study the effect of migration on the general population dynamics, and the consequences of fragmentation on the persistence or extinction of the population.

The simplest realistic model of population dynamics is the one with exponential growth

$$\frac{dx}{dt} = rx,$$

where r is the intrinsic growth rate. To remove unrestricted growth, Verhulst [33] considered that a stable population would have a saturation level characteristic of the environment. To achieve this the exponential model was augmented by a multiplicative factor $1 - \frac{x}{K}$, which represents the fractional deficiency of the current size from the saturation level K. In Lotka's analysis [21] of the logistic growth concept, the rate of population growth dx/dt, at any moment t is a function of the population size at that moment, $x(t)$, namely,

$$\frac{dx}{dt} = f(x).$$

Since a zero population has zero growth, $x = 0$ is an algebraic root of the function $f(x)$. By expanding f as a Taylor series near $x = 0$ and setting $f(0) = 0$, Lotka obtained the following power series: $f(x) = x(f'(0) + \frac{x}{2}f''(0))$, where higher terms are assumed negligible. By setting $f'(0) = r$ and $f''(0) = -2r/K$, where r is the intrinsic growth rate of the population and K is the carrying capacity, one is led to the Verhulst logistic equation

$$\frac{dx}{dt} = rx\left(1 - \frac{x}{K}\right). \tag{1.1}$$

Turner and co-authors [32] proposed a modified Verhulst logistic equation (1.1) which they termed the generic growth function. It has the form

$$\frac{dx}{dt} = rx^{1+\mu_2(1-\mu_3)}\left[1 - \left(\frac{x}{K}\right)^{\mu_2}\right]^{\mu_3}, \tag{1.2}$$

where μ_2, μ_3 are positive exponents and $\mu_2 < 1 + \frac{1}{\mu_3}$.

Blumberg [4] introduced another growth equation based on a modification of the Verhulst logistic growth equation (1.1) to model population dynamics or organ size evolution. Blumberg observed that the major limitation of the logistic curve was the inflexibility of the inflection point. Blumberg, therefore, introduced what he called the hyperlogistic function, accordingly

$$\frac{dx}{dt} = rx^{\mu_1}\left(1 - \frac{x}{K}\right)^{\mu_3}. \tag{1.3}$$

Blumberg's equation (1.3) is consistent with the Turner and co-author's generic equation (1.2) when $\mu_1 = 2 - \mu_3, \mu_3 < 2$, and $\mu_2 = 1$. Von Bertalanffy [3] introduced his growth equation to model fish weight growth. He proposed the form given below which can be seen to be a special case of the Bernoulli differential equation:

$$\frac{dx}{dt} = rx^{\frac{2}{3}}\left[1 - \left(\frac{x}{K}\right)^{\frac{1}{3}}\right]. \tag{1.4}$$

The Turner model does not contain the Bertalanffy one, as the values of the exponents $\mu_1 = 2/3, \mu_2 = 1/3, \mu_3 = 1$, violate the condition $\mu_1 = 1 + \mu_2(1 - \mu_3)$ stipulated by Turner et al. [32]. It cannot therefore be seen as a special case of Blumberg's equation (1.3). Richards [27] extended the growth equation developed by Von Bertalanffy to fit empirical plant data.

Richards's suggestion was to use the following equation which is also a Bernoulli differential equation

$$\frac{dx}{dt} = rx\left[1 - \left(\frac{x}{K}\right)^{\mu_2}\right]. \tag{1.5}$$

Unlike its Von Bertalanffy antecedent however, the Richards growth function does follow from the Turner model (1.2) in the case where $\mu_3 = 1$. For $\mu_2 = 1$, (1.5) trivially reduces to the Verhulst logistic growth equation (1.1), but for $\mu_2 > 1$ the maximum slope of the curve is when $x > K/2$, and when $0 < \mu_2 < 1$, the maximum slope of the curve is when $x < K/2$. This allows a wider range of curves to be produced, but as μ_2 tends towards zero, the lowest value of x at the point of inflexion remains greater than K/e, where e represents the universal constant, the base of the natural logarithm. In fact, as μ_2 tends towards zero the Richards growth curve tends towards the Gompertz growth curve, which can be derived from the following form of the logistic equation as a limiting case:

$$\frac{dx}{dt} = \frac{r}{\mu_2{}^{\mu_3}}x\left[1 - \left(\frac{x}{K}\right)^{\mu_2}\right]^{\mu_3} = \frac{r}{K^{\mu_2\mu_3}}x\left(\frac{K^{\mu_2} - x^{\mu_2}}{\mu_2}\right)^{\mu_3}.$$

When $\mu_2 \to 0$, we obtain the growth rate modeled by the Gompertz function given by:

$$\frac{dx}{dt} = rx\left[\ln\left(\frac{x}{K}\right)\right]^{\mu_3}, \tag{1.6}$$

with $\mu_3 > 0$ and $\mu_3 \neq 1$. This special case is more usually known as the hyper Gompertz, generalized ecological growth function, or simply generalized Gompertz function. For $\mu_3 = 1$ the equation (1.6) is the ordinary Gompertz growth (see [12,24]).

In [31], Tsoularis et al. proposed a new growth rate that includes all the previous growth rates given by:

$$\frac{dx}{dt} = rx^{\mu_1}\left[1 - \left(\frac{x}{K}\right)^{\mu_2}\right]^{\mu_3}, \tag{1.7}$$

where μ_1, μ_2 and μ_3 are positive real numbers. Unlike Lotka's derivation of the Verhulst logistic growth equation from the truncation of the Taylor series expansion of $f(x)$ near $x = 0$, (1.7) cannot be derived from such an expansion unless μ_1, μ_2 and μ_3 are all positive integers.

In 1977, Freedman and Waltman [9] consider a two-patch model with a single species in logistic population growth as follows:

$$\begin{cases} \dfrac{dx_1}{dt} = r_1x_1\left(1 - \dfrac{x_1}{K_1}\right) + m(x_2 - x_1), \\ \dfrac{dx_2}{dt} = r_2x_2\left(1 - \dfrac{x_2}{K_2}\right) + m(x_1 - x_2), \end{cases} \tag{1.8}$$

where x_i represents the population density in patch i, the parameter r_i is the intrinsic growth rate, K_i is carrying capacity and m is the dispersal rate. Freedman and Waltman show that under certain conditions, the total population abundance can be larger than the total carrying capacities $K_1 + K_2$. Holt [15] generalized these results to a source-sink system. In 2015, Arditi et al. [1] gave a full mathematical analysis of the model (1.8) of Freedman and Waltman with symmetric dispersal.

In 2018, Arditi et al. [2] extended the model (1.8) by considering asymmetric dispersal, i.e. the model:

$$\begin{cases} \dfrac{dx_1}{dt} = r_1x_1\left(1-\dfrac{x_1}{K_1}\right) + m(m_{12}x_2 - m_{21}x_1), \\ \dfrac{dx_2}{dt} = r_2x_2\left(1-\dfrac{x_2}{K_2}\right) + m(m_{21}x_1 - m_{12}x_2), \end{cases} \tag{1.9}$$

where mm_{12} and mm_{21} with $m_{ij} > 0, i \neq j$ and $m \geq 0$, are the migration terms which describe the flows of individuals from the patch 2 to the patch 1, and from the patch 1 to the patch 2 respectively. These flows can for example depend on the distance between the patches. By noting that the positive equilibrium (x_1^*, x_2^*) of model (1.9) is the unique positive solution to

$$\begin{cases} r_1x_1\left(1-\dfrac{x_1}{K_1}\right) + r_2x_2\left(1-\dfrac{x_2}{K_2}\right) = 0, \\ x_2 = \frac{1}{m_{12}}\left(m_{21}x_1 - \frac{r_1}{m}x_1\left(1-\dfrac{x_1}{K_1}\right)\right), \end{cases}$$

i.e., the intersection of an ellipse and a parabola, they used a graphical method to completely analyze model (1.9) in order to determine when dispersal is either favorable or unfavorable to total population abundance (see Appendix B).

Wu et al. [35] studied the following two-patch source-sink model:

$$\begin{cases} \dfrac{dx_1}{dt} = r_1x_1\left(1-\dfrac{x_1}{K_1}\right) + m(x_2 - sx_1), \\ \dfrac{dx_2}{dt} = r_2x_2\left(-1-\dfrac{x_2}{K_2}\right) + m(sx_1 - x_2), \end{cases} \tag{1.10}$$

where the parameter s reflects the dispersal asymmetry. The authors show that the dispersal asymmetry can lead to either an increased total size of the species population in two patches, a decreased total size with persistence in the patches, or even extinction in both patches. They show also that for a large growth rate of the species in the source and a fixed dispersal intensity:

- If the asymmetry is small, the population would persist in both patches and reach a density higher than that without dispersal, in which the population approaches its maximal density at an appropriate asymmetry.
- If the asymmetry is intermediate, the population persists in both patches but reaches a density less than that without dispersal.
- If the asymmetry is large, the population goes to extinction in both patches, and asymmetric dispersal is more favorable than symmetric dispersal under certain conditions.

Kang et al. [16] have considered a two-patch model with Allee effect and dispersal:

$$\begin{cases} \frac{dx_1}{dt} = r_1x_1\left(x_1-\theta\right)\left(1-x_1\right) + m(x_2 - x_1), \\ \frac{dx_2}{dt} = r_2x_2\left(x_2-\theta\right)\left(1-x_2\right) + m(x_1 - x_2), \end{cases} \tag{1.11}$$

where x_1 and x_2 denote the population density in two patches. The parameters $m \in [0,1]$ and θ represent the dispersal intensity and Allee threshold, respectively. It was shown that the dispersal parameter m and the Allee threshold θ will affect the global dynamics. Another important two-patch model with additive Allee effect is proposed and studied in [5], given by:

$$\begin{cases} \dfrac{dx_1}{dt} = -x_1 + m(m_{12}x_2 - m_{21}x_1), \\ \dfrac{dx_2}{dt} = x_2\left(1 - x_2 - \dfrac{\sigma}{x_2 + a}\right) + m(m_{21}x_1 - m_{12}x_2), \end{cases} \tag{1.12}$$

where the positive parameters σ and a are the Allee effect constants. Note that, the additive Allee effect consists of two cases, i.e., weak and strong Allee effects. That is, if $0 < \sigma < a$, it is the weak Allee effect; if $\sigma > a$, it is the strong Allee effect. The authors show that dispersal and Allee effect may lead to persistence or extinction in both patches. Also, by mathematical analysis with numerical simulation, they verified that the total population abundance will increase when the Allee effect constant a increases or σ decreases. And the total population density increases when the dispersal rate m_{12} increases or the dispersal rate m_{21} decreases. The reader may refer to [16, 22, 23, 25, 28] for more references and details on the effects of dispersal on the total population in discrete space additive Allee effect. For more details and information on the maximization of the total population with logistic growth in a multi-patchy environment, the reader is referred to [7, 8, 11] and the references therein.

This paper is organized as follows: in Section 2, we introduce Richard's model in two patches. Next, in Section 3, we study the behavior of the system (2.1) in the case when the migration rate goes to infinity using perturbation arguments. In Section 4, we compare the total equilibrium population with the sum of the two carrying capacities for all parameter space by using the same method as Arditi et al. [2]. In Section 5, two-patch model (2.1) where one growth rate is much larger than the second one is considered, we compare the total equilibrium population with the sum of two capacities in this case. In Appendix A, we analyze the existence of equilibrium point by geometrical method and we prove also the global stability of the system (2.1) and in Appendix B, we recall some result on two-patch logistic model.

2 Two-patch Richards model

Taking the case of two patches, coupled by asymmetric migration terms, and assuming that each patch follows the same Richards law (1.5), the two-patch Richards model can be written in the following form:

$$\begin{cases} \dfrac{dx_1}{dt} = r_1x_1\left[1 - \left(\dfrac{x_1}{K_1}\right)^{\mu}\right] + m(m_{12}x_2 - m_{21}x_1), \\ \dfrac{dx_2}{dt} = r_2x_2\left[1 - \left(\dfrac{x_2}{K_2}\right)^{\mu}\right] + m(m_{21}x_1 - m_{12}x_2), \end{cases} \tag{2.1}$$

where x_i is the population in the patch i, the parameters r_i and K_i are respectively the intrinsic growth rate and the carrying capacity in the patch i, and μ is a positive number. The parameters mm_{12} and mm_{21} with $m_{12} > 0$ and $m_{21} > 0$, represent the migration terms which describe the flows of individuals from the patch 2 to the patch 1, and from the patch 1 to the patch 2 respectively. For $\mu = 1$, the system (2.1) trivially reduces to Two-patch logistic model (1.9). Note that the system (1.9) is studied in [1, 6, 9, 10, 15] in the case where the migration rates satisfy $m_{12} = m_{21}$, and in [2, 26] for general migration rates. Model (2.1) has always a unique positive equilibrium, again denoted by $\mathcal{E}^*(m) := (x_1^*(m), x_2^*(m))$ which satisfies

$$\begin{cases} 0 = r_1 x_1^*(m)\left[1 - \left(\dfrac{x_1^*(m)}{K_1}\right)^{\mu}\right] + m(m_{12}x_2^*(m) - m_{21}x_1^*(m)), \\ 0 = r_2 x_2^*(m)\left[1 - \left(\dfrac{x_2^*(m)}{K_2}\right)^{\mu}\right] + m(m_{21}x_1^*(m) - m_{12}x_2^*(m)). \end{cases}$$

The equilibrium $\mathcal{E}^*$ is GAS in $\mathbb{R}^2 \setminus \{0\}$ (see Appendix A). We thus define the total equilibrium population at the positive equilibrium under dispersal rate , i.e.

$$X_T^*(m) = x_1^*(m) + x_2^*(m), \tag{2.2}$$

as the total realized asymptotic population abundance.

The main aim of this paper is to study the effect of population dispersal on total population size and to perform the mathematical analysis of the two-patch Richards model (2.1) in the full parameter space. Thus, we extend [1,2] by considering the case $\mu \neq 1$.

3 The behavior of the model for a large migration rate

In this section, we aim to study the behavior of the system (2.1) for a large migration rate, i.e. when $m \to \infty$. We have the following result:

Theorem 3.1. Let $\mathcal{E}^*(m)$ be the positive equilibrium of the system (2.1). We then have :

$$\lim_{m\to\infty} \mathcal{E}^*(m) = \left(\frac{m_{12}r_1 + m_{21}r_2}{m_{12}^{\mu+1}\frac{r_1}{K_1^{\mu}} + m_{21}^{\mu+1}\frac{r_2}{K_2^{\mu}}}\right)^{\frac{1}{\mu}} (m_{12}, m_{21})\,. \tag{3.1}$$

Proof. Denote $\mathcal{E}^*(\infty)$ the limit (3.1). The equilibrium point $\mathcal{E}^*(m)$ of the system (2.1) is the solution of the equation $F_m = 0$, where:

$$F_m(x_1, x_2) = \left(\ r_1 x_1\left[1 - \left(\tfrac{x_1}{K_1}\right)^{\mu}\right] + r_2 x_2\left[1 - \left(\tfrac{x_2}{K_2}\right)^{\mu}\right], r_2 x_2\left[1 - \left(\tfrac{x_2}{K_2}\right)^{\mu}\right] + m(m_{21}x_1 - m_{12}x_2)\ \right). \tag{3.2}$$

When $m \to \infty$, Equation (3.2) becomes:

$$F_\infty(x_1, x_2) = \left(\ r_1 x_1\left[1 - \left(\tfrac{x_1}{K_1}\right)^{\mu}\right] + r_2 x_2\left[1 - \left(\tfrac{x_2}{K_2}\right)^{\mu}\right], m_{21}x_1 - m_{12}x_2\ \right). \tag{3.3}$$

The solutions of the equation $F_\infty = 0$ are given by 0 and $\mathcal{E}^*(\infty)$. Therefore, to prove the convergence of $\mathcal{E}^*(m)$ to $\mathcal{E}^*(\infty)$, it suffices to prove that the origin cannot be a limit point of $\mathcal{E}^*(m)$. We claim that for any m, there exists $i \in \{1,2\}$ such that $x_i^*(m) \geq K_i$, which entails that $E^*(m)$ is bounded away from the origin. If $m_{12}x_2^*(m) \leq m_{21}x_1^*(m)$ then we have

$$r_2 x_2^*(m)\left[1 - \left(\frac{x_2^*(m)}{K_2}\right)^{\mu}\right] \leq 0,$$

and since x_2^* cannot be negative or 0, we have $x_2^*(m) \geq K_2$. Therefore, $\mathcal{E}^*(m) \to \mathcal{E}^*(+\infty)$ as $m \to \infty$. □

As a first corollary of the previous theorem we obtain the following result which describes the total equilibrium population when $m \to \infty$:

Corollary 3.2. Consider the total equilibrium population (2.2). We have:

$$X_T^*(+\infty) = (m_{12} + m_{21}) \left(\frac{m_{12}r_1 + m_{21}r_2}{m_{12}^{\mu+1}\frac{r_1}{K_1^\mu} + m_{21}^{\mu+1}\frac{r_2}{K_2^\mu}} \right)^{\frac{1}{\mu}}. \quad (3.4)$$

Notice that, the formula (3.4) shows that the total equilibrium population depends on the migration terms m_{12}, m_{21} and the parameter μ . For $\mu = 1$, this formula was obtained for the 2-patch logistic model (1.9) by Freedman and Waltman [10, Theorem 1]. It was also obtained by Arditi et al. [1, Formula (A.13)]. If the migration is symmetric (i.e. $m_{12} = m_{21}$), then the total equilibrium population (3.4) does not depend on the flux of migration m_{12} and m_{21} and (3.4) becomes:

$$X_T^*(+\infty) = 2 \left(\frac{r_1 + r_2}{\frac{r_1}{K_1^\mu} + \frac{r_2}{K_2^\mu}} \right)^{\frac{1}{\mu}}.$$

In [1], Arditi et al. also obtained the formula (3.4), in the 2-patch case with logistic model and symmetric migration, (i.e. the system (1.9) with $m_{12} = m_{21} = 1$) by using singular perturbation theory, see [1, Formula (A.13)]. They showed that, if $(x_1(t,m), x_2(t,m))$ is the solution of (1.9), with initial condition (x_1^0, x_2^0), then, when $m \to \infty$, the total population $x_1(t,m) + x_2(t,m)$ is approximated by $X(t)$, the solution of the logistic equation:

$$\begin{cases} \dfrac{dX}{dt} = rX\left(1 - \dfrac{X}{2K}\right), \\ X(0) = x_1^0 + x_2^0, \end{cases} \quad (3.5)$$

where $r = \frac{r_1+r_2}{2}, K = \frac{r_1+r_2}{\alpha_1+\alpha_2}$ and $\alpha_i = \frac{r_i}{K_i}$. Therefore the total population behaves like the unique logistic equation given by (3.5). In addition, one obtains the following property: with the exception of a small initial interval, the populations density $x_1(t,m)$ and $x_2(t,m)$ are both approximated by $X(t)/2$, see [1, Proposition 3]. Therefore, this approximation shows that, when t and m tend to ∞, the density population $x_i(t,m)$ tends toward $\frac{r_1+r_2}{\alpha_1+\alpha 2}$, and in addition, $x_i(t,m)$ quickly jumps from its initial condition x_i^0 to the average $X_0/2$ and then is very close to $X(t)/2$. Our aim is to generalize this result for the 2-patch model (2.1) for all μ positive. To avoid any confusion with $X(t)$, which is the total population, we denote $Z(t)$ the solution of the equation (3.6), and we prove that $X(t)$ is asymptotically equivalent, when m goes to infinity, to $Z(t)$. We have the following result

Theorem 3.3. Let $(x_1(t,m), x_2(t,m))$ be the solution of the system (2.1) with initial condition (x_1^0, x_2^0) satisfying $x_i^0 \geq 0$ for $i = 1, 2$. Let $Z(t)$ be the solution of the Richards equation

$$\begin{cases} \dfrac{dX}{dt} = rX\left[1 - \left(\dfrac{X}{(m_{12}+m_{21})K}\right)^\mu\right], \\ X(0) = x_1^0 + x_2^0, \end{cases} \quad (3.6)$$

where $r = \frac{m_{12}r_1+m_{21}r_2}{m_{12}+m_{21}}$ and $K = \left[\frac{m_{12}r_1+m_{21}r_2}{m_{12}^{\mu+1}\frac{r_1}{K_1^\mu}+m_{21}^{\mu+1}\frac{r_2}{K_2^\mu}}\right]^{\frac{1}{\mu}}$. Then, when $m \to \infty$, we have

$$x_1(t,m) + x_2(t,m) = Z(t) + o_m(1), \quad \text{uniformly for } t \in [0, +\infty) \quad (3.7)$$

and, for any $t_0 > 0$, we have

$$\begin{cases} x_1(t,m) = \dfrac{m_{12}}{m_{12}+m_{21}} Z(t) + o_m(1), \\ x_2(t,m) = \dfrac{m_{21}}{m_{12}+m_{21}} Z(t) + o_m(1) \quad \text{uniformly for } t \in [t_0, +\infty). \end{cases} \tag{3.8}$$

Proof. Let $X(t,m) = x_1(t,m) + x_2(t,m)$. We rewrite the system (2.1) using the variables (X, x_1). One obtains:

$$\begin{cases} \dfrac{dX}{dt} = r_1 x_1 \left[1 - \left(\dfrac{x_1}{K_1}\right)^{\mu}\right] + r_2(X - x_1)\left[1 - \left(\dfrac{X - x_1}{K_2}\right)^{\mu}\right], \\ \dfrac{dx_1}{dt} = r_1 x_1 \left[1 - \left(\dfrac{x_1}{K_1}\right)^{\mu}\right] + m\left(m_{12}X - (m_{12}+m_{21})x_1\right). \end{cases} \tag{3.9}$$

When $m \to \infty$, (3.9) is a *slow-fast* system, with one *slow variable*, X, and one *fast variable* x_1. According to Tikhonov's Theorem [17, 30, 34] we consider the dynamics of the fast variable in the time scale $\tau = mt$. One obtains

$$\frac{dx_1}{d\tau} = \frac{1}{m} r_1 x_1 \left[1 - \left(\frac{x_1}{K_1}\right)^{\mu}\right] + m_{12}X - (m_{12}+m_{21})x_1.$$

In the limit $m \to \infty$, we find the *fast dynamics*

$$\frac{dx_1}{d\tau} = m_{12}X - (m_{12}+m_{21})x_1. \tag{3.10}$$

The *slow manifold* is formed by the equilibrium points of the fast equation (3.10), which given by:

$$x_1^* = \frac{m_{12}}{m_{12}+m_{21}} X. \tag{3.11}$$

Since x_1^* is GAS for the system (3.10), the Theorem of Tikhonov ensures that after a fast transition toward the slow manifold, the solutions of (3.9) are approximated by the solutions of the *reduced model* which is obtained by replacing (3.11) into the dynamics of the slow variable, that is:

$$\frac{dX}{dt} = r_1 \frac{m_{12}}{m_{12}+m_{21}} X \left[1 - \left(\frac{m_{12}X}{(m_{12}+m_{21})K_1}\right)^{\mu}\right] + r_2 \frac{m_{21}}{m_{12}+m_{21}} X \left[1 - \left(\frac{m_{21}X}{(m_{12}+m_{21})K_2}\right)^{\mu}\right], \tag{3.12}$$

which gives the equation (3.6). Since (3.6) admits

$$X^* = (m_{12}+m_{21})K = (m_{12}+m_{21}) \left[\frac{m_{12}r_1 + m_{21}r_2}{m_{12}^{\mu+1}\frac{r_1}{K_1^{\mu}} + m_{21}^{\mu+1}\frac{r_2}{K_2^{\mu}}}\right]^{\frac{1}{\mu}}$$

as a positive equilibrium point, which is GAS in the positive axis, the approximation given by Tikhonov's Theorem holds for all $t \geq 0$ for the slow variable and for all $t \geq t_0 > 0$ for the fast variable, where t_0 is small as we want. Therefore, let $Z(t)$ be the solution of the reduced model (3.12) of initial condition $Z(0) = X(0,m) = x_1^0 + x_2^0$, then, when $m \to \infty$, we have the approximations (3.7) and (3.8). □

In the case where the migration rate tends to infinity, the approximation (3.7) shows that the total population behaves like a unique equation of Richards (3.6) and then, when t and m tend to ∞, the total population $x_1(t,m) + x_2(t,m)$ tends towards $X_T^*(\infty)$ defined by (3.4) as stated in Corollary 3.2. The approximation (3.8) shows that, with the exception of a thin initial boundary layer, where the density population $x_1(t,m)$ and $x_2(t,m)$ quickly jumps from its initial condition x_1^0 and x_2^0 to $m_{12}X_0/(m_{12}+m_{12})$ and $m_{21}X_0/(m_{12}+m_{12})$ respectively. The first (resp. second) patch behaves like the single Richards equation

$$\frac{dz}{dt} = rz\left[1-\left(\frac{z}{m_{12}K}\right)^{\mu}\right] \quad \left(\text{resp.} \quad \frac{dz}{dt} = rz\left[1-\left(\frac{z}{m_{21}K}\right)^{\mu}\right]\right), \tag{3.13}$$

where r and K are defined in (3.6). Hence, when t and m tend to ∞, the density population $x_1(t,m)$ and $x_2(t,m)$ tends toward $m_{12}K$ and $m_{21}K$ respectively, as stated in Theorem 3.1.

4 Influence of dispersal on the total population size

In [2], Arditi et al. have considered the system (1.9) and they showed that there are only three cases that can occur: the case where the total equilibrium population is always greater than the sum of carrying capacities, the case where it is always smaller, and a third case, where the effect of dispersal is beneficial for lower values of the migration rate m and detrimental for the higher values. More precisely, it was shown in [2], that the following trichotomy holds

- If $X_T^*(+\infty) > K_1 + K_2$ then $X_T^*(m) > K_1 + K_2$ for all $m > 0$.
- If $\frac{d}{dm}X_T^*(0) > 0$ and $X_T^*(+\infty) < K_1 + K_2$, then there exists $m_0 > 0$ such that $X_T^*(m) > K_1 + K_2$ for $0 < m < m_0$, $X_T^*(m) < K_1 + K_2$ for $m > m_0$ and $X_T^*(m_0) = K_1 + K_2$.
- If $\frac{d}{dm}X_T^*(0) < 0$, then $X_T^*(m) < K_1 + K_2$ for all $m > 0$.

Therefore, the condition $X_T^*(m) = K_1 + K_2$ holds only for $m = 0$ and at most for one positive value $m = m_0$. The value m_0 exists if and only if $\frac{d}{dm}X_T^*(0) > 0$ and $X_T^*(+\infty) < K_1 + K_2$.

In this section, we generalize the result of Arditi et al. [2] by considering the case where $\mu \neq 1$ in the system (2.1). We analyze the effect of dispersal on the total equilibrium population for the Richards system (2.1). Using the method of Arditi et al. [2], we describe the position affects the equilibrium $\mathcal{E}^*(m)$ of (2.1) when the migration rate varies from zero to infinity. The total equilibrium population $X_T^*(+\infty)$, given by equation (3.4), play a vary important role in the characterization of the different possible positions of the equilibrium $\mathcal{E}^*$. As for the 2-patch logistic model (1.9), we prove that exactly three cases can occur. More precisely we have the following theorem:

Theorem 4.1. Consider the system (2.1). Let $X_T^*(\infty)$ be defined by (3.4). Then,

1. If $r_1 = r_2$, then $X_T^*(m) \leq K_1 + K_2$ for all $m \geq 0$.
2. If $r_1 < r_2$, then
   (a) If $\frac{m_{21}}{m_{12}} < \frac{K_1}{K_2}$, then
      i. If $X_T^*(\infty) \geq K_1 + K_2$, then $X_T^*(m) \geq K_1 + K_2$ for all $m \geq 0$.
      ii. If $X_T^*(\infty) < K_1 + K_2$, there is an $m_0 > 0$ such that:
         A. If $m < m_0$, then $X_T^*(m) \geq K_1 + K_2$.

B. If $m \geq m_0$, then $X_T^*(m) \leq K_1 + K_2$.

(b) If $\frac{m_{21}}{m_{12}} > \frac{K_1}{K_2}$, then $X_T^*(m) \leq K_1 + K_2$ for all $m \geq 0$.

(c) If $\frac{m_{21}}{m_{12}} = \frac{K_1}{K_2}$, then $X_T^*(m) = K_1 + K_2$ for all $m \geq 0$, i.e. the equilibrium $\mathcal{E}^*$ does not depend on m.

3. If $r_1 > r_2$, then

(a) If $\frac{m_{21}}{m_{12}} > \frac{K_1}{K_2}$, then

i. If $X_T^*(\infty) \geq K_1 + K_2$, then $X_T^*(m) \geq K_1 + K_2$.

ii. If $X_T^*(\infty) < K_1 + K_2$, there is a $m_0 > 0$ such that:

A. If $m < m_0$, then $X_T^*(m) \geq K_1 + K_2$.

B. If $m \geq m_0$, then $X_T^*(m) \leq K_1 + K_2$.

(b) If $\frac{m_{21}}{m_{12}} < \frac{K_1}{K_2}$, then $X_T^*(m) \leq K_1 + K_2$ for all $m \geq 0$.

(c) If $\frac{m_{21}}{m_{12}} = \frac{K_1}{K_2}$, then $X_T^*(m) = K_1 + K_2$ for all $m \geq 0$, i.e. the equilibrium $\mathcal{E}^*$ does not depend on m.

Proof. First, we consider the line Δ with Cartesian equation $x_1 + x_2 = K_1 + K_2$, of slope -1 and passing through the point $A = (K_1, K_2)$. The equilibrium point $\mathcal{E}^*$ is always on the curve $\mathcal{C}_\mu$ (see Appendix A). For $m = 0$, $\mathcal{E}^*$ coincides with A. When m increases, $\mathcal{E}^*$ describes an arc of the curve $\mathcal{C}_\mu$ and ends at point $\mathcal{E}^*(\infty)$ given in equation (3.1).

1. The equation of the tangent line to the curve $\mathcal{C}_\mu$ at the point $\mathcal{A}$ is given by:

$$(x_1 - K_1)\frac{\partial \Phi_\mu}{\partial x_1}(\mathcal{A}) + (x_2 - K_2)\frac{\partial \Phi_\mu}{\partial x_2}(\mathcal{A}) = 0, \tag{4.1}$$

where the function Φ_μ is given by the equation (A.2). Since $\frac{\partial \Phi_\mu}{\partial x_1}(\mathcal{A}) = -\mu r_1$ and $\frac{\partial \Phi_\mu}{\partial x_2}(\mathcal{A}) = -\mu r_2$, Equation (4.1) becomes simply

$$r_1 x_1 + r_2 x_2 = r_1 K_1 + r_2 K_2. \tag{4.2}$$

If $r_1 = r_2$ in the equation (4.2), the tangent space to the the curve $\mathcal{C}_\mu$ at $\mathcal{A}$ is the line Δ. By the concavity of $\mathcal{C}_\mu$, any point of $\mathcal{C}_\mu$ lies below the line Δ. Therefore $\mathcal{E}^*(m)$ satisfies $x_1^*(m) + x_2^*(m) \leq K_1 + K_2$, for all $m \geq 0$ (see figure 4.1), which completes the proof of item 1.

2. We suppose now that $r_1 < r_2$, then the line Δ makes a second intersection with the curve $\mathcal{C}_\mu$ at a point noted C. This intersection is below the line $\Sigma : x_2 = \dfrac{K_2}{K_1}x_1$ (as shown in the figures 4.2, 4.3 and 4.4). When $m \to \infty$, the curve $M_{m,\mu}$ defined by (A.3), goes to the oblique line $M_{\infty,\mu} : x_2 = \frac{m_{21}}{m_{12}}x_1$. The intersection points between the line $M_{\infty,\mu}$ and the curve $\mathcal{C}_\mu$ are the origin and $\mathcal{E}^*(\infty)$. If the line $M_{\infty,\mu}$ is below the line Σ, that is $m_{21}/m_{12} < K_1/K_2$, we have two possible cases for the relative positions of the point $\mathcal{E}^*(\infty)$ and the line Δ. In the case where $\mathcal{E}^*(\infty)$ is above the line Δ, that is $X_T^*(\infty) \geq K_1 + K_2$, then the equilibrium point start at point A and when m increases from 0 to ∞, $\mathcal{E}^*(m)$ moves along the curve $\mathcal{C}_\mu$ and ends at the point $\mathcal{E}^*(\infty)$. Equivalently, the total equilibrium population start, for $m = 0$, with the value $K_1 + K_2$ and satisfies

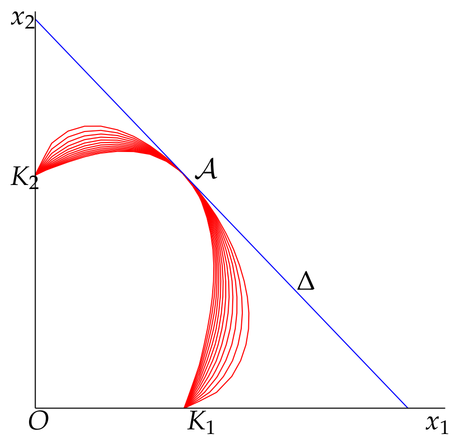

Figure 4.1: The illustration of item 1 of Theorem 4.1. The curve $\mathcal{C}_\mu$ is shown in red for some values of μ and the straight line Δ in blue. The total equilibrium population is always smaller than $K_1 + K_2$ for all m because it belongs to the curve $\mathcal{C}_\mu$.

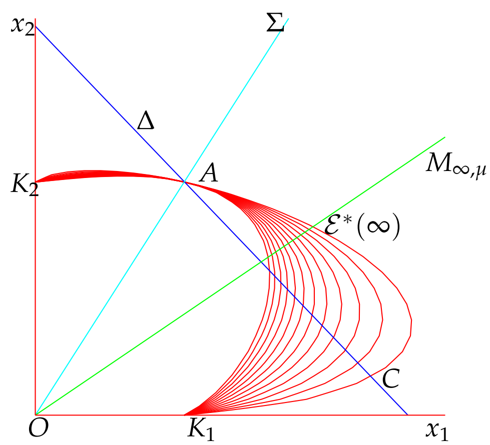

Figure 4.2: The illustration of item (2.a.i) of Theorem 4.1. The curve $\mathcal{C}_\mu$ is shown in red for some values of μ, the straight lines Δ, Σ and $M_{\infty,\mu}$ are shown in blue, cyan and green respectively. The total equilibrium point is always greater than $K_1 + K_2$ for all m, because it belongs to the curve $\mathcal{C}_\mu$ and the limit point $\mathcal{E}^*(\infty)$ is above Δ. As the migration rate increases from 0 to ∞, the equilibrium point varies along the curve $\mathcal{C}_\mu$ from A to $\mathcal{E}^*(\infty)$.

the inequality $x_1^*(m) + x_2^*(m) \geq K_1 + K_2$ for all m, which completes the proof of item (2.a.i). (see figure 4.2).

In the case where $\mathcal{E}^*(\infty)$ is below the line Δ, that is $X_T^*(\infty) < K_1 + K_2$, the equilibrium point $\mathcal{E}^*(m)$ start, for $m = 0$, at point A and when m increases from 0 to ∞, it moves along the curve $\mathcal{C}_\mu$, passes through the point $\mathcal{C}$ for a certain m_0 and ends at the point $\mathcal{E}^*(\infty)$. Therefore, the total equilibrium is greater than $K_1 + K_2$ for $m < m_0$ and smaller than $K_1 + K_2$ for all $m \geq m_0$, which completes the proof of item (2.a.ii) (see figure 4.3).

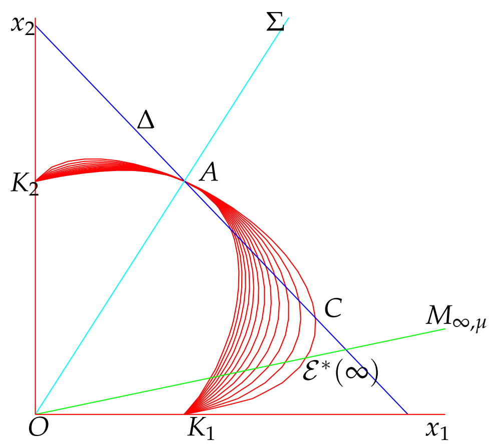

Figure 4.3: The illustration of item (2.a-ii) of Theorem 4.1. The curve $\mathcal{C}_\mu$ is shown in red for some values of μ, the straight lines Δ, Σ and $M_{\infty,\mu}$ are shown in blue, cyan and green respectively. As the limit point $\mathcal{E}^*(\infty)$ is above Δ, then, when the migration rate increases from 0 to ∞, the equilibrium point varies along the curve $\mathcal{C}_\mu$ from A to $\mathcal{E}^*(\infty)$, passing through the point C which is the other point of intersection between the curve $\mathcal{C}_\mu$ and the line Δ.

If the line $M_{\infty,\mu}$ is above the line Σ, that is $m_{21}/m_{12} > K_1/K_2$, then the total equilibrium population is smaller than the sum of carrying capacities for all m. This completes the proof of item (2.b). (see figure 4.4).

It is clear that if the two lines Σ and $M_{\infty,\mu}$ are identical, i.e. $\mathcal{A} = \mathcal{E}^*(\infty)$, then the total equilibrium population does not depend on migration rate m. Therefore, $x_1^*(m) = K_1$ and $x_2^*(m) = K_2$ for all $m \geq 0$. This gives the proof of item (2.c).

3. As the role of the variables of the system (2.1) is symmetrical, this case is analogous to case 2.

□

According to the previous theorem, we concluded that, the dispersal can lead to an increased or decreased the total equilibrium population with persistence in each patch.

Proposition 4.2. The derivative of the total equilibrium population X_T^* at $m = 0$ is given by:

$$\frac{dX_T^*}{dm}(0) = \frac{1}{\mu}\left(m_{12}K_2 - m_{21}K_1\right)\left(\frac{1}{r_1} - \frac{1}{r_2}\right). \tag{4.3}$$

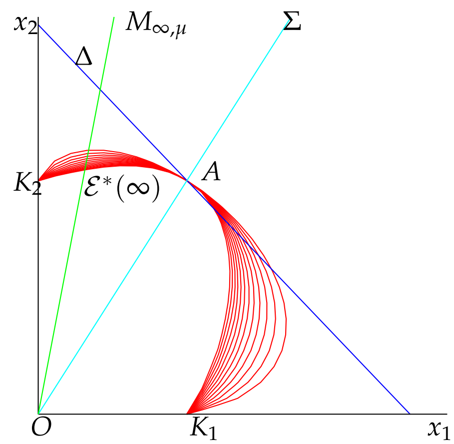

Figure 4.4: The illustration of item (b) of Theorem 4.1. The curve $\mathcal{C}_\mu$ is shown in red for some values of μ, the straight lines Δ, Σ and $M_{\infty,\mu}$ are shown in blue, cyan and green respectively. The total equilibrium is always smaller than $K_1 + K_2$ for all m.

In particular, $\frac{dX_T^*}{dm}(0) = 0$ if and only if, $r_1 = r_2$ or $\frac{K_1}{K_2} = \frac{m_{12}}{m_{21}}$.

Proof. The equilibrium point $\mathcal{E}^*(m)$ satisfies the system

$$\begin{cases} 0 = r_1 x_1^*(m)\left[1 - \left(\frac{x_1^*(m)}{K_1}\right)^\mu\right] + m(m_{12}x_2^*(m) - m_{21}x_1^*(m)), \\ 0 = r_2 x_2^*(m)\left[1 - \left(\frac{x_2^*(m)}{K_2}\right)^\mu\right] + m(m_{21}x_1^*(m) - m_{12}x_2^*(m)). \end{cases} \tag{4.4}$$

Dividing the first and the second equation by $\frac{r_1}{K_1^\mu}x_1^*(m)$ and $\frac{r_2}{K_2^\mu}x_2^*(m)$ respectively, one obtains

$$\begin{cases} x_1^*(m) = \left(K_1^\mu + m\dfrac{m_{12}x_2^*(m) - m_{21}x_1^*(m)}{\frac{r_1}{K_1^\mu}x_1^*(m)}\right)^{\frac{1}{\mu}}, \\ x_2^*(m) = \left(K_2^\mu + m\dfrac{m_{21}x_1^*(m) - m_{12}x_2^*(m)}{\frac{r_2}{K_2^\mu}x_2^*(m)}\right)^{\frac{1}{\mu}}. \end{cases} \tag{4.5}$$

Hence, the total equilibrium population X_T^* is given by

$$X_T^*(m) = \left(K_1^\mu + m\frac{m_{12}x_2^*(m) - m_{21}x_1^*(m)}{\frac{r_1}{K_1^\mu}x_1^*(m)}\right)^{\frac{1}{\mu}} + \left(K_2^\mu + m\frac{m_{21}x_1^*(m) - m_{12}x_2^*(m)}{\frac{r_2}{K_2^\mu}x_2^*(m)}\right)^{\frac{1}{\mu}}. \tag{4.6}$$

By differentiating the equation (4.6) at $m = 0$, we get:

$$\frac{dX_T^*}{dm}(0) = \frac{1}{\mu}\left(\frac{m_{12}x_2^*(0) - m_{21}x_1^*(0)}{\frac{r_1}{K_1^\mu}x_1^*(0)}\right)K_1^{1-\mu} + \frac{1}{\mu}\left(\frac{m_{21}x_1^*(0) - m_{12}x_2^*(0)}{\frac{r_2}{K_2^\mu}x_2^*(0)}\right)K_2^{1-\mu}, \tag{4.7}$$

which gives (4.3), since $x_1^*(0) = K_1$ and $x_2^*(0) = K_2$. □

Note that, the derivative (4.3) is dependent on all the parameters of the model. it is equal to zero if and only if both patches have the same growth rates or $m_{12}K_2 = m_{21}K_1$, positive if $r_1 < r_2$ and $m_{12}K_2 > m_{21}K_1$, or $r_1 > r_2$ and $m_{12}K_2 < m_{21}K_1$.

As a corollary of the previous theorem, we have the result:

Corollary 4.3. Let $\mu_i, i = 1, \ldots, n$, be a positive number such that $0 < \mu_0 < \ldots < \mu_n$. Consider the following systems:

$$\begin{cases} \dfrac{dx_1}{dt} = r_1 x_1 \left[1 - \left(\dfrac{x_1}{K_1}\right)^{\mu_i}\right] + m(m_{12}x_2 - m_{21}x_1), \\ \dfrac{dx_2}{dt} = r_2 x_2 \left[1 - \left(\dfrac{x_2}{K_2}\right)^{\mu_i}\right] + m(m_{21}x_1 - m_{12}x_2), \end{cases} \tag{4.8}$$

where the parameters r_i, K_i, m_{12} and m_{21} are as in (2.1). Let $X_T^*(m, \mu_i), i = 1, \ldots, n$ be the total equilibrium population of (4.8). Then, the sequence $(X_T^*(m, \mu_i))_{1 \le i \le n}$ is increasing. In particular, when $m \to \infty$, we have:

$$X_T^*(\infty, \mu_1) < \ldots < X_T^*(\infty, \mu_n).$$

Proof. The equilibrium point of the system (4.8) is always on the curve noted $\mathcal{C}_{\mu_i}$ given by

$$\mathcal{C}_{\mu_i}: \quad r_1 x_1 \left[1 - \left(\frac{x_1}{K_1}\right)^{\mu_i}\right] + r_2 x_2 \left[1 - \left(\frac{x_2}{K_2}\right)^{\mu_i}\right] = 0.$$

These curves intersect at four points $(0,0), (0, K_2), (K_1, 0)$ and (K_1, K_2). If $\mu_i < \mu_j$ for some i and j, then the curve $\mathcal{C}_{\mu_i}$ is below the curve $\mathcal{C}_{\mu_j}$ as shown in the figure A.1 and in the others figures 4.1, 4.2, 4.3 and 4.4. Therefore, the total equilibrium population $X_T^*(m, \mu_i) < X_T^*(m, \mu_j)$ for all $m > 0$ and for all $i, j \in \{1, \ldots, n\}$. □

5 Two-patch model where one growth rate is much larger than the second one

In this section, we consider the two-patch model (2.1) and we assume that the growth rate in the second patch is much larger than in the first. For simplicity we denote $m_2 := m_{12} > 0$ the migration rate from patch 2 to patch 1 and $m_1 := m_{21} > 0$ from patch 1 to patch 2. Mathematically, the model (2.1) is written under this assumption as follows:

$$\begin{cases} \frac{dx_1}{dt} = r_1 x_1 \left[1 - \left(\frac{x_1}{K_1}\right)^{\mu}\right] + m\left(m_2 x_2 - m_1 x_1\right), \\ \frac{dx_2}{dt} = \frac{r_2}{\epsilon} x_2 \left[1 - \left(\frac{x_2}{K_2}\right)^{\mu}\right] + m\left(m_1 x_1 - m_2 x_2\right), \end{cases} \tag{5.1}$$

where ϵ is assumed to be a small positive number. We denote $E^*(m, \epsilon) = (x_1^*(m, \epsilon), x_2^*(m, \epsilon))$, the positive equilibrium of (5.1), which is GAS, and $X_T^*(m, \epsilon) := x_1^*(m, \epsilon) + x_2^*(m, \epsilon)$ the total equilibrium. The behavior of the model (5.1) for perfect mixing (i.e. $m \to \infty$) is given by the following formula:

$$X_T^*(+\infty, \epsilon) = (m_1 + m_2)\left(\frac{\epsilon m_2 r_1 + m_1 r_2}{\epsilon m_2^{\mu+1} r_1 / K_1^{\mu} + m_1^{\mu+1} r_2 / K_2^{\mu}}\right)^{\frac{1}{\mu}}, \tag{5.2}$$

and the derivative of the total equilibrium population $X_T^*(m,\epsilon)$ at $m = 0$ becomes

$$\frac{dX_T^*}{dt}(0,\epsilon) = \frac{1}{\mu}\left(m_{12}K_2 - m_{21}K_1\right)\left(\frac{1}{r_1} - \frac{\epsilon}{r_2}\right). \tag{5.3}$$

First, we have the result:

Theorem 5.1. Let $(x_1(t,\epsilon), x_2(t,\epsilon))$ be the solution of the system (5.1) with initial condition (x_1^0, x_2^0) satisfying $x_i^0 \geq 0$ for $i = 1,2$. Let $z(t)$ be the solution of the differential equation

$$\frac{dx_1}{dt} = r_1 x_1\left[1 - \left(\frac{x_1}{K_1}\right)^{\mu}\right] + m(m_2K_2 - m_1x_1) =: \varphi_\mu(x_1), \tag{5.4}$$

with initial condition $z(0) = x_1^0$. Then, when $\epsilon \to 0$, we have

$$x_1(t,\epsilon) = z(t) + o_\epsilon(1), \qquad \text{uniformly for } t \in [0,+\infty) \tag{5.5}$$

and, for any $t_0 > 0$, we have

$$x_2(t,\epsilon) = K_2 + o_\epsilon(1), \quad \text{uniformly for} \quad t \in [t_0,+\infty). \tag{5.6}$$

Proof. When $\epsilon \to 0$, the system (5.1) is a *slow-fast* system, with one *slow variable*, x_1, and one *fast variable*, x_2. Tikhonov's Theorem [17,30,34] prompts us to consider the dynamics of the fast variable in the time scale $\tau = \frac{1}{\epsilon}t$. One obtains

$$\frac{dx_2}{d\tau} = r_2x_2\left[1 - \left(\frac{x_2}{K_2}\right)^{\mu}\right] + \epsilon m(m_1x_1 - m_2x_2).$$

In the limit $\epsilon \to 0$, we find the *fast dynamics*

$$\frac{dx_2}{d\tau} = r_2x_2\left[1 - \left(\frac{x_2}{K_2}\right)^{\mu}\right]. \tag{5.7}$$

The slow manifold is given by the positive equilibrium of the system (5.7), i.e. $x_2 = K_2$, which is GAS in the positive axis. When ϵ goes to zero, Tikhonov's Theorem ensures that after a fast transition toward the slow manifold, the solutions of (5.1) converge to the solutions of the *reduced model* (5.4), obtained by replacing $x_2 = K_2$ into the dynamics of the slow variable.

The differential equation (5.4) admits unique positive equilibrium, which is GAS. Indeed, we distinguish two cases according to sign of $r_1 - mm_1$. First, note that, if $r_1 - mm_1 = 0$, then $\frac{d\varphi_\mu}{dx_1}(x_1) = -(\mu+1)\frac{r_1}{K_1^\mu}x_1^\mu + r_1 - mm_1 = 0$ if and only if $x_1 = 0$.

If $r_1 - mm_1 < 0$, then $\frac{d\varphi_\mu}{dx_1}(x_1) = -(\mu+1)\frac{r_1}{K_1^\mu}x_1^\mu + r_1 - mm_1 < 0$, for all $x_1 \geq 0$. In addition, $\varphi_\mu(0) > 0$ and $\varphi_\mu \to -\infty$ when x_1 goes to infinity. So, there exists a unique positive solution of $\varphi_\mu(x_1) = 0$. Denote $x_1^*(m,0^+)$ this solution. As $\varphi_\mu(x_1) > 0$ for all $0 \leq x_1 < x_1^*(m,0^+)$ and $\varphi_\mu(x_1) < 0$ for all $x_1 > x_1^*(m,0^+)$ then, the equilibrium $x_1^*(m,0^+)$ is GAS in the positive axis.

If $r_1 - mm_1 > 0$, then $\frac{d\varphi_\mu}{dx_1}(x_1) = 0$ implies $\tilde{x_1} := \left(\frac{r_1 - mm_1}{(\mu+1)r_1/K_1^\mu}\right)^{\frac{1}{\mu}} > 0$. So φ_μ is increasing on $[0,\tilde{x_1}[$ and decreasing on $]\tilde{x_1},\infty[$. In addition, $\varphi_\mu(0) > 0$ and $\varphi_\mu \to -\infty$ when x_1 goes to infinity. So, there exists unique positive solution of $\varphi_\mu(x_1) = 0$ denoted $x_1^*(m,0^+)$. As $\varphi_\mu(x_1) > 0$ for all $0 \leq x_1 < x_1^*(m,0^+)$ and $\varphi_\mu(x_1) < 0$ for all $x_1 > x_1^*(m,0^+)$ then, the equilibrium $x_1^*(m,0^+)$ is GAS in the positive axis. Therefore, the approximation given by Tikhonov's Theorem holds for all $t \geq 0$ for the slow variable and for all $t \geq t_0 > 0$ for the fast variable, where t_0 is as small as we want. Therefore, if $z(t)$ is the solution of the reduced model (5.4) of initial condition $z(0) = x_1^0$, then, when $\epsilon \to 0$, we have the approximations (5.5) and (5.6). □

As a corollary of the previous theorem, we have the following result which gives the limit of the total equilibrium population $X_T^*(m,\epsilon)$ of the model (5.1) when ϵ goes to zero:

Corollary 5.2. We have:

$$X_T^*(m,0^+) := \lim_{\epsilon\to 0} X_T^*(m,\epsilon) = \lim_{\epsilon\to 0}(x_1^*(m,\epsilon)+x_2^*(m,\epsilon)) = x_1^*(m,0^+)+K_2, \tag{5.8}$$

where $x_1^*(m,0^+)$ is the equilibrium of the reduced model (5.4).

Proposition 5.3. Consider the total equilibrium population (5.8). Then,

$$\frac{dX_T^*}{dm}(0,0^+) := \frac{1}{\mu}\frac{-m_1K_1+m_2K_2}{r_1}, \tag{5.9}$$

and

$$X_T^*(+\infty,0^+) := \frac{m_1+m_2}{m_1}K_2. \tag{5.10}$$

Proof. The equilibrium $x_1^*(m,0^+)$ satisfies:

$$r_1x_1^*(m,0^+)\left[1-\left(\frac{x_1^*(m,0^+)}{K_1}\right)^{\mu}\right]+m(m_2K_2-m_1x_1^*(m,0^+))=0. \tag{5.11}$$

Dividing (5.11) by $\frac{r_1}{K_1^\mu}x_1^*(m,0^+)$, we obtain:

$$x_1^*(m,0^+) = \left[{K_1}^{\mu}+m\frac{m_2K_2-m_1x_1^*(m,0^+)}{\frac{r_1}{K_1^\mu}x_1^*(m,0^+)}\right]^{\frac{1}{\mu}}. \tag{5.12}$$

The derivative of (5.12) with respect to m, gives

$$\frac{dx_1^*}{dm}(m,0^+) = \frac{1}{\mu}\left[m\frac{d}{dm}\left(\frac{m_2K_2-m_1x_1^*(m,0^+)}{\frac{r_1}{K_1^\mu}x_1^*(m,0^+)}\right)\right. \tag{5.13}$$

$$\left.+\frac{m_2K_2-m_1x_1^*(m,0^+)}{\frac{r_1}{K_1^\mu}x_1^*(m,0^+)}\right]\left[{K_1}^{\mu}+m\frac{m_2K_2-m_1x_1^*(m,0^+)}{\frac{r_1}{K_1^\mu}x_1^*(m,0^+)}\right]^{\frac{1}{\mu}-1}.$$

For $m=0$, we have $x_1^*(0,0^+)=K_1$, therefore, the equation (5.13) gives the derivative (5.9).

For the formula of perfect mixing, dividing (5.11) by m, and taking the limit when $m\to\infty$, we get:

$$m_2K_2-m_1x_1^*(+\infty,0^+)=0,$$

Hence, as $x_2^*(+\infty,0^+)=K_2$, the sum of $x_1^*(+\infty,0^+)$ and $x_2^*(+\infty,0^+)$ gives the formula (5.10). □

Remark 5.4. We can deduce the formula of perfect mixing $X_T^*(+\infty,0^+)$ and the derivative of the total equilibrium population $\frac{dX_T^*}{dm}(0,0^+)$ by computing the limit of the equations (5.2) and (5.3) when ϵ goes to zero respectively.

We consider the regions in the set of the parameters m_1 and m_2, denoted $\mathcal{J}_0$ and $\mathcal{J}_1$ defined by:

$$\mathcal{J}_0 = \left\{(m_1, m_2) : \frac{m_2}{m_1} > \frac{K_1}{K_2}\right\}, \quad \mathcal{J}_1 = \left\{(m_1, m_2) : \frac{m_2}{m_1} < \frac{K_1}{K_2}\right\}. \tag{5.14}$$

We have the following result which gives the conditions for which patchiness is beneficial or detrimental in model (5.1) when ϵ goes to zero.

Theorem 5.5. Let $\mathcal{J}_0$ and $\mathcal{J}_1$ be the domains defined in (5.14). Consider the total equilibrium population $X_T^*(m, 0^+)$ given by (5.8). Then, we have:

- If $(m_1, m_2) \in \mathcal{J}_0$ then $X_T^*(m, 0^+) > K_1 + K_2$, for all $m > 0$.
- If $(m_1, m_2) \in \mathcal{J}_1$ then $X_T^*(m, 0^+) < K_1 + K_2$, for all $m > 0$.
- If $\frac{m_2}{m_1} = \frac{K_1}{K_2}$, then $x_1^*(m, 0^+) = K_1$ and $x_2^*(m, 0^+) = K_2$ for all $m \geq 0$. Therefore $X_T^*(m, 0^+) = K_1 + K_2$ for all $m \geq 0$.

Proof. First, we try to solve the equation $X_T^*(m, 0^+) = K_1 + K_2$ with respect to m, to obtain the intersection points between the curve of the total equilibrium population $m \mapsto X_T^*(m, 0^+)$ and the straight line $m \mapsto K_1 + K_2$. For any $m > 0$, we have

$$\begin{aligned} x_1^*(m, 0^+) = K_1 \iff & \left[{K_1}^{\mu} + m \frac{m_2 K_2 - m_1 x_1^*(m, 0^+)}{\frac{r_1}{K_1^{\mu}} x_1^*(m, 0^+)} \right]^{\frac{1}{\mu}} = K_1 \\ \iff & m_2 K_2 = m_1 x_1^*(m, 0^+) \\ \iff & m_2 K_2 = K_1 m_1 \iff \frac{dX_T^*}{dm}(0, 0^+) = 0. \end{aligned}$$

So, if $\frac{dX_T^*}{dm}(0, 0^+) \neq 0$ then $m = 0$ and the curve of the total equilibrium population intersects the straight line $m \mapsto K_1 + K_2$ in a unique point which is $(0, K_1 + K_2)$. Therefore, we conclude that the first and second items of the theorem hold. □

Biologically speaking, according to the result of the previous theorem, the existence of a faster growing sub-population compared to the second one causes the critical value of migration rate m_0 (see Theorem 4.1) to disappear.

6 Conclusion

The goal of this paper was to generalize to some general growth rates the results obtained in [2] for a two-patch logistic model. In particular, we considered the model of two patches with Richards growth rate.

In Section 3, we looked at the case when migration rate goes to infinity. We computed the equilibrium in this situation (Theorem 3.1) and we proved that the dynamics of the system (3.6) provide a good approximation of the model (2.1) by using singular perturbation arguments (Theorem 3.3). In Section 4, we have given a complete classification of the conditions under which dispersal is either beneficial or detrimental to total equilibrium population. The important result is, even with more general dynamics, the effect of migration is the same as with logistic dynamic: either patchiness always has a beneficial effect on the total equilibrium population, or this effect is always detrimental, or there exists a critical value m_0 of the migration rate m, such that, the effect is beneficial for $m < m_0$, and detrimental for $m < m_0$ (see Theorem 4.1). In Section 5, we considered the two-patch model (2.1), in the case where one growth rate is much larger than the last. First, by perturbation arguments, we have given an approximation of the solutions of the system in this case. Next, we compared the total equilibrium population with the sum of two carrying capacities.

Some question remains open: how do our results generalize to situations with more than two patches? If we consider a more general growth dynamic than the growth of Richards (1.5), this has an effect on the total equilibrium population. I think these questions are difficult to answer, and require a lot of work and mathematical tools.

Appendix

A Equilibria and stability of (2.1)

In this section, our goal is to prove the global stability of the positive equilibrium of the system (2.1). In the absence of migration, i.e. the case where $m = 0$, the system (2.1) admits (K_1, K_2) as a non trivial equilibrium point, which furthermore is globally asymptotically stable (GAS) in the interior of the positive cone $\mathbb{R}^2_+$. The problem is whether the equilibrium continues to be positive and globally stable for any $m > 0$ or not. We first prove the non negativity of the solution of System (2.1). We have the following proposition:

Proposition A.1. The positive cone $\mathbb{R}^2_+$ is positively invariant for the system (2.1).

Proof. Suppose that, at a given time t, one of the state variables of the system (2.1) is at a boundary of $\mathbb{R}^2_+$, meaning that at least one population is at 0. We suppose first that $x_1 = 0$, and $x_2 \geq 0$, then the dynamics of x_1 is given by $\frac{dx_1}{dt} = m_{21}x_2 \geq 0$, and, if $x_2 = 0$, and $x_1 \geq 0$, then we have $\frac{dx_2}{dt} = m_{12}x_1 \geq 0$. So each trajectory initiated at a boundary of $\mathbb{R}^2_+$ either remains at the boundary or goes to the interior of $\mathbb{R}^2_+$. According to [29, Proposition B.7, page 267], no trajectory comes out of $\mathbb{R}^2_+$. Therefore, $\mathbb{R}^2_+$ is positively invariant for (2.1). □

The equilibrium of the system (2.1) is the solutions of the following algebraic system:

$$\begin{cases} 0 = r_1 x_1 \left[1 - \left(\frac{x_1}{K_1}\right)^{\mu}\right] + m(m_{12}x_2 - m_{21}x_1), \\ 0 = r_2 x_2 \left[1 - \left(\frac{x_2}{K_2}\right)^{\mu}\right] + m(m_{21}x_1 - m_{12}x_2). \end{cases} \tag{A.1}$$

The sum of the two equations of (A.1) shows that the equilibrium points are in a curve noted $\mathcal{C}_\mu$, which its equation is given by:

$$\Phi_\mu(x_1, x_2) := r_1 x_1 \left[1 - \left(\frac{x_1}{K_1}\right)^{\mu}\right] + r_2 x_2 \left[1 - \left(\frac{x_2}{K_2}\right)^{\mu}\right] = 0. \tag{A.2}$$

The curve $\mathcal{C}_\mu$ passes through the points $(0,0), (K_1, 0), (0, K_2)$ and $\mathcal{A} := (K_1, K_2)$ for all value positive of parameter μ. Note that, it is independent of migration rate m and m_{ij}. For the particular value $\mu = 1$, the curve $\mathcal{C}_1$ is an ellipse centered in $\left(\frac{K_1}{2}, \frac{K_2}{2}\right)$ (shown in black in Figure A.1). For $\mu > 1$, the curve $\mathcal{C}_\mu$ is below the ellipse $\mathcal{C}_1$ (shown in green and brown in the figure A.1) and for $0 < \mu < 1$, the curve $\mathcal{C}_\mu$ is above the ellipse $\mathcal{C}_1$ (shown in red and blue in Figure A.1). The function $\Phi_\mu(x_1, x_2) = \Phi_{\mu,1}(x_1) + \Phi_{\mu,2}(x_2)$, with $\Phi_{\mu,i}(x_i) = r_i x_i \left[1 - \left(\frac{x_i}{K_i}\right)^\mu\right]$ is concave since $\Phi_{\mu,1}$ and $\Phi_{\mu,2}$ are two concave functions. Another property of the curve $\mathcal{C}_\mu$, if is that if a point (x_1, x_2) belongs to $\mathcal{C}_\mu$ with $x_1 < K_1$ (resp. $x_2 > K_2$) then $x_2 > K_2$ (resp. $x_1 < K_1$) (see figure A.1).

Solving the first equation of system (A.1) for x_2 yields a curve noted $M_{m,\mu}$ of equation $x_2 = \varphi_{m,\mu}(x_1)$, where the function $\varphi_{m,\mu}$ is given by the following equation:

$$\varphi_{m,\mu}(x_1) := \frac{1}{m_{12}} \left(m_{21} x_1 - \frac{r_1}{m} x_1 \left[1 - \left(\frac{x_1}{K_1}\right)^\mu\right]\right). \tag{A.3}$$

The curve $M_{m,\mu}$ (shown in the figure A.1 for some values of μ) depends on the migration rate m and the parameter μ. It always passes through the origin and the point $\mathcal{B} := \left(K_1, \frac{m_{21}}{m_{12}} K_2\right)$. So, the equilibrium points are the non-negative intersection between the curves $\mathcal{C}_\mu$ and $M_{m,\mu}$. There are two equilibrium points. The first is the trivial point $(0,0)$ and the second is a non trivial point noted $\mathcal{E}^*(m) := (x_1^*(m), x_2^*(m))$ whose position depend on migration rate m (see Figure A.2).

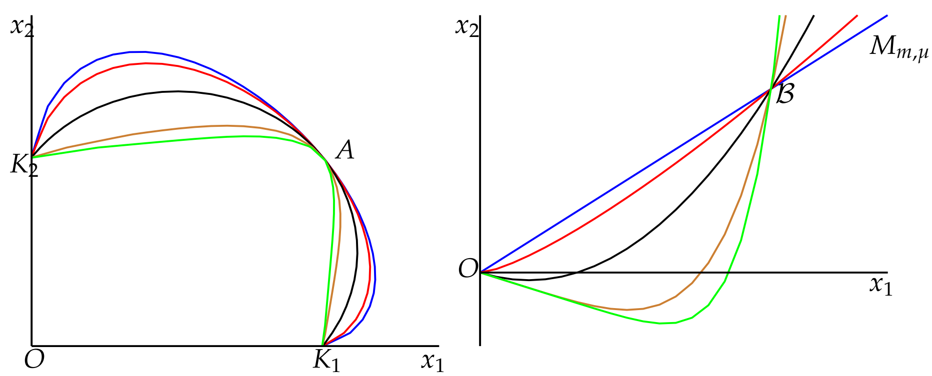

Figure A.1: The curves $\mathcal{C}_\mu$ (left) and $M_{m,\mu}$ (right) for $r_1 = 3, r_2 = 2, K_1 = 5, K_2 = 4, m_{12} = m_{21} = m = 1$ and $\mu = 0.001$ (green curves), $\mu = 0.2$ (gold curves), $\mu = 1$ (black curves), $\mu = 4$ (red curves) and $\mu = 7$ (blue curves).

In the following, our aim is to show the global stability of the equilibrium $\mathcal{E}^*(m)$. For this, we need some results. First, for the non-negativity and boundedness of the solution of the system (2.1), we have the following result:

Lemma A.2. For any non-negative initial condition, the solutions of the system (2.1) remain bounded, for all $t \geq 0$. Moreover, the set

$$\Sigma = \left\{ (x_1, x_2) \in \mathbb{R}_+^2 / x_1 + x_2 \leq \frac{\xi_2^*}{\xi_1^*} \right\},$$

where $\xi_1^* = \mu \min\{r_1, r_2\}$ and $\xi_2^* = \mu(r_1 K_1 + r_2 K_2)$, is positively invariant and is a global attractor for the system (2.1).

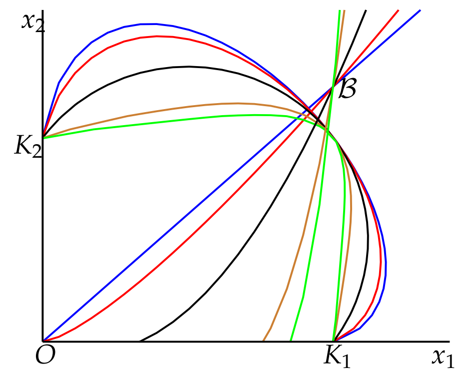

Figure A.2: Intersection between $\mathcal{C}_\mu$ and $M_{m,\mu}$, which are drawn in the same color.

Proof. To show that all solutions are bounded, we consider the quantity defined by $X_T(t) = x_1(t) + x_2(t)$. So, we have

$$\dot{X}_T(t) = r_1 x_1(t) \left[1 - \left(\frac{x_1(t)}{K_1}\right)^\mu\right] + r_2 x_2(t) \left[1 - \left(\frac{x_2(t)}{K_2}\right)^\mu\right]. \tag{A.4}$$

For all r_i and K_i, we have the inequality:

$$r_i x_i \left[1 - \left(\frac{x_i}{K_i}\right)^\mu\right] \leq \mu r_i (K_i - x_i), \quad i = 1, 2. \tag{A.5}$$

Substituting Equation (A.5) into (A.4), we get

$$\dot{X}_T(t) \leq -\xi_1^* X_T(t) + \xi_2^* \qquad \text{for all } t \geq 0,$$

which gives

$$X_T(t) \leq \left(X_T(0) - \frac{\xi_2^*}{\xi_1^*}\right) e^{-\xi_1 t} + \frac{\xi_2^*}{\xi_1^*}, \qquad \text{for all } t \geq 0. \tag{A.6}$$

Hence,

$$X_T(t) \leq \max\left(X_T(0), \frac{\xi_2^*}{\xi_1^*}\right), \qquad \text{for all } t \geq 0.$$

Therefore, the solutions of System (2.1) are positively bounded and defined for all $t \geq 0$. From (A.6), it can be deduced that the set Σ is positively invariant and it is a global attractor for the system (2.1). □

We have also the following property:

Lemma A.3. System (2.1) admits no periodic solution.

Proof. The isoclines of the system (2.1) are given by the two equations:

$$\begin{cases} \mathcal{P}_1(x_1) = -\frac{r_1}{mm_{12}}x_1\left[1-\left(\frac{x_1}{K_1}\right)^{\mu}\right]+\frac{m_{21}}{m_{12}}x_1, \\ \mathcal{P}_2(x_2) = -\frac{r_2}{mm_{21}}x_2\left[1-\left(\frac{x_2}{K_2}\right)^{\mu}\right]+\frac{m_{12}}{m_{21}}x_2. \end{cases}$$

Let f_i be the right hand side of the system (2.1). Then, for all m we have:

$$\begin{aligned} \frac{\partial f_1}{\partial x_1}+\frac{\partial f_2}{\partial x_2} &= r_1+r_2-(\mu+1)\left[r_1\left(\frac{x_1}{K_1}\right)^{\mu}+r_2\left(\frac{x_2}{K_2}\right)^{\mu}\right] \\ &\quad -m(m_{21}+m_{12}) = -m\left(m_{12}\frac{d\mathcal{P}_1}{dx_1}+m_{21}\frac{d\mathcal{P}_2}{dx_2}\right)<0. \end{aligned}$$

So, by Dulac's Criterion [14, Theorem 4.1.1], the system (2.1) admits no periodic solution. □

Theorem A.4. The equilibrium $\mathcal{E}^*(m)$ of (2.1) is GAS in the positive cone $\mathbb{R}^2_+ \setminus \{0\}$.

Proof. The Jacobian matrix of the system (2.1) at $\mathcal{E}^*(m)$ is given by:

$$\mathbb{J}(\mathcal{E}^*) = \begin{bmatrix} \kappa_1 & mm_{12} \\ mm_{21} & \kappa_2 \end{bmatrix},$$

where $\kappa_1 = r_1-(\mu+1)r_1\left(\frac{x_1^*(m)}{K_1}\right)^{\mu}-mm_{21}$, and $\kappa_2 = r_2-(\mu+1)r_2\left(\frac{x_2^*(m)}{K_2}\right)^{\mu}-mm_{12}$. We have: $0<\frac{d\mathcal{P}_1}{dx_1}(x_1^*(m),x_2^*(m)) = -\frac{1}{mm_{12}}\kappa_1$, and $0<\frac{d\mathcal{P}_2}{dx_2}(x_1^*(m),x_2^*(m)) = -\frac{1}{mm_{21}}\kappa_2$. Therefore, $\kappa_1<0$ and $\kappa_2<0$. This implies that $\mathrm{tr}(\mathbb{J}(\mathcal{E}^*)) = \kappa_1+\kappa_2<0$, where tr means the trace.

It's clear that, in the figures A.3, at the equilibrium $\mathcal{E}^*$, we have: $\frac{d\mathcal{P}_1}{dx_1}(\mathcal{E}^*) > \left(\frac{d\mathcal{P}_2}{dx_2}(\mathcal{E}^*)\right)^{-1}$, which gives $\frac{\kappa_1}{-mm_{12}} > \frac{-mm_{21}}{\kappa_2}$. Thus, $\det\mathbb{J}(\mathcal{E}^*) = \kappa_1\kappa_2-m^2m_{12}m_{21}>0$.
Hence by the Routh-Hurwitz criteria for stability, the real parts of the eigenvalues value of the Jacobian matrix $\mathbb{J}(\mathcal{E}^*)$ are negative, proving that $\mathcal{E}^*$ is asymptotically stable. Lemmas A.2 and A.3 imply that there cannot be any non-trivial closed paths lying in the interior of the positive quadrant and hence the asymptotic stability must be global. □

B Two-patch logistic model

We consider the 2-patch logistic equation with asymmetric migrations. We denote by m_{12} the migration rate from patch 2 to patch 1, m_{21} from patch 1 to patch 2, and m is the dispersal rate between two patches. The model is written:

$$\begin{cases} \frac{dx_1}{dt} = r_1x_1\left(1-\frac{x_1}{K_1}\right)+m\left(m_{12}x_2-m_{21}x_1\right), \\ \frac{dx_2}{dt} = r_2x_2\left(1-\frac{x_2}{K_2}\right)+m\left(m_{21}x_1-m_{12}x_2\right). \end{cases} \quad \text{(B.1)}$$

Note that the system (B.1) is studied in [1, 6, 9, 10, 15] in the case where the migration rates satisfy $m_{21} = m_{12}$, and in [2] for general migration rates. If we denote $\gamma = \frac{m_{12}}{m_{21}}$, then the system (B.1) becomes:

$$\begin{cases} \frac{dx_1}{dt} = r_1x_1\left(1-\frac{x_1}{K_1}\right)+m\left(\gamma x_2-x_1\right), \\ \frac{dx_2}{dt} = r_2x_2\left(1-\frac{x_2}{K_2}\right)+m\left(x_1-\gamma x_2\right), \end{cases} \quad \text{(B.2)}$$

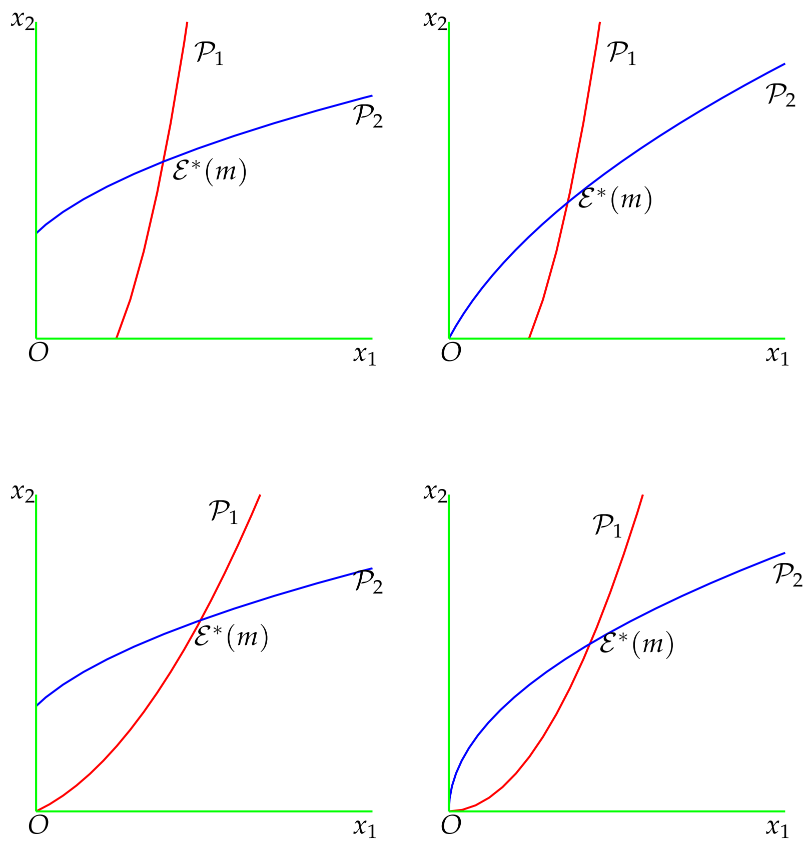

Figure A.3: All possible configurations for the isoclines of the system (2.1) (in red for x_1 and in blue for x_2) for certain parameters. The equilibrium points are the intersection between these two isoclines: the origin and the positive equilibrium $\mathcal{E}^*(m)$.

The system (B.2) has always a unique positive equilibrium, still denoted by $E^*(m,\gamma) = (x_1^*(m,\gamma), x_2^*(m,\gamma))$, which is GAS in the interior of positive cone $\mathbb{R}^2 \setminus \{0\}$. We thus define the total population abundance at the positive equilibrium under dispersal rate m and dispersal asymmetry γ by

$$X_T^*(m,\gamma) = x_1^*(m,\gamma) + x_2^*(m,\gamma),$$

as the total realized asymptotic population abundance.

B.1 Total population size for fixed γ

In all of this part, we assume that γ is positive and fixed parameter and m varies in $[0,\infty[$. We recall that the derivative of $X_T^*(m,\gamma)$ with respect to m at $m = 0$ is given by the following formula [8]:

$$\frac{dX_T^*}{dm}(0,\gamma) = (\gamma K_2 - K_1)\left(\frac{1}{r_1} - \frac{1}{r_2}\right). \tag{B.3}$$

The behavior of the model (B.2) for perfect mixing (i.e. $m \to \infty$) is given by the following formula [2, 8]:

$$X_T^*(\infty,\gamma) = (1+\gamma)\frac{\gamma r_1 + r_2}{\gamma^2\alpha_1 + \alpha_2}, \qquad \text{where } \alpha_i = r_i/K_i. \tag{B.4}$$

We consider the regions in the set of the parameter γ denoted $\mathcal{J}_0$, $\mathcal{J}_1$ and $\mathcal{J}_2$, defined by:

$$\begin{cases} \text{If } r_2 > r_1 \text{ then } \begin{cases} \mathcal{J}_1 = \left\{\gamma : \gamma > \frac{\alpha_2}{\alpha_1}\right\}, \\ \mathcal{J}_0 = \left\{\gamma : \frac{\alpha_2}{\alpha_1} \geq \gamma > \frac{K_1}{K_2}\right\}, \\ \mathcal{J}_2 = \left\{\gamma : \frac{K_1}{K_2} > \gamma\right\}. \end{cases} \\ \text{If } r_2 < r_1 \text{ then } \begin{cases} \mathcal{J}_1 = \left\{\gamma : \gamma < \frac{\alpha_2}{\alpha_1}\right\}, \\ \mathcal{J}_0 = \left\{\gamma : \frac{\alpha_2}{\alpha_1} \leq \gamma < \frac{K_1}{K_2}\right\}, \\ \mathcal{J}_2 = \left\{\gamma : \frac{K_1}{K_2} < \gamma\right\}. \end{cases} \end{cases} \tag{B.5}$$

We recall the following result of Arditi et al. [2] which gives the conditions for which patchiness is beneficial or detrimental in model (B.2).

Proposition B.1. The total equilibrium population X_T^* of (B.2) for γ fixed satisfies the following properties

1. If $r_1 = r_2$ then $X_T^*(m,\gamma) \leq K_1 + K_2$ for all $m \geq 0$.
2. If $r_2 \neq r_1$, let $\mathcal{J}_0$, $\mathcal{J}_1$ and $\mathcal{J}_2$, be defined by (B.5). Then we have:
   - if $\gamma \in \mathcal{J}_0$ then $X_T^*(m,\gamma) > K_1 + K_2$ for all $m > 0$
   - if $\gamma \in \mathcal{J}_1$ then $X_T^*(m,\gamma) > K_1 + K_2$ for $0 < m < m_0$ and $X_T^*(m,\gamma) < K_1 + K_2$ for $m > m_0$, where
   $$m_0 = \frac{r_2 - r_1}{\frac{\gamma}{\alpha_2} - \frac{1}{\alpha_1}}\frac{1}{\alpha_1 + \alpha_2}.$$
   - if $\gamma \in \mathcal{J}_2$ then $X_T^*(m,\gamma) < K_1 + K_2$ for any $m > 0$
   - If $\gamma = \frac{K_1}{K_2}$, then $x_1^*(m,\gamma) = K_1$ and $x_2^*(m,\gamma) = K_2$ for all $m \geq 0$. Therefore $X_T^*(m,\gamma) = K_1 + K_2$ for all $m \geq 0$.

B.2 Total population size for fixed m

In all of this section, we assume that m is fixed parameter and γ varies from 0 to ∞.

B.2.1 The model when $\gamma \to 0$

We have the following result

Proposition B.2. Consider the system (B.2). Then,

$$\lim_{\gamma\to 0} E^*(m,\gamma) = \begin{cases} (0, K_2), & if \quad m \geq r_1, \\ \left(\left(1-\frac{m}{r_1}\right)K_1, \frac{1}{2}K_2 + \frac{1}{2\alpha_2}\sqrt{r_2^2 + 4m\alpha_2\left(1-\frac{m}{r_1}\right)K_1}\right), & if \quad m < r_1. \end{cases} \tag{B.6}$$

Proof. Denote $E^*(m,0^+) = (x_1^*(m,0^+), x_2^*(m,0^+)) := \lim_{\gamma\to 0} E^*(m,\gamma)$. When $\gamma \to 0$, the equilibrium equations of (B.2) take the following form:

$$\begin{cases} 0 = r_1 x_1^*(m,0^+)\left(1-\dfrac{x_1^*(m,0^+)}{K_1}\right) - m x_1^*(m,0^+), \\ 0 = r_2 x_2^*(m,0^+)\left(1-\dfrac{x_2^*(m,0^+)}{K_2}\right) + m x_1^*(m,0^+), \end{cases} \tag{B.7}$$

which implies

$$\begin{cases} 0 = (r_1 - m)x_1^*(m,0^+) - \alpha_1(x_1^*(m,0^+))^2 = 0, \\ -\alpha_1(x_2^*(m,0^+))^2 + m x_1^*(m,0^+) + r_2 x_2^*(m,0^+) = 0. \end{cases} \tag{B.8}$$

If $m \geq r_1$, then the system (B.8) admits $(0,0)$ and $(0,K_2)$ as solutions. Since $(0,0)$ is unstable for (B.2), then $E^*(m,\gamma) \to (0,K_2)$ as $\gamma \to 0$.

If $m < r_1$, the first equation in (B.8) gives $x_1^*(m,0^+) = 0$ or $x_1^*(m,0^+) = \frac{r_1 - m}{\alpha_1}$. If we replace $x_1^*(m,0^+) = 0$ in the second equation of (B.8) we get $x_2^*(m,0^+) = 0$ or $x_2^*(m,0^+) = K_2$, and if we replace $x_1^*(m,0^+) = \frac{r_1-m}{\alpha_1}$ in the second equation of (B.8) we obtain the following equation:

$$-\alpha_2(x_2^*(m,0^+))^2 + r_2 x_2^*(m,0^+) + \frac{m\,(r_1 - m)}{\alpha_1} = 0, \tag{B.9}$$

which admits as positive solution

$$x_2^*(m,0^+) = \frac{1}{2}K_2 + \frac{1}{2\alpha_2}\sqrt{r_2^2 + 4m\alpha_2\left(1-\frac{m}{r_1}\right)K_1}.$$

Therefore, if $r_1 > m$, then the system (B.8) admits three solutions: $(0,0)$, $(0,K_2)$ and

$$E^*(m,0^+) := \left(\left(1-\frac{m}{r_1}\right)K_1, \frac{1}{2}K_2 + \frac{1}{2\alpha_2}\sqrt{r_2^2 + 4m\alpha_2\left(1-\frac{m}{r_1}\right)K_1}\right), \tag{B.10}$$

Since, $(0,0)$, and $(0,K_2)$ are unstable, so $E^*(m,\lambda)$ converge to $E^*(m,0^+)$ as $\gamma \to 0$. □

As a corollary of the previous proposition, we obtain the following result which describes the total equilibrium population $X_T^*(m,\gamma)$ when $\gamma \to 0$.

Corollary B.3. we have:

$$\lim_{\gamma\to 0} X_T^*(m,\gamma) := X_T^*(m,0^+) = \begin{cases} K_2, & if \quad m \geq r_1, \\ \left(1-\frac{m}{r_1}\right)K_1 + \frac{1}{2}K_2 + \frac{1}{2\alpha_2}\sqrt{r_2^2 + 4m\alpha_2\left(1-\frac{m}{r_1}\right)K_1}, & if \quad m < r_1. \end{cases} \tag{B.11}$$

B.2.2 The model when $\gamma \to \infty$

In the next theorem, we give the behavior of the model (B.2) when $\gamma \to \infty$.

Proposition B.4. Let $(x_1(t,\gamma), x_2(t,\gamma))$ be the solution of the system (B.2) with initial condition (x_1^0, x_2^0) satisfying $x_i^0 \geq 0$ for $i = 1,2$. Let $z(t)$ be the solution of the differential equation

$$\frac{dX}{dt} = r_1 X \left(1 - \frac{X}{K_1}\right), \tag{B.12}$$

with initial condition $z(0) = x_1^0 + x_1^0$. Then, when $\gamma \to \infty$, we have

$$x_1(t,\gamma) + x_2(t,\gamma) = z(t) + o_\gamma(1), \qquad \text{uniformly for } t \in [0, +\infty) \tag{B.13}$$

and, for any $t_0 > 0$, we have

$$\begin{cases} x_1(t,\gamma) = z(t) + o_\gamma(1), \\ x_2(t,\gamma) = o_\gamma(1), \end{cases} \qquad \text{uniformly for} \quad t \in [t_0, +\infty). \tag{B.14}$$

Proof. Let $X = x_1 + x_2$. We rewrite the system (B.2) using the variables (X, x_1), and get:

$$\begin{cases} \dfrac{dx_1}{dt} = r_1 x_1 \left(1 - \dfrac{x_1}{K_1}\right) + m\left(\gamma(X - x_1) - x_1\right), \\ \dfrac{dX}{dt} = r_1 x_1 \left(1 - \dfrac{x_1}{K_1}\right) + r_2(X - x_1)\left(1 - \dfrac{(X - x_1)}{K_2}\right). \end{cases} \tag{B.15}$$

When $\gamma \to \infty$, (B.15) is a slow-fast system, with one slow variable, X, and one fast variable x_1. As suggested by Tikhonov's Theorem [17, 30, 34] we consider the dynamics of the fast variable in the time scale $\tau = \gamma t$. One obtains

$$\frac{dx_1}{d\tau} = m(X - x_1). \tag{B.16}$$

The *slow manifold*, which is the equilibrium point of the fast dynamics (B.16), is given by $x_1 = X$. As this manifold is GAS for the system (B.16), the Theorem of Tikhonov ensures that after a fast transition toward the slow manifold, the solutions of (B.15) are approximated by the solutions of the *reduced model* which is obtained by replacing $x_1 = X$ into the dynamics of the slow variable, which gives (B.12).

Since (B.12) admits $X = K_1$ as a positive equilibrium point, which is GAS in the positive axis, the approximation given by Tikhonov's Theorem holds for all $t \geq 0$ for the slow variable and for all $t \geq t_0 > 0$ for the fast variable, where t_0 is small as we want. Therefore, let $z(t)$ be the solution of the reduced model (B.12) of initial condition $z(0) = X(0,\gamma) = x_1^0 + x_2^0$, then, when $m \to \infty$, we have the approximations (B.13) and (B.14). □

According to previous proposition, when $\gamma \to \infty$, the equilibrium $E^*(m,\gamma)$ converge to $(K_1, 0)$ and $X_T^*(m, +\infty) = K_1$.

For more details on the effects of dispersal intensity and dispersal asymmetry on the total population abundance, the reader may refer to the recent work of Gao et al. [11].

Acknowledgments.

The author thanks the Editor and the two anonymous reviewers for their constructive comments which have greatly improved this work.

Conflict of Interest

The author has no conflicts of interest to declare.

References

[1] R. Arditi, C. Lobry and T. Sari, *In dispersal always beneficial to carrying capacity? New insights from the multi-patch logistic equation*, Theor. Popul. Biol., **106** (2015), 45-59. DOI

[2] R. Arditi, C. Lobry and T.Sari, *Asymmetric dispersal in the multi-patch logistic equation*, Theor. Popul. Biol., **1206** (2018), 11-15. DOI

[3] L. Von. Bertalanffyi, *A quantitative theory of organic growth*, Human Biology., **10**(2) (1938), 181-213. DOI

[4] A. A. Blumberg, *Logistic Growth rate functions*, J. Theor. Biol., **21** (1968), 42-443. DOI

[5] L. Chen, T. Liu and F. Chen, *Stability and bifurcation in a two-patch model with additive Allee effect*, AIMS Math., **7**(1) (2021), 536-551. DOI

[6] D. L. DeAngelis, C. C. Travis and W. M. Post, *Persistence and stability of seed-dispersel species in a patchy environment*. Theor. Popul. Biol., **16** (1979), 107-125. DOI

[7] B. Elbetch, T. Benzekri, D. Massart and T. Sari, *The multi-patch logistic equation*. Discrete Contin. Dyn. Syst. - B., **26**(12) (2020), 6405-6424. DOI

[8] B. Elbetch, T. Benzekri, D. Massart and T. Sari, *The multi-patch logistic equation with asymmetric migration*, Rev. Integr. Temas Mat., **40**(1) (2022), 25-57. DOI

[9] H. I. Freedman and P. Waltman, *Mathematical Models of Population Interactions with Dispersal I: Stability of two habitats with and without a predator*. SIAM J. Appl Math., **32** (1977), 631-648. DOI

[10] H. I. Freedman, B. Rai and P. Waltman, *Mathematical Models of Population Interactions with Dispersal II: Differential Survival in a Change of Habitat*. J. Math. Anal. Appl., **115** (1986), 140-154. DOI

[11] D. Gao and Y. Lou, *Total biomass of a single population in two-patch environments*. Theor. Popul. Biol., **(146)** (2022), 1-14. DOI

[12] J. W. Haefner, *Modelling Biological Systems: Principles and Applications*, ITP Chapman and Hall, New York, 1996. URL

[13] I. A. Hanski and M. E. Gilpin, *Metapopulation Biology: Ecology, Genetics, and Evolution*. Academic Press, 1997.

[14] J. Hofbauer and K. Sigmund, *Evolutionary Games and Population Dynamics*. Cambridge University Press, Cambridge, 1998. URL

[15] R. D. Holt, *Population dynamics in two patch environments: some anomalous consequences of an optimal habitat distribution*. Theor. Popul. Biol., **28** (1985), 181-201. DOI

[16] Y. Kang and N. Lanchier, *Expansion or extinction: Deterministic and stochastic two-patch models with Allee effects*, J. Math. Biol., **62** (2011), 925-973. DOI

[17] C. Lobry, T. Sari and S. Touhami, *On Tykhonov's theorem for convergence of solutions of slow and fast systems*. Electron. J. Differ. Equ., **19**(1998), 1-22. URL

[18] S. A. Levin, *Dispersion and population interactions*. Amer. Natur., **108** (1974), 207-228. DOI

[19] S. A. Levin, *Spatial patterning and the structure of ecological communities, in Some Mathematical Questions in Biology VII*. American Mathematical Society, 1976. URL

[20] S. A. Levin, T. M. Powell and J. H. Steele, *Patch Dynamics*, volume **96** of Lecture Notes in Biomathematics. Springer-Verlag, 1993. DOI

[21] A. J. Lotka, *Elements of Mathematical Biology*. DOVER, New York, 1956. URL

[22] Y. Y. Lv, L. J. Chen and F. D. Chen, *Stability and bifurcation in a single species logistic model with additive Allee effect and feedback control*, Adv. Differ. Equ., **8** (2020), 2686-2697. DOI

[23] Y. Y. Lv, L. J. Chen, F. D. Chen and Z. Li, *Stability and bifurcation in an SI epidemic model with additive Allee effect and time delay*, Int. J. Bifurcat. Chaos, **31**(2021), 2150060. DOI

[24] H. McCallum, *Population Parameters: Estimation for Ecological Models*, Blackwell Science, UK 2008. URL

[25] D. Pal and G. P. Samanta, *Effects of dispersal speed and strong Allee effect on stability of a two-patch predator-prey model*, Int. J. Dyn. Control, **6** (2018), 1484-1495. DOI

[26] J.-C. Poggiale, P. Auger, D. Nérini, C. Manté and F. Gilbert, *Global production increased spatial heterogeneity in a population dynamics model*. Acta Biotheor., **53** (2005), 359-370. DOI

[27] F. J. Richards, *A Flexible Growth Function for Empirical Use*, J. Exp. Bot., **10**(29) (1959), 290-300. DOI

[28] S. Saha and G. P. Samanta, *Influence of dispersal and strong Allee effect on a two-patch predator-prey model*, Int. J. Dyn. Control, **7** (2009), 1321-1349. DOI

[29] H. L. Smith and P. Waltman, *The Theory of the Chemostat : Dynamics of Microbial Competition*, Cambridge Studies in Mathematical Biology, **13** (1995). DOI

[30] A. N. Tikhonov, *Systems of differential equations containing small parameters in the derivatives*. Mat. Sb. (N.S.), **31**(73):3 (1952), 575-586. URL

[31] A. Tsoularis and J. Wallace, *Analysis of Logistic Growth Models*. Math. Biosci., **179** (2002), 21-55. DOI

[32] M. E. Turner, E. Bradley , K. Kirk and K. Pruitt, *A Theory of Growth*. Math. Biosci., **29** (1976), 367-373. DOI

[33] P. F. Verhulst, *Notice sur la loi que la population suit dans son accroissement*. Corr. Math. Physics, **10**(1838), 113. DOI

[34] W. R. Wasow, *Asymptotic Expansions for Ordinary Differential Equations*. Robert E. Krieger Publishing Company, Huntington, New York, 1976.

[35] H. Wu, Y. Wang, Y. Li and D. DeAngelis, *Dispersal asymmetry in a two-patch system with source-sink populations*. Theor. Popul. Biol., **131** (2020), 54-65. DOI

Journal of Innovative Applied Mathematics and Computational Sciences

J. Innov. Appl. Math. Comput. Sci. **2**(3) (2022), 69–85. n2t.net/ark:/49935/jiamcs.v2i3.25

http://jiamcs.centre-univ-mila.dz/

Modified projective synchronization of fractional-order hyperchaotic memristor-based Chua's circuit

Nadjet Boudjerida ✉[1], Mohammed Salah Abdelouahab [1, 2] and René Lozi [3]

[1]Departement of Mathematics, Mentouri Brothers University of Constantine 1, Constantine, 25000, Algeria
[2]Laboratory of Mathematics and their interactions, Abdelhafid Boussouf University Center, Mila, 43000, Algeria
[3]Université Côte d'Azur, CNRS, LJAD, Nice 06108 France

Received 5 February 2022, Accepted 15 December 2022, Published 31 December 2022

Abstract. This paper investigates the modified projective synchronization (MPS) between two hyperchaotic memristor-based Chua circuits modeled by two nonlinear integer-order and fractional-order systems. First, a hyperchaotic memristor-based Chua circuit is suggested, and its dynamics are explored using different tools, including stability theory, phase portraits, Lyapunov exponents, and bifurcation diagrams. Another interesting property of this circuit was the coexistence of attractors and the appearance of mixed-mode oscillations. It has been shown that one can achieve MPS with integer-order and incommensurate fractional order memristor-based Chua circuits. Finally, examples of numerical simulation are presented, showing that the theoretical results are in good agreement with the numerical ones.

Keywords: Memristor; hyperchaotic system; Chua's circuit; Caputo derivative; incommensurate fractional order Hyperchaotic System; modified projective synchronization.
2020 Mathematics Subject Classification: 37M05, 37M20, 37M22, 37M25, 93D05

1 Introduction

In 1971, the circuit theorist Leon Chua had published a study entitled "Memristor: the missing circuit element". This achievement has attracted a great research attention across a wide range of disciplines, such as programmable logic [14] and electronics [33] as well as neural networks [42]. Because memristors are non-linear components, their application to build chaotic or hyperchaotic systems has received significant attention in recent decades [9,23,30]. For example, the canonical Chua's circuit has been improved by replacing its diode with a memristor whose output is monotone-increasing [8]. Both chaotic and hyperchaotic systems are clearly

✉Corresponding author. Email: boudjnadj1843@gmail.com

ISSN (electronic): 2773-4196

defined as nonlinear systems that are highly dependent on initial conditions, unpredictable in the long run and non-periodic. The fact that hyper-chaotic systems have at least two positive Lyapunov exponents makes their dynamics more complex. And hence favourable for many applications. Mainly, for encryption and secure communications [12,17,35,36]. Various models of commensurate fractional-order memristor-based systems have been designed [11,13,21]. However, because of the different fractional-order characteristics of each circuit component, it is more important to consider fractional-order circuits or systems with incommensurate fractional order. Meanwhile, synchronization of chaotic and hyperchaotic systems has become a crucial research domain, especially in secure communication [19]. Various techniques have been proposed for the synchronization of chaotic systems, such as Active control [31], adaptive control [4,35], Feedback control, Prediction based feedback control, Sliding mode control and adaptive fuzzy control [2,5,6,10,31,34,38]. Using these methods, many works for the synchronization problem have been extended to the scope, such as phase synchronization, complete synchronization, anti-synchronization, projective synchronization, generalized projective synchronization, inverse hybrid function projective synchronization, generalized synchronization and MPS [4,18,29,31,41,43], but there are few studies on the MPS between integer-order and incommensurate fractional order hyperchaotic systems.

Motivated by the precedent reasons, a hyperchaotic memristor-based Chua's circuit is suggested, and its dynamics are explored using different tools, including stability theory, phase portraits, Lyapunov exponents, and bifurcation diagrams. Then, using an active control strategy, the problem of MPS between integer-order and incommensurate fractional order hyperchaotic memristor-based systems is explored, and synchronization is proved using the Lyapunov stability theory of fractional systems.

The present paper is organized as follows: in section 2, a mathematical model of the memristor is described, and the Caputo fractional derivative is discussed. In section 3, a novel memristor-based hyperchaotic system is introduced and its dynamical behavior is investigated. MPS between integer-order and incommensurate fractional order hyperchaotic systems is applied using the active control method in section 4. To illustrate the theoretical results, numerical simulations are presented using MATLAB programs. Finally, in the last section, this study concludes with a summary of the accomplished results and a conclusion.

2 Preliminaries

2.1 Basic memristor model

A memristor is a nonlinear resistor with a memory effect that can be either flux-controlled or charge-controlled [8]. It can be defined as a dual-terminal device having the relationship

$$f(\varphi, q) = 0.$$

Equations (2.1) and (2.2) describe a charge-controlled and a flux-controlled memristor, respectively [20,26]

$$M(q) = \frac{d\varphi(q)}{dq}, v = M(q)i, \tag{2.1}$$

$$W(\varphi) = \frac{dq(\varphi)}{d\varphi}, i = W(\varphi)v, \tag{2.2}$$

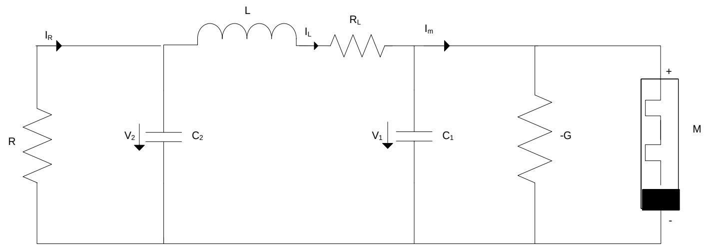

Figure 2.1: Modified memristor-based Chua's circuit

Where φ denotes the magnetic flux and q the charge, $W(\varphi)$ and $M(q)$ are called the memductance and memristance respectively.
This study considers a flux-controlled memristor whose characteristics are described by a piecewise quadratic function $q(\varphi)$ given by

$$q(\varphi) = -a\varphi + 0.5b\varphi|\varphi|.$$

With a and b being positive parameters.
Hence, its memductance function is

$$W(\varphi) = \frac{dq(\varphi)}{d\varphi} = -a + b|\varphi|.$$

2.2 Caputo fractional derivative

Definition 2.1. The Caputo fractional derivative of order α of a continuous function $f : \mathbb{R}^+ \mapsto \mathbb{R}$ is defined by:

$$D_t^\alpha f(t) = \begin{cases} \frac{1}{\Gamma(m-\alpha)} \int_0^t \frac{f^{(m)}(\tau)}{(t-\tau)^{\alpha-m+1}} d\tau, & m-1 < \alpha < m, \\ \frac{d^m}{dt^m} f(t), & \alpha = m, \end{cases}$$

where $m = \lceil \alpha \rceil$, and Γ is the Γ-function defined by

$$\Gamma(z) = \int_0^{+\infty} e^{-t} t^{z-1} dt, \quad \Gamma(z+1) = z\Gamma(z).$$

Theorem 2.2. *Consider the incommensurate fractional order system*

$$D^{\alpha_i} x_i = f(x_1, x_2, ..., x_n, t), i = 1, 2, ..., n, \tag{2.3}$$

Where $\alpha_1 \neq \alpha_2 \neq ... \neq \alpha_n$. Suppose that m is the least common multiple of the denominators u_i's of α_i's, where $\alpha_i = \frac{v_i}{u_i}$, $u_i, v_i \in \mathbb{Z}^+$ for $i = 1, 2, ..., n$. Denote $\gamma = \frac{1}{m}$ and J be the Jacobian matrix $J = \frac{df}{dx}$ evaluated at the equilibrium, where $f = [f_1, f_2, ..., f_n]^T$, $x = [x_1, x_2, ..., x_n]^T$. System (2.3) is asymptotically stable if $|arg(\lambda_i)| > \gamma\frac{\pi}{2}$ is satisfied for all roots λ_i of the following equation :

$$det(diag([\lambda^{m\alpha_1}, \lambda^{m\alpha_2}, ..., \lambda^{m\alpha_n}]) - J) = 0, \tag{2.4}$$

3 Building a memristor-based system and its analysis

In this section, an alternative memristor-based Chua's circuit is proposed by replacing the nonlinear diode in the original circuit with a negative conductance and a passive flux-controlled memristor described by (2.2) in parallel and changing the inductance's position that becomes between the two capacitances as shown in Figure 2.1.
Kirchhoff Laws allow us to describe the suggested circuit theoretically by the following four-dimensional differential system

$$\begin{cases} \dfrac{dV_1(t)}{dt} = \dfrac{1}{C_1}\left[I_L(t) + GV_1(t) - W(\phi)\,V_1(t)\right], \\ \dfrac{dV_2(t)}{dt} = \dfrac{1}{C_2}\left[\dfrac{V_2(t)}{R} - I_L(t)\right], \\ \dfrac{dI_L(t)}{dt} = \dfrac{1}{L}\left[-V_1(t) + V_2(t) - R_L I_L(t)\right], \\ \dfrac{d\phi(t)}{dt} = V_1(t), \end{cases} \tag{3.1}$$

where $W(\phi)$ is defined by (2.2) and $V_i, i = 1.2$ voltages, R, R_L and G resistances, $C_i, i = 1.2$ capacitances, I_L current, L the inductance and ϕ the magnetic flux through the memristor.
By setting $x = V_1,\ y = V_2,\ z = I_L,\ \omega = \phi,\ C_2 = 1, R = 1,\ \alpha = \dfrac{1}{C_1},\ \beta = \dfrac{1}{L},\ \gamma = \dfrac{R_L}{L}$ and $\xi = G$ then (3.1) can be converted into its dimensionless form

$$\begin{cases} \dot{x} = \alpha[z + \xi x - (-a + b|\omega|)x], \\ \dot{y} = y - z, \\ \dot{z} = -\beta(x - y) - \gamma z, \\ \dot{w} = x, \end{cases} \tag{3.2}$$

where x, y, z and ω are the states and α, β, γ, ξ, a and b are assumed to be positive constant parameters.

3.1 Stability analysis

The equilibrium points of system (3.2) are its solutions, taking each equation of the system equal to zero. Thus, the following equilibrium points are obtained

$$P_e = \{(x, y, z, \omega);\ x = 0,\ y = 0,\ z = 0 \text{ and } \omega = \omega_e \in \mathbb{R}\}. \tag{3.3}$$

Hence, each point on the $\omega -$ axis is an equilibrium point of (3.2), and (3.3) is called the equilibrium set.
The Jacobian matrix at each equilibrium point P_e is

$$J(P_e) = \begin{bmatrix} \alpha(\xi - W(w_e)) & 0 & \alpha & 0 \\ 0 & 1 & -1 & 0 \\ -\beta & \beta & -\gamma & 0 \\ 1 & 0 & 0 & 0 \end{bmatrix} \tag{3.4}$$

The characteristic polynomial of the system (3.2) is given by

$$\begin{aligned} P(\lambda) &= \lambda\left[\lambda^3 + [\gamma - 1 - \alpha(\xi - W(w_e))]\lambda^2 + [(-\gamma+1)\alpha(\xi - W(w_e)) + (1+\alpha)\beta - \gamma]\lambda \right. \\ &\quad \left. + \alpha[(\gamma-\beta)(\xi - W(w_e)) - \beta]\right] = \lambda Q(\lambda). \end{aligned} \tag{3.5}$$

Setting the system parameters as

$$\alpha = 5,\ \beta = 5,\ \gamma = 0.11,\ \xi = 3,\ a = 1.5,\ b = 1\ \ and\ \ W(\omega_e) = -a + b|\omega_e|. \tag{3.6}$$

Then, the characteristic polynomial (3.5) becomes

$$\begin{aligned} P(\lambda) &= \lambda Q(\lambda) \\ &= \lambda\left[\lambda^3 + (5\,|w_e| - 23.4)\,\lambda^2 + (50.15 - 4.5\,|w_e|)\,\lambda + 24.5\,|w_e| - 135.25\right] = 0. \end{aligned} \tag{3.7}$$

In order to find the range ω_e for which the system (3.2) has a three-dimensional stable manifold (Regardless of the eigenvalue being zero), one applies Routh-Hurwitz stability criterion to $Q(\lambda)$. So, all its roots have negative real parts if and only if the following conditions are satisfied

$$\begin{cases} 5\,|w_e| - 23.4 > 0, \\ 24.5\,|w_e| - 135.25 > 0, \\ -22.5\,|w_e|^2 + 331.55\,|w_e| - 1038.3 > 0, \end{cases} \tag{3.8}$$

Hence,

$$5.5204 < |w_e| < 10.221,$$

In contrast, chaos has a greater possibility of occurrence if (3.7) has one or more roots with positive real parts, that is

$$|w_e| < 5.5204, \ \text{ or } \ |w_e| > 10.221. \tag{3.9}$$

According to the above results, we deduce that the initial value of the state variable $\omega(t)$ can affect considerably the dynamical behavior of the system (3.2).

3.2 Bifurcation and Lyapunov Exponents spectrum

3.2.1 Dynamical behaviors versus the parameter a

In this section, the parameters take the following values $\alpha = 5, \beta = 5, \gamma = 0.1, b = 1, \xi = 3$ and let a vary over a certain interval to discuss the complex dynamics of the system (3.2) with the initial condition $(x, y, z, w_0) = (-0.5, 0.1, 0.01, -1)$. The bifurcation diagram of y and the corresponding Lyapunov exponents spectrum for a varying from 0 to 6 with a step size $h = 0.001$ are obtained as depicted in Figure 3.1 and Figure 3.2, respectively, which are in good coincidence.

From these figures it is obvious that system (3.2) displays period 1 orbit for $a \in]0.02, 1.41[\cup]2.04, 3.24[$. For $a \in]1.41, 2.1[\cup]3.24, 6[$ system (3.2) demonstrates chaotic and hyperchaotic behavior.

In particular, for $a = 3$ the Lyapunov exponents are

$$L_1 \approx 0.1417,\ L_2 \approx 0.0942,\ L_3 \approx 0.042,\ L_4 \approx -52.2119. \tag{3.10}$$

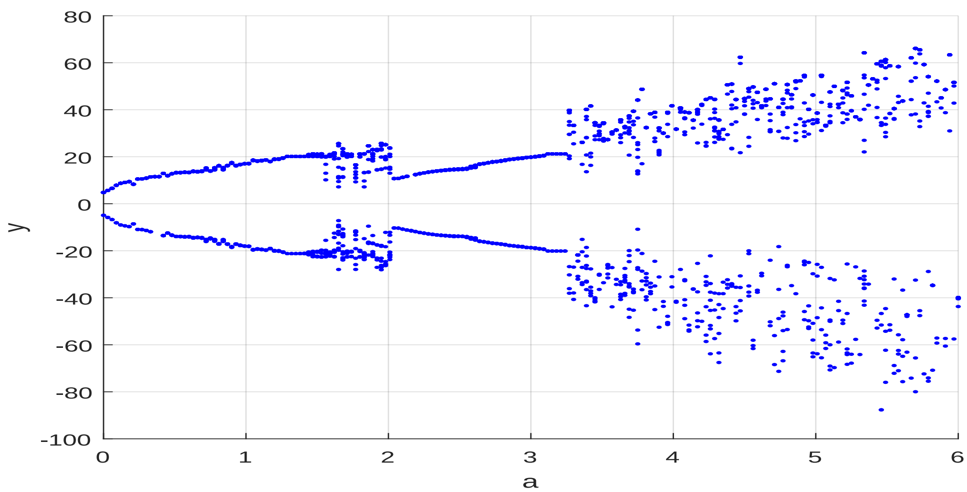

Figure 3.1: Bifurcation diagram with respect to the parameter a for $w_0 = -1$

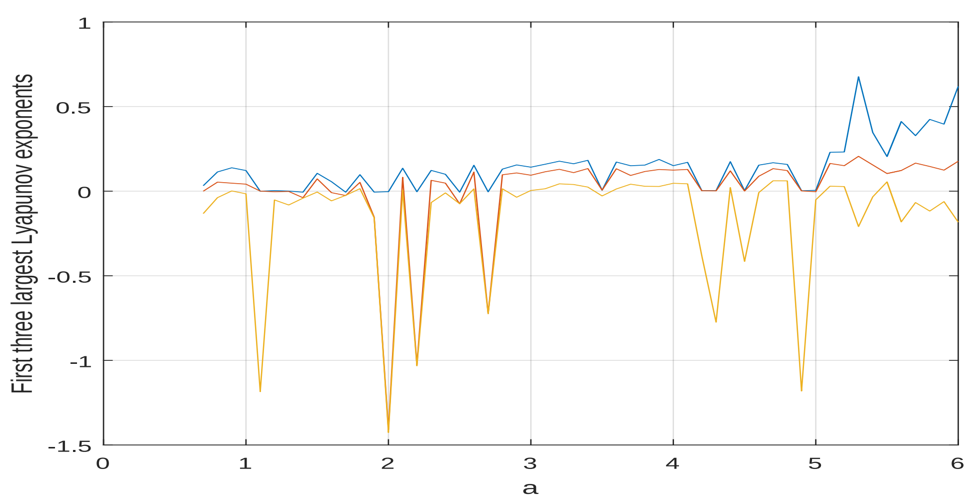

Figure 3.2: The three largest Lyapunov exponents of the system (3.2) versus the parameter a for $w_0 = -1$

Since $L_1 + L_2 + L_3 + L_4 = -51.9719 < 0$, $L_1 > 0, L_2 > 0$, then the system (3.2) is hyperchaotic. The Kaplan-Yorke dimension of its attractor is

$$D_{KY} \approx 3 + \frac{L_1 + L_2 + L_3}{|L_4|} = 3 + \frac{0.1417 + 0.0942 + 0.042}{51.2119} = 3.0046, \tag{3.11}$$

which is a fractal dimension.

3.2.2 Dynamical behaviors versus the initial state w_0

In the aim to study the impact of initial condition values on the dynamical behavior of the system (3.2), for the set of parameter values (7), different diagrams are presented to identify chaos.
Considering the initial condition $(x, y, z, w_0) = (-0.5, 0.1, 0.01, w_0)$, the Lyapunov exponents spectrum and the corresponding bifurcation diagram of y, for w_0 varying from -15 to 15 with step 0.01 are obtained as shown in Figure 3.4 and Figure 3.5, respectively. From these diagrams, one observes that when the value of initial state w_0 belongs to the following four intervals: $[-15, -11.91]$, $[-5.52, -0.9]$, $[0.9, 5.52]$, $[11.91, 15]$, then system (3.2) exhibits chaos. Furthermore, the two diagrams indicate symmetry versus $w_0 = 0$.

Particularly, for $w_0 = -1$ the Lyapunov exponents are [7]

$$L_1 = 0.1485,\ L_2 = 0.0420,\ L_3 = -0.0154,\ L_4 = -31.7725. \tag{3.12}$$

Since $L_1 + L_2 + L_3 + L_4 = -31.5975 < 0$, $L_1 > 0, L_2 > 0$, then the system (3.2) is hyperchaotic. The Kaplan-Yorke dimension of its attractor is

$$D_{KY} = 3 + \frac{L_1 + L_2 + L_3}{|L_4|} = 3 + \frac{0.1485 + 0.0420 - 0.0154}{31.7725} = 3.0055, \tag{3.13}$$

which is a fractal dimension.
Some phase portraits are depicted in Figure 3.3 for different values of the initial condition w_0. In particular, a period-1 orbits are shown in 3.3(b), 3.3(e), and 3.3(h). Moreover, 3.3(c), 3.3(g) represents a stable equilibrium point, and 3.3(a), 3.3(d), 3.3(f) and 3.3(i) displays chaotic attractors.

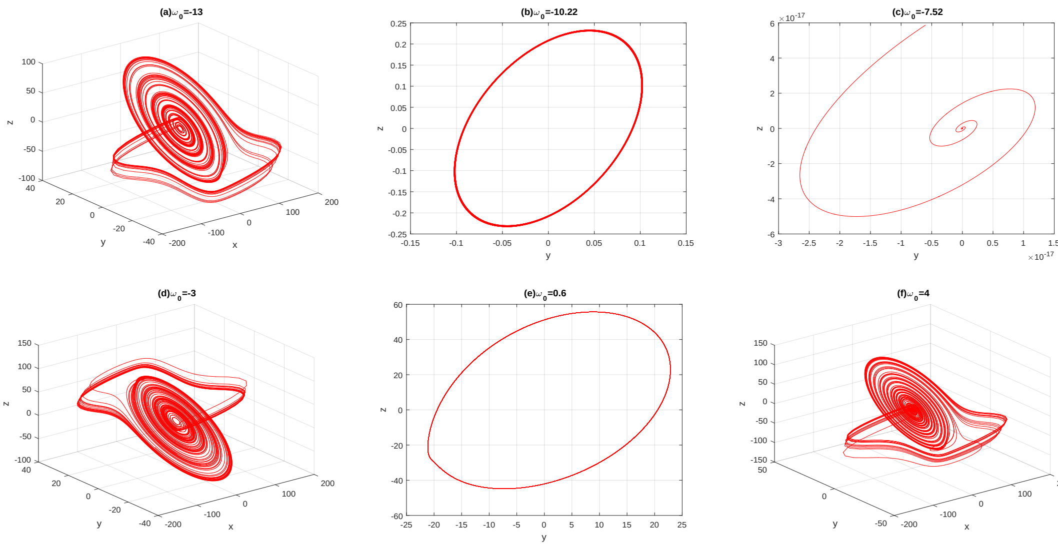

Figure 3.3: Some attractors for different values of initial condition w_0 : (a) $w_0 = -13$, (b) $w_0 = -10.22$, (c) $w_0 = -7.52$, (d) $w_0 = -3$, (e) $w_0 = 0.6$, (f) $w_0 = 4$, (g)

4 Modified projective synchronization between integer-order and incommensurate fractional order hyperchaotic systems

This section presents a theoretical analysis of the modified projective synchronization between integer-order and incommensurate fractional order hyperchaotic systems by applying the active control method based on the stability theorem of fractional-order linear systems.

4.1 Theoretical analysis

Giving two hyperchaotic systems: master and slave described respectively by :

$$\dot{X} = F(X), \tag{4.1}$$

$$D^{\alpha} Y = G(Y), \tag{4.2}$$

in order to make the study easier, (4.2) is rewritten as:

$$D^{\alpha} Y = AY + g(Y) + U, \tag{4.3}$$

where $X(t) = (x_1, x_2, ..., x_n)$, $Y(t) = (y_1, y_2, ..., y_n)$ are states of the master and the slave systems, respectively, $\alpha = (\alpha_1, \alpha_2, ..., \alpha_n)$ where $0 < \alpha_i < 1$ is the fractional-order,
$A \in \mathbb{R}^{n \times n}$, g are the linear part and the nonlinear part of the system (4.3), respectively, and $U = (u_1, u_2, ..., u_n)$ is a control input vector.
The error state is defined as:

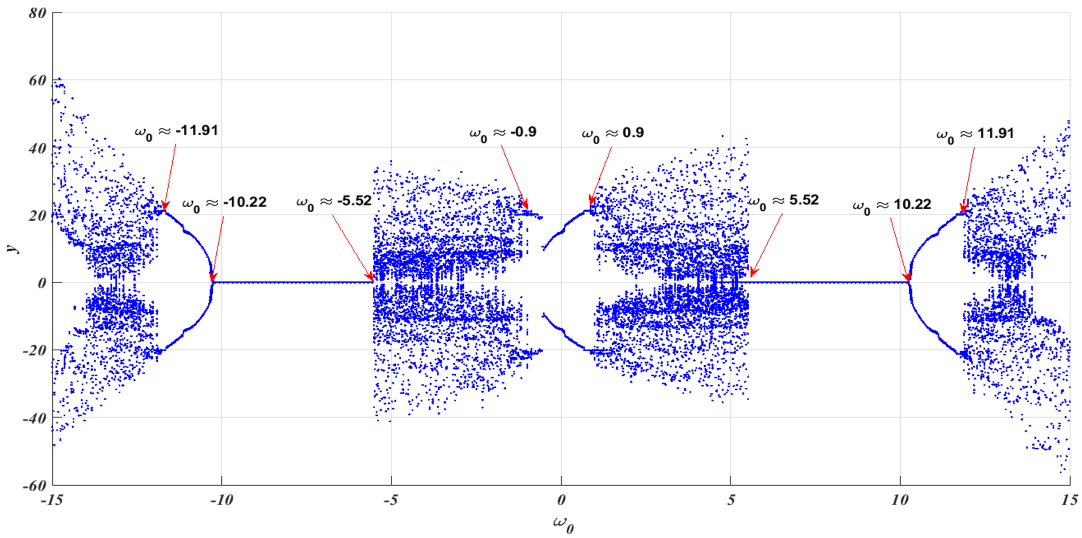

Figure 3.4: Bifurcation diagram with respect to the fourth coordinate w_0 of initial condition for $b = 1$

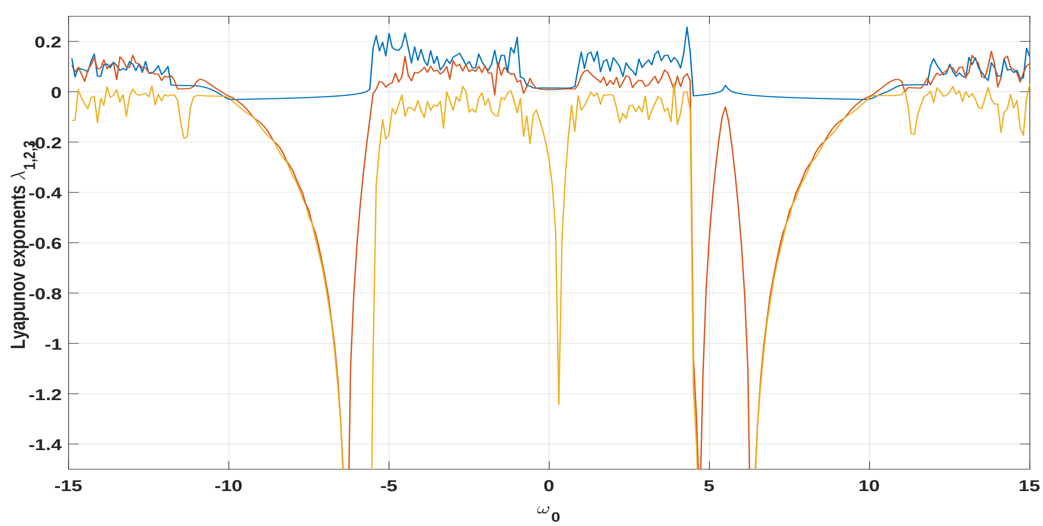

Figure 3.5: The three largest Lyapunov exponents of the system (3.2) versus the parameter w_0 for $b = 1$

$$e(t) = CY - X. \tag{4.4}$$

Where $C = diag(c_1, c_2, ..., c_n)$ denotes a scaling matrix. The objective of our work is to achieve synchronization between the two hyperchaotic systems (4.1) and (4.2) which could be achieved using the MPS technique when:

$$\lim_{t\to+\infty} e(t) = \lim_{t\to+\infty} \|CY(t) - X(t)\| = 0. \tag{4.5}$$

Hence the error system from equations (4.1) and (4.3) is as follows:

$$\begin{aligned} D^{\alpha}e &= CD^{\alpha}Y - D^{\alpha}X, &(4.6)\\ &= CAY + Cg(Y) + CU - D^{\alpha}X. &(4.7)\end{aligned}$$

In order to realize the MPS between integer order and incommensurate fractional order hyperchaotic systems, an active control U is chosen whereas the error system (4.4) asymptotically converges to zero. To achieve the stability of the system, we take the active control $U = (u_1, u_2, ..., u_n)^T$, such that:

$$U = C^{-1}((A + M)e - CAY - Cg(Y) + D^{\alpha}X), \tag{4.8}$$

where $M \in \mathbb{R}^{n\times n}$ is a gain matrix to be determined.
Substituting (4.8) into (4.7)yields :

$$D^{\alpha}e = (A + M)e. \tag{4.9}$$

Proposition 4.1. *If the matrix M is selected such that all roots λ_i of the characteristic equation:*

$$det(diag([\lambda^{m\alpha_1}, \lambda^{m\alpha_2}, ..., \lambda^{m\alpha_n}]) - (A + M)) = 0,$$

satisfy $|arg(\lambda_i)| > \frac{\pi}{2m}$, $i = 1, 2, ..., n$, where m is the least common multiple of the denominators of α_i, then the master system (4.1) and slave system (4.3) can be synchronized under the controller (4.8).

Proof. Immediately, using **theorem** 2.2. □

4.2 Numerical example and simulation results

To confirm the theoretical results obtained in the above sections, we perform numerical simulation by adopting the novel hyperchaotic system as a master system and its incommensurate fractional order version as a slave system.
The master system is defined as

$$\begin{cases} \dot{x}_1 = \alpha[x_3 + \xi x_1 - (-a + b|\omega|)x_1], \\ \dot{x}_2 = x_2 - x_3, \\ \dot{x}_3 = -\beta(x_1 - x_2) - \gamma x_3, \\ \dot{x}_4 = x_1, \end{cases} \tag{4.10}$$

The slave system is expressed by

$$\begin{cases} D^{\alpha_1} y_1 = \alpha[y_3 + \xi y_1 - (-a + b|\omega|)y_1] + u_1, \\ D^{\alpha_2} y_2 = y_2 - y_3 + u_2, \\ D^{\alpha_3} y_3 = -\beta(y_1 - y_2) - \gamma y_3 + u_3, \\ D^{\alpha_4} y_4 = y_1 + u_4, \end{cases} \tag{4.11}$$

where $u_1, u_2, ..., u_4$ are the active control functions, and α is a rational number between 0 and 1. The linear part of the system (4.3) is given by

$$A = \begin{bmatrix} \alpha(a+\xi) & 0 & \alpha & 0 \\ 0 & 1 & -1 & 0 \\ -\beta & \beta & -\gamma & 0 \\ 1 & 0 & 0 & 0 \end{bmatrix} \tag{4.12}$$

The matrix C is picked out in agreement with the MPS control technique proposed in equation (4.4) then

$$C = diag(5, 10, 0.1, 12), \tag{4.13}$$

and the gain matrix M is chosen as

$$M = \begin{bmatrix} -\alpha\xi - 2\alpha a & 0 & 1-\alpha & 0 \\ 0 & -2 & 1 & 0 \\ \beta & -\beta & -\gamma & 0 \\ -1 & 0 & 0 & -1 \end{bmatrix} \tag{4.14}$$

With the values given in (4.8) and (4.14), the error system becomes

$$\begin{bmatrix} D^{\alpha_1} e_1 \\ D^{\alpha_2} e_2 \\ D^{\alpha_3} e_3 \\ D^{\alpha_4} e_4 \end{bmatrix} = \begin{bmatrix} -\alpha a & 0 & 1 & 0 \\ 0 & -1 & 1 & 0.11 \\ 0 & 0 & -\gamma & 0 \\ -1.5 & 0 & 0 & -1 \end{bmatrix} \begin{bmatrix} e_1 \\ e_2 \\ e_3 \\ e_4 \end{bmatrix} \tag{4.15}$$

and the characteristic equation:

$$det(diag([\lambda^{m\alpha_1}, \lambda^{m\alpha_2}, \lambda^{m\alpha_3}, \lambda^{m\alpha_4}]) - (A + M)) = 0, \tag{4.16}$$

it can be transformed to:

$$(\lambda^{m\alpha_1} + 7.5)(\lambda^{m\alpha_2} + 1)(\lambda^{m\alpha_3} + 0.11)(\lambda^{m\alpha_4} + 1) = 0, \tag{4.17}$$

Where m is the least common multiple of the denominators of α_i, for $i = 1, 2, 3$ and 4, the master system (4.10) and the slave system (4.11) are synchronized if all roots λ of (4.17) satisfy

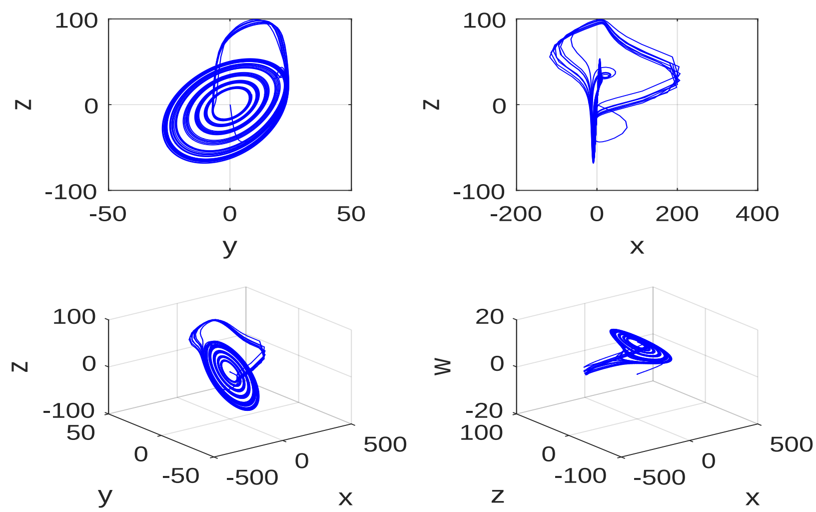

Figure 4.1: Some chaotic attractors of novel incommensurate fractional order system (4.11)

$|arg(\lambda_i)| > \frac{\pi}{2m}$.

Let us take $(\alpha, \beta, \xi, a, \gamma) = (5, 5, 3, 1.5, 0.11)$ and $(\alpha_1, \alpha_2, \alpha_3, \alpha_4) = (0.95, 1, 1, 1)$, substituting in (4.17) yields:

$$(\lambda^{19} + 7.5)(\lambda^{20} + 1)(\lambda^{20} + 0.11)(\lambda^{20} + 1) \quad = \quad 0, \tag{4.18}$$

Obviously, all roots λ_i of (4.18) must satisfy the condition $|arg(\lambda_i)| > \frac{\pi}{40}$, consequently the master system (4.10) and the slave system (4.11) are synchronized, under the controller (4.8).

Finally, for numerical simulation, the Adams method [16] is used to solve the systems with time step size $h = 0.02$, the error system has the initial values:

$$e_1(0) = 0.1, e_2(0) = 0.2, e_3(0) = 0.1, e_4(0) = -1.$$

The parameter values of the hyperchaotic systems are taken as in the hyperchaotic case (**??**) and the different fractional-orders are taken as:

$$(\alpha_1,\ \alpha_2,\ \alpha_3,\ \alpha_4) = (0.95, 1, 1, 1).$$

Figure 4.1 illustrates the attractors of the novel incommensurate fractional order system (4.11).
Figure 4.2 illustrates the synchronization errors between integer-order and incommensurate fractional order systems.
Figure 4.3 illustrates the error functions evolution (4.15).
From Figure 4.3, for the given parameters, numerical results clearly show that errors converge to zero, and so the MPS is effectively implemented under the controller (4.8).

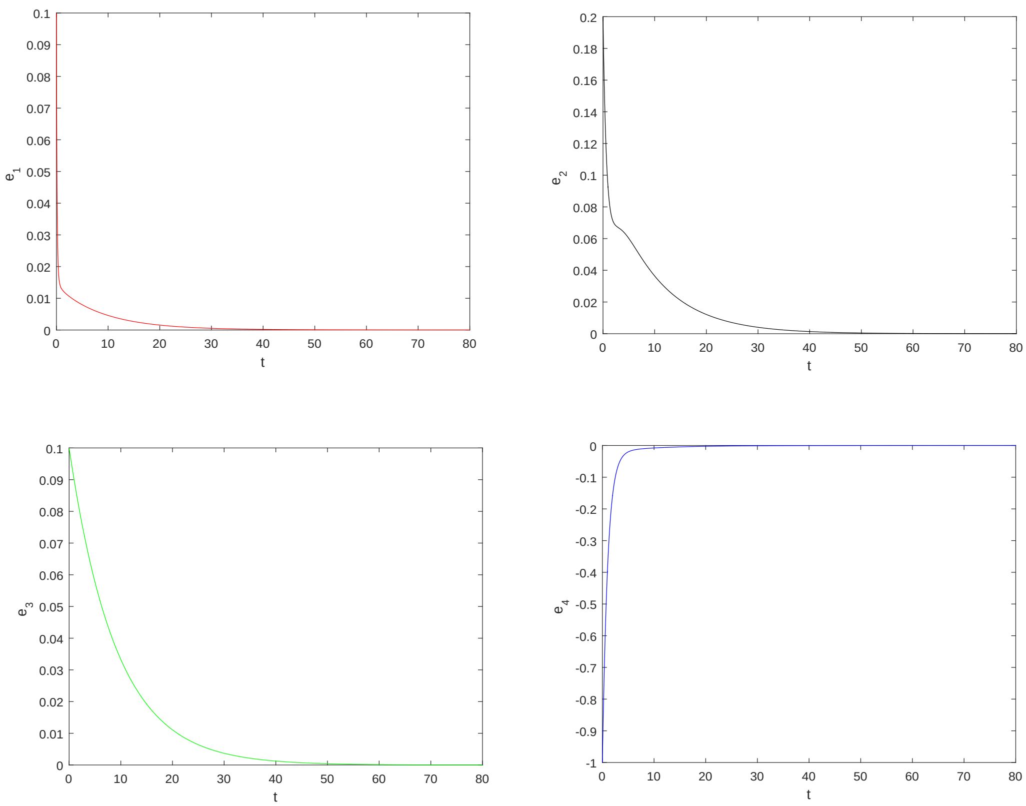

Figure 4.2: Synchronization errors between integer order and incommensurate fractional order systems

5 Conclusion

The synchronization between integer-order and fractional-order versions of a new memristor-based circuit with hyperchaotic dynamics was examined in this study. In order to derive the dynamical analysis, the stability theorems for fractional-order systems were applied, and the findings show that the variation of the fractional-order derivative significantly affects the proposed model's dynamical behavior. An MPS controller for synchronizing two hyperchaotic systems with integer and incommensurate fractional orders has been developed. Some numerical simulations have been provided to illustrate the theoretical results. We will use the proposed memristor-based hyperchaotic circuit for secure communication in the future by modulating the original signals into the chaotic sequences generated by the master circuit and transferring the combined signals to the receiver over a communication channel. Signals are received, and the MPS controller decodes them using the slave memristor-based circuit. Therefore, the relevant research is still in its early stages, and our next articles will discuss circuit implementations.

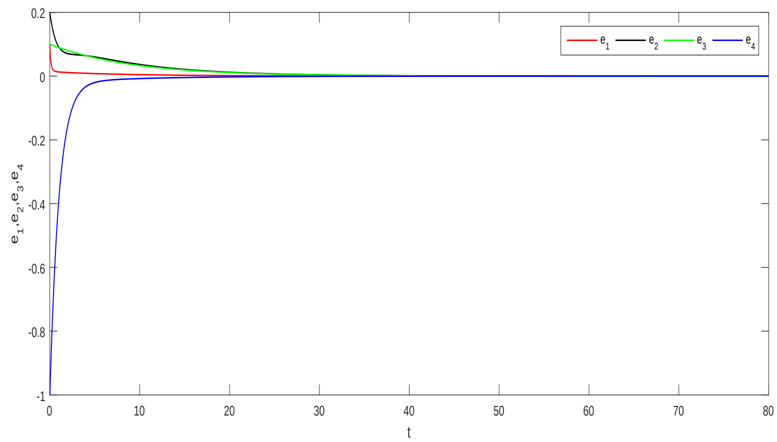

Figure 4.3: The synchronization errors of (4.10) and (4.11)

Declarations

Availability of data and materials

Data sharing not applicable to this article.

Funding

Not applicable.

Conflict of Interest

The authors have no conflicts of interest to declare.

References

[1] A. Boulkroune and M. Msaad, *On the design of observer-based fuzzy adaptive controller for nonlinear systems with unknown control gain sign*, Fuzzy Sets. Syst., **201** (2012), 71-85. DOI

[2] A. Boulkroune, S. Hamel, F. Zouari, and A. Leas, *Output-Feedback Controller Based Projective Lag Synchronization of Uncertain Chaotic Systems in the Presence of Input Nonlinearities*, Mathematical Problems in Engineering, **81** (2017), 1-12. DOI

[3] A. Chen, J. Lu, Jinhu Lü and S. Yu, *Generating hyperchaotic Lü attractor via state feedback control*, Physica A, **364** (2006), 103-110. DOI

[4] M. M. Al-Sawalha, and A. Al-Sawalha, *Anti-synchronization of fractional-order chaotic and hyperchaotic systems with fully unknown parameters using modified adaptive control*, Open Phys., **14**(1) (2016), 304-313.

DOI

[5] A. Soukkou and S. Leulmi, *Controlling and Synchronizing of Fractional-Order Chaotic Systems via Simple and Optimal Fractional-Order Feedback Controller*, International Journal of Intelligent Systems Technologies and Applications., **8**(6) (2016), 56-69. DOI

[6] A. Soukkou, A. Boukabou and S. Leulmi, *Prediction-based feedback control and synchronization algorithm of fractional-order chaotic systems*, Nonlinear Dyn. **58**(4) (2016), 2183-2206. DOI

[7] A. Wolf, J. B. Swift, H. L. Swinney and J. A. Vastano, *Determning Lyapunov Exponents from a Time Series*, Physica D., **16** (1985), 285-317. DOI

[8] B. C. Bao, J. P. Xu and Z. Liu, *Initial state dependent dynamical behaviors in memristor based chaotic circuit*, Chinese Physics Letters, **27**(7) (2010), 070504. DOI

[9] B. Muthuswamy and P. P. Kokate, *Memristor based chaotic circuits*, IETE Technical Review. **26**(6) (2009), 415-426. DOI

[10] B. Wang, J. Jian and H. Yu, *Adaptive synchronization of fractional-order memristor-based Chuas system*, Systems Science, (2014), 291-296. DOI

[11] D. Cafagna and G. Grassi, *On the simplest fractional-order memristor-based chaotic system*, Nonlinear Dyn., **70**(2)(2012), 1185-1197. DOI

[12] G. Ye and J. Zhou, *A block chaotic image encryption scheme based on self-adaptive modelling*, Applied Soft Computing, **22**(2014), 351-357. DOI

[13] I. Petráš, *Fractional-order memristor-based Chua's circuit*, IEEE Trans. Circuits Syst. II., **57**(12) (2010), 975-979. DOI

[14] J. Borghetti, G. S. Snider , P. J. Kuekes, J. J. Yang, D. R. Stewart and R. S. Williams, *Memristive switches enable tateful logic operations via material implication*, **64**(4) (2010), 873-876. DOI

[15] J. Wang and Z. Chen, *A novel hyperchaotic system and its complex dynamics*, Int. J. Bifurcation Chaos, **18**(11) (2008), 3309-3324. DOI

[16] K. Diethelm, N. J. Ford and A. D. Freed, *Detailed error analysis for a fractional Adams method*, Numer. Algorithms., **36** (2004), 31-52. DOI

[17] K. Murali and M. Lakshmanan, *Secure communication using a compound signal from generalized chaotic systems*, Phys. Lett. A., **241**(6) (1998), 303-310. DOI

[18] L. Jian , L. Shutang and Y. Chunhua, *Modified generalized projective synchronization of fractional-order chaotic Lü systems*, Adv. Differ. Equations, (2013), 2013-374. DOI

[19] L. Kocarev and U. Parlitz, *General approach for chaotic synchronization with application to communication*, Phys. Rev. Lett., **74** (1995), 5028-5031. DOI

[20] L. O. Chua, *Memristor, the missing circuit element*, IEEE Trans. circuit. Theory., **18** (1971), 507-519. DOI

[21] L. Teng, H. C. Iu Herbert , X. Y. Wang and X. K. Wang, *Chaotic behavior in fractional-order memristor-based simplest chaotic circuit using fourth degree polynomial*, Nonlinear Dyn., **77**(1-2) (2014), 231-241. DOI

[22] M-S. Abdelouahab, N-E. Hamri and J. Wang, *Hopf bifurcation and chaos in fractional-order modified hybrid optical system*, Nonlinear Dyn., **69**(1) (2012), 275–284. DOI

[23] M-S. Abdelouahab and R. Lozi, *Hopf bifurcation and chaos in simplest fractional-order memristors-based electrical circuit*, Indian Journal of Industrial and Applied Mathematics, **6**(2)(2015), 105-119. DOI

[24] M-S. Abdelouahab, R. Lozi and L. O. Chua, *Memfractance: a mathematical paradigm for circuit elements with memory*, Int. J. Bifurcation Chaos., **24**(9) (2014), 1430023 (29 pages). DOI

[25] M. Bharathwaj, Khalil, *Implementing memristor based chaotic circuit*, Int. J. Bifurcation Chaos, **20**(5) (2010), 1335-1350. DOI

[26] M. Itoh and L. O. Chua, *Memristor Oscillators*, Int. J. Bifurcation Chaos, **18**(11) (2008), 3183-3206. DOI

[27] O. E. Rossler, *An equation for hyperchaos*, Phys. Lett. A., **71**(2-3) (1979), 155-177. DOI

[28] Q. Li, S. Hu, S. Tang and G. Zeng, *Hyperchaos and horseshoe in a* $4-D$ *memristive system with a line of equilibria and its implementation*, Int. J. Circuit Theory Appl., **42**(11) (2014), 1172-1188. DOI

[29] R. Suresh, and V. Sundarapandian, *Hybrid synchronization of n–scroll Chua and Lur'e chaotic systems via backstepping control with novel feedback*. Arch. Control Sci., **3** (2012), 343-365. DOI

[30] Sh. Wang, Xi. Wang and Y. Zhou, *A Memristor-Based Complex Lorenz System and Its Modified Projective Synchronization*, Entropy.,**17**(11) (2015), 7628-7644. DOI

[31] S. Kaouache and M-S. Abdelouahab, *Modified Projective Synchronization between Integer Order and fractional-order Hyperchaotic Systems*, Journal of Adv Research in Dynamical and Control Systems, **10**(5) (2018), 96-104.

[32] S. Rasappan, Y. Li , X. Huang, Y. Song and J. Lin, *A new fourth-order memristive chaotic system and its generation*, Int. J. Bifurcation Chaos, **25**(11) (2015), 1550151. DOI

[33] S. Shin, K. Kim and S. M. Kang , *Memristor applications for programmable analog ICs*, IEEE Transactions in Nanotechnology, **10**(2) (2011), 266-274. DOI

[34] S. Vaidyanathan, Ch. K. Volos and V.-T. Pham, *Analysis, Control, Synchronization and SPICE Implementation of a Novel 4-D Hyperchaotic Rikitake Dynamo System without Equilibrium*, Journal of Engineering Science and Technology Review, **8** (2)(2015), 232-244. DOI

[35] S. Vaidyanathan, Ch. K. Volos and V. -T. Pham, *Analysis, adaptive control and adaptive synchronization of a nine-term novel 3-D chaotic system with four quadratic nonlinearities and its circuit simulation*, Journal of Engineering Science and Technology Review, **8**(2) (2015), 174–184. DOI

[36] T. I. Chien and T. L. Liao, *Design of secure digital communication systems using chaotic modulation, cryptography and chaotic synchronization*, Chaos, Solitons Fractals, **24** (2005), 241-245. DOI

[37] V. T. Pham, Ch. Volos and L. V. Gambuzza, *A Memristive Hyperchaotic System without Equilibrium*, The Scientific World Journal, 368986 (2014), 1-9. DOI

[38] W. Zhen, H. Xia and S. Hao, *Control of an uncertain fractional-order economic system via adaptive sliding mode*, Neurocomputing, **83** (2012), 83-88. DOI

[39] X. Huang, J. Jia, Y. Li and Z. Wang, *Complex Nonlinear Dynamics in fractional and integer order memristor-based systems*, Neurocomputing., **218**(19) (2016), 296-306. DOI

[40] H. Xi, Y. Li, and X. Huang. *Generation and Nonlinear Dynamical Analyses of Fractional-Order Memristor-Based Lorenz Systems*, Entropy, **16**(12) (2014), 6240-6253. DOI

[41] X. J. Wu and Y. Lu, *Generalized projective synchronization of the fractional-order Chen hyperchaotic system*, Nonlinear Dyn., **57**(1-2) (2009), 25-35. DOI

[42] Y. V. Pershin and M. D. Ventra , *Experimental demonstration of associative memory with memristive neural networks*, Neural Networks, **23**(7) (2010), 881-886. DOI

[43] Y. Yu and H. Li, *The synchronization of fractional-order Rossler hyperchaotic systems*, Physica A, **387** (5-6)(2008), 1393-1403. DOI

[44] Z. Elhadj, *Dynamical Analysis of a* $3-D$ *Chaotic System with only Two Quadratic Nonlinearities*, J. Syst. Sci. Complex., **21**(1) (2008), 67-75. DOI

[45] Z. Hrubš and T. Gotthans, *Analysis and synthesis of chaotic circuits using memristor properies*, Journal of electrical engineering, **65**(3) (2014), 129-136. DOI